Image-Guided Intensity-Modulated Radiotherapy for Single Vocal Cord Irradiation in Early Glottic Cancers

Printed by: Ridderprint
Cover drawing: Amira Osman
Cover design: Ridderprint, Sarah Osman
Layout: Eliana Vásquez Osorio

ISBN: 978-90-5335-460-5

Image-Guided Intensity-Modulated Radiotherapy for Single Vocal Cord Irradiation in Early Glottic Cancers

Beeldgestuurde, intensiteitsgemoduleerde radiotherapie voor bestraling van een enkele stemband bij vroege glottische tumoren

Proefschrift

ter verkrijging van de graad van doctor aan de
Erasmus Universiteit Rotterdam
op gezag van de Rector Magnificus

Prof.dr. H.G. Schmidt

en volgens besluit van het College voor Promoties

De openbare verdediging zal plaatsvinden op
vrijdag 21 oktober 2011 om 11.30 uur

door

Sarah Omer Siddig Osman
geboren te Bristol, UK

Promotiecommissie

Promotor:	Prof. dr. B.J.M. Heijmen
	Prof. dr. P.C. Levendag
Overige leden:	Prof. dr. G.C. van Rhoon
	Prof. dr. M. van Herk
	Prof. dr. S. Leenstra

This thesis has been prepared at the Department of Radiation Oncology, Erasmus MC - Daniel den Hoed Cancer Center, Rotterdam, The Netherlands.

The printing of this thesis was partially funded by Elekta B.V.

E-mail for correspondence: osman.sarah@gmail.com

To my parents

Contents

Chapter 1

Introduction

1.1 Cancer of the larynx

The larynx anatomy is graphically presented in figure 1.1 . The vocal cords in the center of the larynx are muscular bands covered by thin mucosa layers. Together, the right and left vocal cords have a V-shape, when viewed from cranial. The vocal cords play key roles in the control of the airflow during breathing, the protection of airway, and in the production of sound for speech.

Cancer of the larynx is one of the most common cancers in Europe, with about 52,000 new cases annually, 90% occurring in men. 95% of all cancers of the larynx are squamous cell carcinomas [65]. Cancer of the larynx is mainly caused by consumption of tobacco and alcohol. Nevertheless, tobacco dominates the risk for cancer of the vocal cords. Over 90% of the present incidences of laryngeal cancers could be prevented by avoiding smoking and alcohol consumption. The most common symptoms observed in early glottic cancers are; the presence of hoarseness, sore throat, shortness of breath, and the feeling of a lump in the throat. Hoarseness, which is a an early symptom for glottic lesions, is the main symptom which causes patients to seek medical consultation [65].

A complete ear, nose, and throat check (with mirrors and laryngscopes) and histology examination are common steps in the examination of suspected laryngeal cancer patients. Vocal cord mobility and exact tumor extension are carefully assessed to aid specifying the exact stage (TNM staging) of the tumor [65]. The stage of the tumor is important for establishing the treatment policy.

This thesis discusses treatment of early stage glottic cancers (Carcinoma in situ (Tis), and tumors limited to one vocal cord (T1a), with no regional/distant lymph node metastasis (N0M0)). Early stage glottic squamous cell carcinomas (SCC) are usually confined to the glottic area. As the true vocal cords essentially have no lymphatic vessels, these tumors are known to be highly localized [97]. It is also known that these cancers are normally limited to the mucosa without the involvement of the underlying muscles.

These early stage glottic tumors are frequently curable using one of the treatment modalities; surgery, endoscopic laser surgery, and radiation therapy (RT), which are equally successful in terms of local control [65, 105]. The probability of cure is $80-90\%$ when using any of the above-mentioned treatment modalities. Nevertheless, the treatment of choice of early glottic cancer is still largely debated (surgery or radiotherapy). It is generally agreed that choice should depend on the functional outcomes.

Comparative studies between endoscopic laser surgery and RT show no differences between either treatment modalities except slightly better voice after RT, which makes RT the favored treatment modality especially for invasive carcinoma [102, 60].

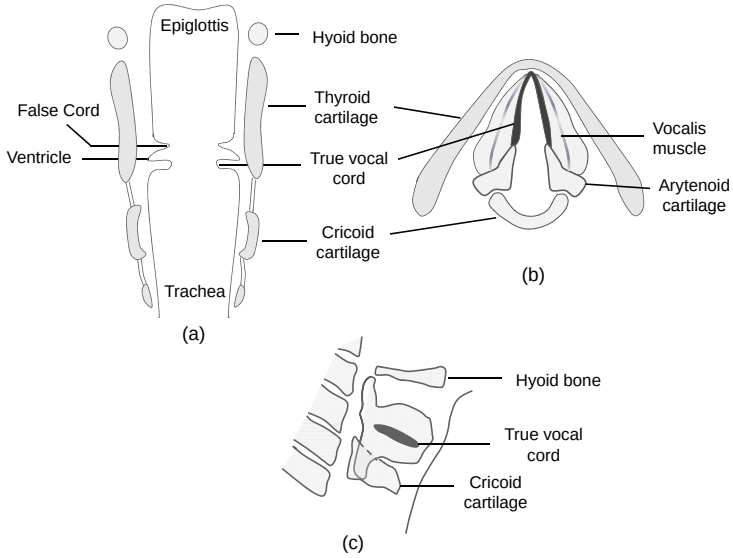

Figure 1.1: *Anatomy of the larynx : schematic representation of the coronal(a), transverse (b) and sagittal (c) planes at the level of the vocal cords.*

1.2 Conventional radiotherapy treatment fields

Early glottic tumors treated with RT are conventionally irradiated using two parallel opposed wedged 6-MV photon beams with field sizes that vary between $25 - 50cm^2$. The superior border of the treatment field is the hyoid bone and the inferior border is the lower edge of the cricoid cartilage. The anterior border is approximately $1cm$ outside the patient's skin and the posterior border covers $\sim 1mm$ of the anterior vertebrae figure 1.2. These fields cover both vocal cords and the surrounding muscles and cartilages conservatively. All the structures receive the total prescribed dose (e.g. in our scheme 66Gy in 33 fractions).

Typical side effects of irradiating normal tissues with conventional RT techniques are poor voice quality, persistent or progressive arytenoid edema, and increased risk of strokes [20, 4, 104].

Considering current developments in the field of RT and the introduction of image-guided radiotherapy (IGRT) techniques, using conventional conservative irradiation techniques with large treatment fields is likely to be sub-optimal, especially in case of a single involved vocal cord.

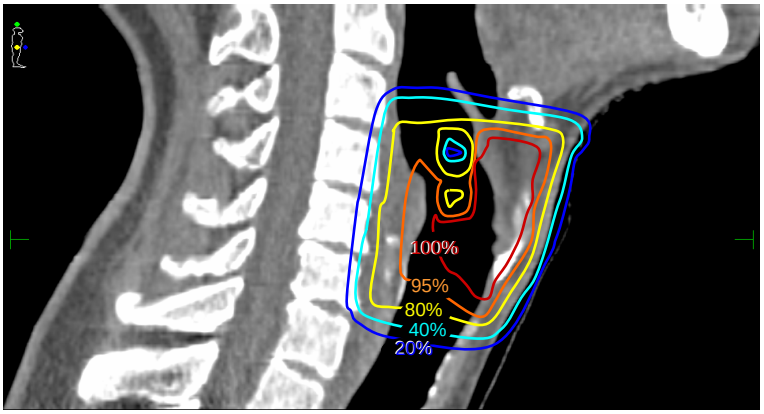

Figure 1.2: *Sagittal CT slice showing the iso-dose lines of conventional RT parallel opposed fields (100%=66 Gy).*

1.3 Single vocal cord irradiation - Outline of the thesis

We have developed a new optimized radiotherapy technique to treat Tis and T1a tumors confined to one vocal cord. The goal was to deliver a highly conformal dose to the tumor, while minimizing radiation damage to the contra-lateral vocal cord and other normal healthy tissues (e.g. surrounding cartilages, muscles, carotid arteries, etc.) on both sides of the neck as much as possible.

Sparing the non-involved normal tissues with the new RT technique might improve voice outcomes, preserve swallowing functionality, prevent arytenoid edema, and reduce the risk of strokes in this group of patients. Moreover, for laryngeal preservation, delivering a more conformal dose might allow re-irradiating the tumors if the need arises in the future due to a regional recurrence or growth of a second primary tumor in the same vicinity.

This thesis describes the steps we have taken to arrive at a highly focused, image-guided radiation therapy (IGRT) technique for single vocal cord irradiation for early glottic cancer patients. Chapter (2) covers the issue of internal organ motion of the vocal cords with breathing. This was done with the aid of time-resolved 4D computed tomography (4D-CT) scans of the region of the vocal cords while monitoring the patient's breathing signal. The extent of the movement of the structures and the uncertainties involved were quantified and discussed in details.

In chapter (3), the feasibility of using in-treatment-room cone beam computed tomography scans (CBCT) for daily-on-line patient set-up corrections is discussed. Guidelines for a fast automatic registration procedure are presented, and the accuracy of this procedure was determined. The residual uncertainties in the

position of the tumor after automatic registration were assessed and quantified. Also a CTV-PTV safety margin was proposed to compensate for residual inter- and intra-treatment set-up errors.

Single vocal cord irradiation (SVCI) with Intensity-modulated radiation therapy (IMRT) for early glottic cancers is presented in chapter (4). An in-house developed beam angle optimization algorithm was employed to find the best beam orientations to deliver intensity modulated fluences (co-planar and non-coplanar) with a maximum sparing of normal tissue and organs at risk. These beam arrangements were then used in a Monte Carlo based (MC) treatment planning system to generate IMRT plans. In Chapter (4) a comparison of plans obtained using IMRT coplanar, IMRT non-coplanar, and conventional parallel opposed wedged fields is presented. Moreover, a class-solution of five coplanar beam angles is researched.

In chapter (5), the sensitivity of the IMRT plans for SVCI to geometrical uncertainties resulting from patient's set-up errors, respiration, and anatomical variation/deformations was investigated. The effect of these uncertainties on dose distribution in the CTV as well as the contra-lateral vocal cord sparing is reported.

In chapter (6), a review of the side effects that are commonly observed after RT for the head and neck cancer is presented. The potential reduction of these side effect with the introduction of SVCI as a standard treatment is discussed based on a comparison of the dose received by different normal tissues. In addition, the role of (hypo) fractionation in SVCI, considering the low probability of normal tissue side-effects, is also discussed. A comparison of SVCI and carbon dioxide endoscopic laser surgery in the management of early glottic cancers is also discussed.

Chapter (7) presents a general discussion of the topics discussed in this thesis. Early reports on the clinical implementation of IMRT for SVCI and proposals for further research are also presented.

Chapter 2

Four-dimensional CT Analysis of Vocal Cords Mobility for Highly Focused Single Vocal Cord Irradiation

Sarah O.S. Osman, Hans C.J. de Boer, Ben J.M. Heijmen and Peter C. Levendag

Published in Radiotherapy and Oncology. Volume 89, Issue 1. Pages 19-27. October 2008

Abstract

Background and Purpose: To quantify respiratory motion of the vocal cords during normal respiration using 4D-CT. The final goal is to develop a technique for single vocal cord irradiation (SVCI) in early glottic carcinoma. Sparing the non-involved cord and surrounding structures has the potential to preserve voice quality and allow re-irradiation of recurrent and second primary tumors.

Methods and Materials: Four-dimensional CTs of 1 mm slice thickness from 10 early glottic carcinoma patients were acquired. The lateral dimensions of the air gap separating the vocal cords were measured anteriorly, at mid-level and posteriorly at each phase of the 4D-CTs. The corresponding anterior-posterior gaps were similarly measured. Cranio-caudal vocal cords movements during breathing were derived from the shifts of the arythenoids.

Results: The population-averaged mean gap size $\pm$ the corresponding standard deviation due to breathing (SD_B) for the lateral gaps was $5.8 \pm 0.7mm$ anteriorly, 8.7 ± 0.9 mm at mid-level, and $11.0 \pm 1.3mm$ posteriorly. Anterior-posterior gap values were $21.7 \pm 0.7mm$, while cranio-caudal shift SD_B was $0.8mm$.

Conclusions: Vocal cords breathing motions were found to be small relative to their separation. Hence, breathing motion does not seem to be a limiting factor for SVCI.

2.1 Introduction

Early stage glottic carcinoma (EGC) is frequently curable using one of the treatment modalities; surgery, laser surgery, and radiation therapy (RT), which are equally successful in terms of local control and cure rates [65, 50, 10, 17, 105, 117, 136]. Speech and voice quality were reported to be significantly better in patients treated with RT as opposed to surgery [60, 106]. Furthermore, comparative studies between endoscopic laser surgery and RT show no differences between either treatment modalities except slightly better voice after RT, which makes RT the favoured treatment modality especially for invasive carcinoma [50, 106, 102, 29, 68, 55]. The aim of the treatment is definite cure with a probability of success that depends on the loco-regional extensions of the disease. Using any of the above-mentioned treatment modalities T1 and T2 tumors have $80 - 90\%$ probability of cure. Nevertheless, some groups reported that local recurrences after RT for glottic lesions occurred in $5 - 20\%$ of T1 tumors and $25 - 30\%$ of T2 tumors [77, 114]. Once a tumor recurrence is confirmed by histological examination it is usually treated surgically. Surgical treatment can be either endoscopic laser surgery, partial or total laryngectomy [99, 84, 54]. In this article, we consider the optimization of radiotherapy treatment of EGC, i.e., T1N0M0 and TisN0M0 according to the UICC classification.

Optimal treatment of laryngeal cancer demands both tumor eradication and the preservation of the laryngeal function. Good results have been obtained with radiotherapy for this group of patients in terms of local control rates, survival, as well as voice quality [59]. However, voice quality following radiotherapy could not be considered normal [20]. Verdonck-De Leeuw et al. [22] showed that self-rated performance (questionnaires) and stroboscopic measurements are highly correlated. Preliminary data obtained in our institute deduced from Voice Handicap Index scores [76] (ongoing study, N = 122 patients with T1N0M0), indicate that 22% of patients treated by radiotherapy alone ended up with poor voice quality. Studies on the influence of voice deterioration on the quality of life (QoL) showed that $27 - 58\%$ of patients with voice problems experienced difficulties in communication that disrupted their social lives [37, 95, 33, 122]. Dornfeld et al. investigated the dose to different laryngeal structures in relation to complaints and found an inverse relationship between radiation doses and speech, diet, as well as other QoL indicators after treatment [26]. These results underlined the need to deliver lower doses to unnecessarily irradiated structures in order to preserve the laryngeal function after RT.

In our clinic as well as most other institutes, the conventional RT technique adopted for EGC is the use of two opposed lateral 6 MV photon beams with field sizes that typically vary between 25 and 50 cm^2 [15, 52]. The superior border of the treatment field is the hyoid bone and the inferior border is the lower edge of the cricoid cartilage. The anterior border is approximately 1 cm falloff and the posterior border covers 1 mm of the anterior vertebrae [52]. Because these fields cover the vocal cords and the surrounding muscles and cartilages so conservatively

there have been attempts to deliver more conformal dose distributions [4, 69, 19]. Potentially this could lead to prevention of persistent or progressive arytenoid edema, preservation of voice, and improvement of the quality of life for the RT patients. No significant degradation in local control was observed when reducing the treatment fields for arytenoid shielding [4, 69]. These results support the use of smaller, highly focused treatment fields to irradiate only the affected vocal cord, while sparing the surrounding structures as well as the healthy cord.

In our institute, we have embarked on a program for optimal conformality in EGC, namely single vocal cord irradiation (SVCI). By thus sparing the non-involved cord, we aim to improve the quality of voice and hence QoL of EGC patients treated with RT while maintaining the very good local control rate that is achieved with conventional radiotherapy. As a corollary, SVCI may allow re-irradiation of recurrent tumors in cases of local failure as well as secondary primary tumors in the vicinity and hence prevent laryngectomy for these cases.

Using 4D-CT and cone beam CTs, it is possible to take practical steps towards SVCI. This paper addresses the issue of intra-fraction motion of the vocal cords due to breathing using 4D-CT data. If breathing motion of the cords is relatively large, for instance when compared to the opening between cords, SCVI might require techniques such as breathing control or gating.

Single vocal cord irradiation requires precise techniques to visualize the cords and to monitor the movements of the cords and the surrounding structures. It was the purpose of this work to quantify the intra-fractional movements of the vocal cords during normal breathing using 4D-CT. These motions may have clinical consequences for the choice of margins around the clinical target volumes, i.e., in the construction of the planning target volumes.

2.2 Methods and Materials

2.2.1 Patients and protocol

Ten patients with early glottic carcinoma were enrolled in this study after having given informed consent. Patients and tumor characteristics are presented in Table 2.1.

In our clinic EGC patients undergo an outpatient examination performed by both a head-and-neck surgeon and a radiation oncologist. For diagnostic-staging purposes, patients are usually re-examined under anesthesia and a biopsy is taken. In the majority of the cases contrast-enhanced CT scan is obtained to stage the laryngeal tumor.

Table 2.1: *Patient characteristics*

Patient	Local tumor stage	Right/left	Age	Sex
1	T1aN0M0	Left	68	M
2	T1aN0M0	Left	64	M
3	T1aN0M0	Left	52	M
4	cT1aN0Mx^a	Left	75	M
5	TisN0M0	Right	62	M
6	T1bN0M0	Left and right	55	M
7	T1aN0M0	Right	48	M
8	T1aN0Mx	Left	67	M
9	T1aN0Mx	Right	59	F
10	T1aN0M0	Right	69	M

[a] This patient was staged clinically, while all the other patients were staged histologically

2.2.2 Immobilization, 4D-CT scan procedure and image reconstruction

Instead of a conventional treatment simulator session to determine and mark the treatment fields, patients included in this study were sent to the multi-slice CT scanner (Siemens Medical Solutions, SOMATOM Sensation Open CT 40-slices). They were immobilized using a thermoplastic mask with five fixation points that is also used during treatment to reduce set-up uncertainties. 4D-CT data sets were acquired using a high-resolution protocol with an acquisition slice thickness of 1.5 mm. The reconstructed length was 12 cm and gantry rotation time 0.5 s (pitch = 0.1). The respiratory signal was obtained from a pressure sensor that is attached to an elastic belt (ANZAI medical; figure 2.1(a) and (b)). Based on this signal, we divided the respiratory cycle into nine discrete respiratory phases: start inhale, early inhale, mid inhale, late inhale, end inhale (start exhale), early exhale, mid exhale, late exhale, and end exhale [133]. CT data were retrospectively reconstructed for each phase of the respiratory cycle with a reconstruction increment (slice thickness) of 1 mm. The reconstruction for each phase bin was obtained by imaging four to five breathing cycles.

2.2.3 Measurements

The mobility of each patient's vocal cords was quantified with the aid of the virtual simulation software available with our scanner (VSIM syngo CT 2006A from Siemens AG).

The lateral gap width (X) between the two vocal cords was measured in three different positions along their length; (anterior) X_{ANT}, (middle) X_{MID},

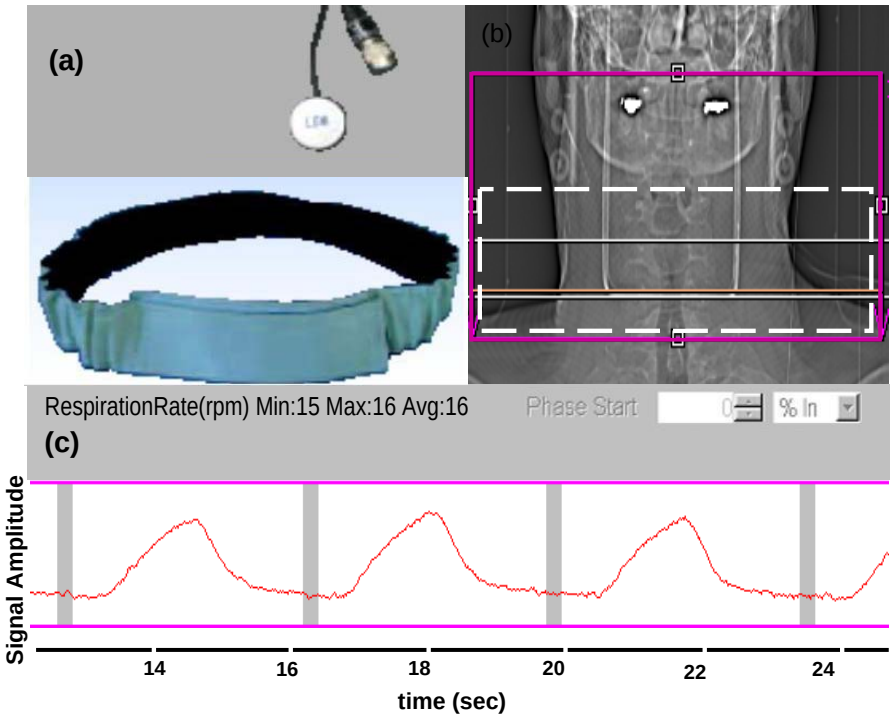

Figure 2.1: *Acquisition of 4D-CTs and reconstruction (a) ANZAI belt with pressure sensor. (b) The dashed rectangular structure represents the area scanned to acquire the 4D-CT. (c) Display of breathing signal in which the gray vertical bars indicates* 0% *inhale (start insp).*

and (posterior) X_{POST}, see figure 2.2. The anterior-posterior gap width (Y) between the anterior commissure and the midpoint between the arytenoids was also measured. To provide a well-defined measurement of the cranial-caudal (Z) movements of the vocal cords, we measured the position of the most cranial extension of the arythenoids. In all measurements the start inspiration phase (0% inhale) was taken as a reference.

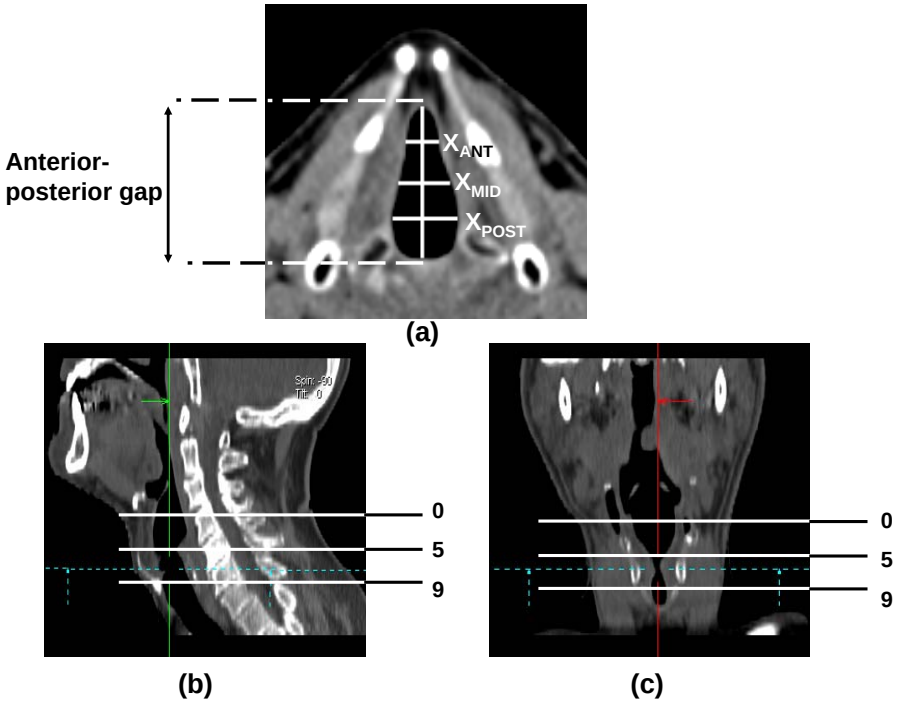

Figure 2.2: *(a) Axial view of the vocal cords and the different values measured with breathing phase. (b and c) Sagittal and coronal images showing schematically the different slices where the vocal cords are located. 0 mm corresponds to the most superior and 9 mm to the most inferior slice.*

2.3 Results

On average, the total time required for the 4D-CT procedure was 10 min. The quality of the CTs allowed good visualization of the vocal cords and the surrounding cartilage tissues especially in the transverse views of the CTs, see [figure 2.2] and [figure 2.3].

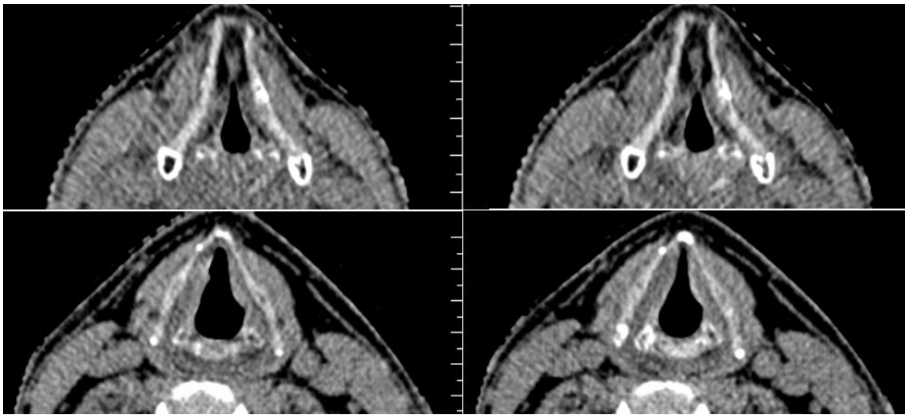

Figure 2.3: *Transverse views showing middle inspiration phase (mid insp.) to the left and the same slice at middle expiration phase to right for patients 4 and 7.*

2.3.1 Variations in the magnitude of the different parameters during respiration

In all the patients the vocal cords were visible in $7 - 10$ transverse slices of 1 mm thickness. figure 2.4 shows an example of the different parameters that were measured in 10 successive transverse slices in patient number 2 (Table 2.1). This figure demonstrates how almost all slices show the same pattern of variation with breathing phase in both the anterior-posterior and the lateral gaps. In the most cranial slices the lateral gaps between the vocal cords were always larger than those in the most caudal slices, reflecting the shape of the cords ((figure 2.2) and (figure 2.4)).

Table 2.2 summarizes the observed intra-fractional movements of the different parts of the vocal cords. The range, the mean magnitude, and the standard deviation from the mean due to breathing of the lateral gaps between the left and the right vocal cords and the anterior-posterior gaps (Y) were calculated from the average values over all slices where the vocal cords were visible for each patient.

As shown in Table 2.2, the largest respiratory variations in the vocal cords gap (SD_B) were noticed posteriorly (X_{POST}), where the mean gap values were also the largest ((figure 2.2) and (figure 2.3)). Two of the 10 patients analyzed showed negligible movements of the vocal cords in these lateral posterior gaps (SD_B of X_{POST} 0.5 mm), and in the remaining patients the standard deviations were in the range of 0.7- 3.0 mm compared with mean X_{POST} gaps of 10.3 and 13.3 mm, respectively.

From the statistics in Table 2.2, it becomes apparent that although there is measurable breathing motion of the vocal cords, the intra-fraction variation in the gap widths is small compared with the average gap width. Furthermore, the

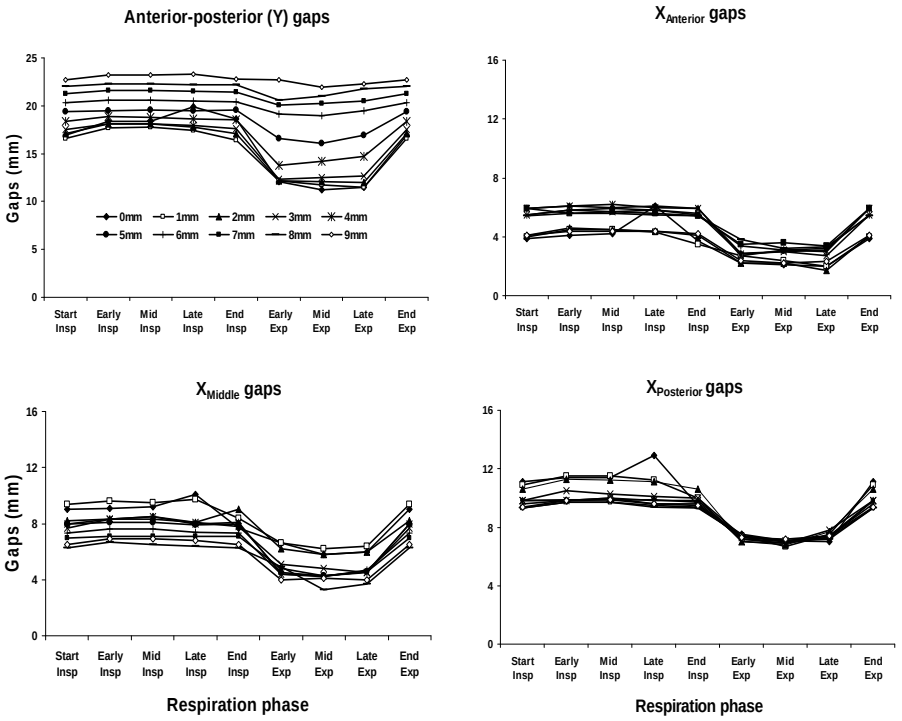

Figure 2.4: *Measured vocal cords dimensions (figure 2.2) for patient 2 in 10 axial slices with visible vocal cords, as a function of the respiration phase. 0 mm corresponds to the most superior and 9 mm to the most inferior slice.*

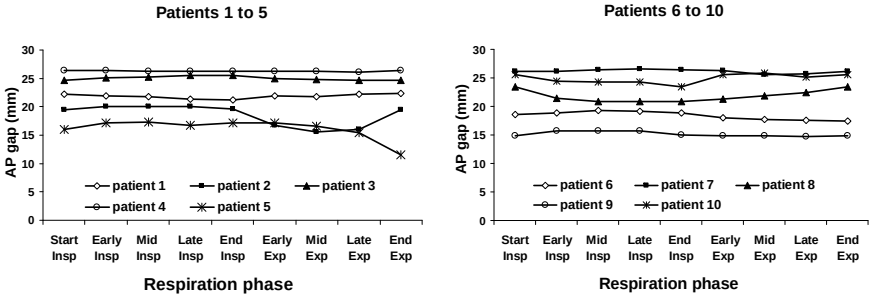

Figure 2.5: *For all patients, anterior-posterior gaps (Y) averaged over the slices with visible vocal cords shown as a function of breathing phases.*

cranio-caudal motion has an average $SD_B < 1mm$. The very limited observed respiratory motion is also illustrated in [figures 2.5 and 2.6].

2.4 Discussion

We are developing a new irradiation technique to treat early glottic carcinoma. Single vocal cord irradiation and sparing of the non-involved cord might help preserving the voice. Our main concern is to safely irradiate a single vocal cord with proper target coverage and simultaneously effectively spare the healthy vocal cord and the surrounding tissues, muscles and cartilages. In cases of no lymph node or anterior commissure involvement, the tumor volumes are usually very localized. In addition, the vocal cords are well visible in CT images being surrounded by the well-defined thyroid cartilage and the air gap which makes it possible to define the CTV clearly. Apart from voice preservation, SVCI will potentially allow re-irradiating recurrent tumors that are usually treated with total or partial laryngectomy and more recently with laser surgery [99, 84, 54]. In the treatment of recurrences the extent of the recurrent tumor after RT is difficult to assess so the surgical margins are usually taken generously. Having the option of re-irradiating these tumors might therefore improve the QoL and voice outcome for these patients in comparison with surgical options.

As a first step in realizing SVCI, we have used 4D-CT to assess respiratory vocal cord mobility. For each patient, vocal cord motion was measured using axial CT slices with visible vocal cord ($7 - 10$ slices, depending on the patient, slice thickness 1 mm). For patient 2, an overview of all obtained data is presented in figure 2.4. This figure shows smooth curves with gradual changes when going from one slice to the next (e.g., figure 2.4, upper left panel). Similar results were obtained for all patients, underlining the validity of the applied 4D-CT procedure for accurate motion measurement.

We have demonstrated that respiration induced intra-fraction motion of vocal cords is small compared with the distance between the vocal cords. Maximum displacements of the vocal cords were observed in the lateral direction towards the back of the larynx (X_{POST}). The patient-average SD_B at this level was 1.3 mm while the corresponding average lateral gap width was 11 mm (Table 2.2). The SD_B values in Table 2 are a measure of the relative displacement of both vocal cords. Because of this, and because we did not correct for gap width measurement inaccuracies, these SD_B-values provide an overestimation of the lateral movement of a single vocal cord during normal respiration. The cranial-caudal movements of the cords are similarly small. The small respiratory cord mobility observed implies that SVCI with substantial sparing of non-involved structures will not be hampered by respiration. Moreover, feasibility of SVCI is unlikely to be enhanced significantly by using respiratory motion compensation techniques such as active breathing control [139], gating [51], or tumor tracking [113].

In an investigation of the laryngeal intra-fraction motion during radiotherapy,

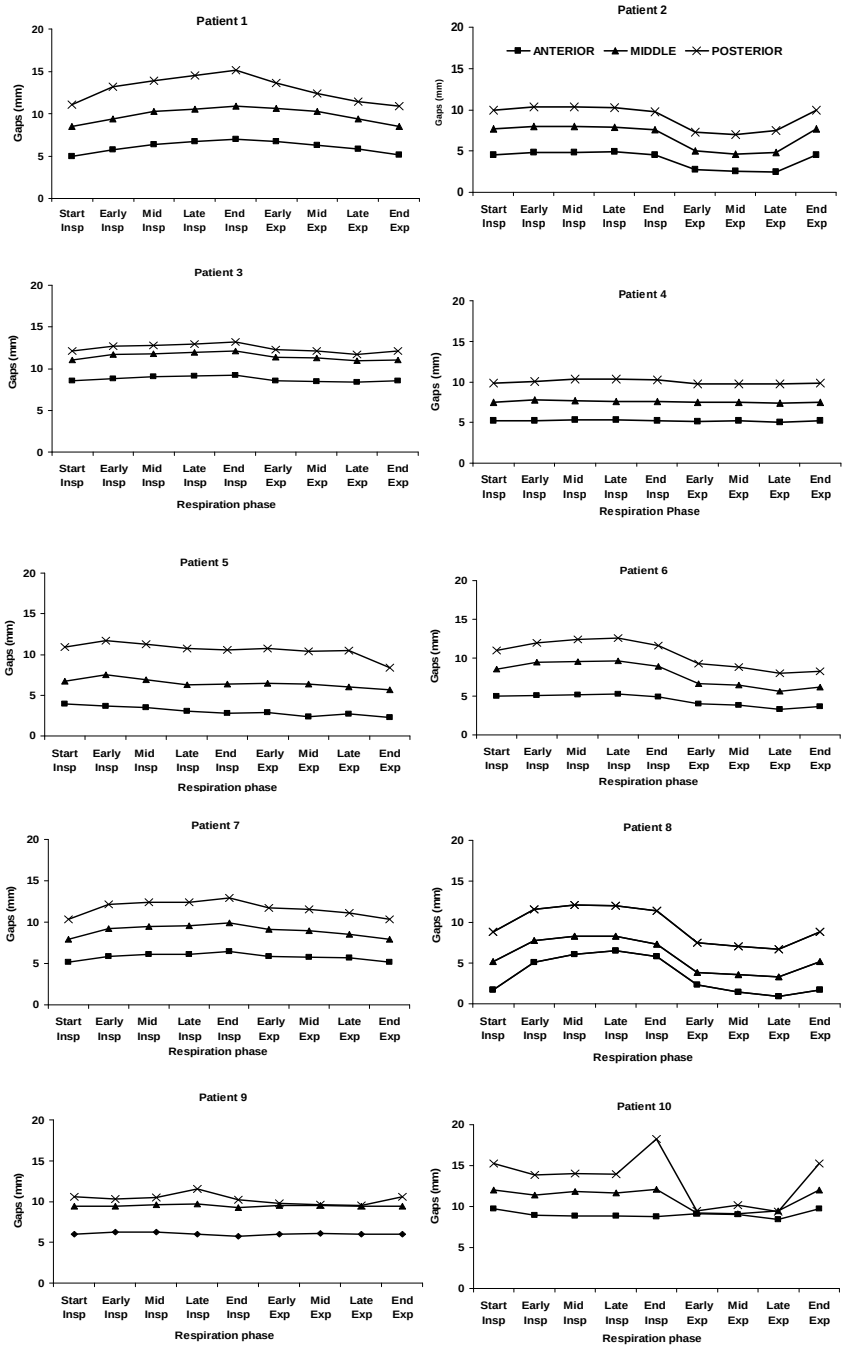

Figure 2.6: *For each patient, lateral gaps (X) averaged over the axial slices with visible vocal cords.*

Table 2.2: *Magnitude (in mm) of intra-fractional motion of the vocal cords relative to the thyroid cartilage as measured from 4D-CTs. The last two rows give the average values of the gaps for the entire population under study and also the inter-patient variations. For example, the mean $X_{POSTERIOR}$ gap width over the population is 11.0 mm and the inter-patient variations SD = 1.5 mm. In this case, the population standard deviation describing respiratory motion is $1.3 \pm 0.8mm$ (0.8 mm is the inter-patient variation).*

	$X_{ANTERIOR}$			X_{MIDDLE}			$X_{POSTERIOR}$			(Y)			(Z)
	Range	Mean	SD_B	Range	Mean	SD_B	Range	Mean	SD_B	Range	Mean	SD_B	SD_B
1	5.0-7.0	6.1	0.7	8.5-11.0	9.8	0.9	11.0-15.1	12.9	1.5	21.3-22.3	21.9	0.4	1.5
2	2.4-5.0	4.0	1.1	4.7-8.0	6.8	1.5	7.0-10.3	9.2	1.4	15.6-20.0	18.6	1.9	1.6
3	8.4-9.2	8.8	0.3	11.0-12.1	11.5	0.4	11.7-13.2	12.4	0.5	24.7-25.6	25.0	0.4	0.5
4	5.0-5.3	5.2	0.1	7.4-7.8	7.6	0.1	9.8-10.4	10.0	0.3	26.1-26.5	26.3	0.1	0.5
5	4.9-6.0	5.4	0.4	7.1-9.7	8.5	0.7	7.8-11.7	10.3	1.1	13.6-20.0	18.9	1.0	0.5
6	3.3-5.3	4.5	0.8	5.7-9.6	7.9	1.6	8.0-12.5	10.4	1.8	17.5-19.2	18.4	0.7	0.5
7	5.2-6.5	5.8	0.4	7.9-9.9	9.0	0.7	0.4-12.4	11.7	0.9	25.6-26.6	26.2	0.4	0.5
8	0.9-7.2	3.5	2.3	3.5- 8.1	5.8	2.1	6.6-12.1	9.5	2.2	20.8-23.5	21.8	1.1	0.7
9	5.7-6.3	6.0	0.2	9.2-9.7	9.5	0.1	9.5-11.6	10.3	0.7	14.8-15.8	15.1	0.5	0.5
10	8.4-9.7	9.0	0.4	9.1-12.1	11.0	1.3	9.4-18.2	13.3	3.0	23.4-25.9	24.9	0.8	1.4
Population average		5.8	0.7		8.7	0.9		11.0	1.3		21.7	0.7	0.8
Inter-patient variation		1.8	0.6		1.8	0.7		1.5	0.8		3.9	0.5	0.5

van Asselen et al. [127] demonstrated that the incidence and total duration of swallowing is small compared with the typical treatment time (10-20 min). They conclude that it is not important to apply an internal margin to take these swallowing displacements into account. Furthermore, because this infrequent motion is also random, the impact on target coverage is small [123]. However, swallowing induced motion during acquisition of the planning CT scan may introduce significant systematic errors. Hence, swallowing must be prevented during the acquisition of the planning CT scan.

To safely irradiate a single vocal cord, random intra-fraction errors caused by internal organ motion, as well as other targeting errors must be controlled. Apart from target definition uncertainties, two of the main remaining sources of errors are (1) inter-fraction systematic and random positioning errors and (2) dosimetric errors due to the application of very small treatment fields and the air-tissue interface at the surface of the target volume. Obviously, these errors must be minimized to allow optimal sparing of the non-involved cord without loss of local control. To minimize both sources of error, we envision the following procedure for the preparation and execution of treatment.

In the preparatory phase a 4D-CT is acquired for each patient, using the methods described in this paper. Based on this 4D-CT scan, the average anatomy and deformation due to breathing motion will be assessed on an individual basis. Hence, although Table 2.2 describes the magnitude of variations to be expected clinically, we will not use population-based statistics to describe vocal cord motion. The results in this paper indicate typical SD_B values of 1 mm. When compared with the effective dosimetric margins that are already required to compensate for the penumbra width ('block margin'), for most patients the additional margin for these random motion errors is expected to be very small [38]. Apart from the intra-fraction respiratory motion, additional random errors will occur due to inaccuracies in the daily patient set-up. Because the latter errors cannot be completely corrected for even with daily CT guidance (see below), the relative contribution of the intra-fraction motion becomes even smaller. Consequently, the purpose of the 4D-CT scan is to get a good definition of the average anatomy to rule out systematic errors as well as to identify outliers in the population that show large breathing motion (e.g., patient 10 in Table 2). The CTV (vocal cord with tumor) in its average position will be expanded with margins to take into account the small residue systematic and random errors. Based on the average anatomy obtained from 4D-CT, a treatment plan will be created using beam angle optimization [24].

It has been reported that incidences of local failure after RT might occur due to the loss of electronic equilibrium at the air tissue interface that results in underdosage of the tumor [120, 3, 94]. Therefore, caution must be applied to prevent tumor underdosage. We will therefore calculate the dose in each breathing phase of the 4D-CT data for SVCI patients using a Monte Carlo dose engine to verify and, if necessary, adapt the treatment plans.

In daily treatment execution, cone beam CT (CB-CT) scans are already being

obtained and on-line corrections will be applied. At present we are performing an analysis of the accuracy of automatic (CT value based) registration for various structures of interest to develop a valid on-line procedure for SVCI. This procedure will be applied in combination with a system that is already in clinical use for precise remote execution of on-line corrections driven by the imaging software [81]. The results of this study on optimal on-line corrections for SVCI will be the subject of a future paper.

2.5 Conclusions

The department of Radiation Oncology of the Erasmus Medical Center has initiated a program to investigate single vocal cord irradiation, aiming at improved voice quality, and also to allow re-irradiation. As a first step, for 10 patients the vocal cord breathing motion was assessed using 4D-CT scans. Observed standard deviations describing this motion around the mean position were generally small (on average 1 mm) compared to the separation between the vocal cords. Therefore, if 4D-CT is used to establish the average position of the cords and their respiratory motion, planning margins required for internal cord motion are small (<1 mm) compared to the average vocal cord opening. Consequently, single vocal cord irradiation is not hampered by respiratory motion.

Chapter 3

On-line Cone Beam CT Image Guidance for Vocal Cord Tumor Targeting

Sarah O.S. Osman, Hans C.J. de Boer, Eleftheria Astreinidou, Anne Gangsaas, Ben J.M. Heijmen, and Peter C. Levendag

Published in Radiotherapy and Oncology. Volume 93, Issue 1. Pages: 8-13. October 2009

Abstract

Background and Purpose: We are developing a technique for highly focused vocal cord irradiation in early glottic carcinoma to optimally treat a target volume confined to a single cord. This technique, in contrast with the conventional methods, aims at sparing the healthy vocal cord. As such a technique requires sub-mm daily targeting accuracy to be effective, we investigate the accuracy achievable with on-line kV-cone beam CT (CBCT) corrections.

Methods and Materials: CBCT scans were obtained in 10 early glottic cancer patients in each treatment fraction. The grey value registration available in X-ray volume imaging (XVI) software (Elekta, Synergy) was applied to a volume of interest encompassing the thyroid cartilage. After application of the thus derived corrections, residue displacements with respect to the planning CT scan were measured at clearly identifiable relevant landmarks. The intra- and inter-observer variations were also measured.

Results: While before correction the systematic displacements of the vocal cords were as large as $2.4 \pm 3.3mm$ (cranial-caudal population mean $\pm SD\Sigma$), daily CBCT registration and correction reduced these values to less than $0.2 \pm 0.5mm$ in all directions. Random positioning errors (SD σ) were reduced to less than $1mm$. Correcting only for translations and not for rotations did not appreciably affect this accuracy. The residue random displacements partly stem from intra-observer variations ($SD = 0.2 - 0.6mm$).

Conclusions: The use of CBCT for daily image guidance in combination with standard mask fixation reduced systematic and random set-up errors of the vocal cords to $< 1mm$ prior to the delivery of each fraction dose. Thus, this facilitates the high targeting precision required for a single vocal cord irradiation.

3.1 Introduction

Early stage glottic squamous cell carcinomas (SCCs) are usually confined to the glottic area; as the true vocal cords essentially have no lymphatic vessels these tumors are known to be highly localized [75, 138]. It is also known that these cancers are normally limited to the mucosa without the involvement of the underlying muscles due to the presence of Reinke's space (superficial lamina propria) [97]. It is a highly curable disease; therefore the aim of the treatment is to cure with the best achievable functional results [56]. Radiotherapy is usually the treatment of choice for these tumors [93]. Considering current developments in the field of RT (e.g. IGRT techniques), using conventional conservative irradiation techniques with large treatment fields is likely to be sub-optimal. At our institute a new optimized radiotherapy technique to treat Tis and T1a tumors confined to one vocal cord is under development. The goal is to deliver a highly conformal dose to the tumor, with the clinical target volume (CTV) confined to one vocal cord, while minimizing radiation damage to the other vocal cord and the surrounding cartilages and muscles. We designate this highly focused irradiation technique single vocal cord irradiation (SVCI). Our hypothesis is that maximally sparing the non-involved vocal cord might improve voice outcomes after RT [1, 26]. In addition, Levendag et al. found a dose-effect relationship between dose to swallowing muscles and dysphagia complaints [62]. In order to improve post radiotherapy QoL, they recommended that precautions must be taken to limit dose received by the swallowing muscles [62, 124]. Furthermore, for laryngeal preservation, delivering a more conformal dose might allow re-irradiating the tumors if the need arises in the future due to a regional recurrence or growth of a second primary tumor in the same vicinity.

To maintain high tumor control probability in SVCI, a number of issues regarding the dose delivery should be fully investigated and controlled, i.e. (1) intra-fractional motion due to breathing and swallowing, (2) inter-fractional position variations and (3) dosimetric accuracy of the highly localized dose distributions. In an earlier investigation on issue (1), we found that respiration-induced intra-fractional movements of the vocal cords are very small and do not obstruct SVCI [93]. What is more, it was found that the incidence and duration of swallowing were low in comparison with treatment times [127, 98]. However, swallowing must be prevented during planning CT acquisition to avoid the introduction of large systematic errors. This paper addresses issue (2) using kilo-voltage cone beam (CBCT) scans to track daily set-up variation in six dimensions (three translational and three rotational) in prospectively enrolled laryngeal cancer patients receiving conventional radiotherapy treatment. We investigate and validate the use of the commercially available X-ray volume imaging software (Elekta Synergy XVI release 3.5b147) for vocal cords positioning and calculate the residual positioning errors after using automatic grey-value-based registration of localization to reference planning CT scans and on-line corrections. The goal is to quantify the residue systematic and random set-up

errors, when an on-line correction protocol is used. These residual errors are used to assess the safety margins needed around the CTV volumes from the statistics of the population under study.

3.2 Methods and Materials

3.2.1 Patients

Ten patients receiving conventional treatment for glottic cancer were analyzed in the context of this study after having given informed consents. For each patient, a 3D planning CT scan was acquired using a multi-slice CT scanner (SOMATOM Sensation Open, Siemens Medical Solutions) with 2.5 mm slice thickness. Patients were instructed not to swallow during the CT acquisition as part of our scanning protocol. The 3D planning CT image was then exported to the XVI system to be used as a reference scan. These patients received doses of 66 Gy in 33 fractions using two laterally opposed photon beams on a 6MV linac (following the conventional treatment protocol). During the course of treatment, patients were immobilized using Posicast thermoplastic masks with five fixation points (CIVCO medical solutions) that were also used during planning CT acquisition.

3.2.2 Imaging system, CBCT acquisition, and 3D matching

Before each treatment fraction, cone beam CT scans were acquired on an Elekta Synergy treatment machine with an integrated kilo-voltage X-ray source. Using the standard "head-and-neck" protocol (100 kV, 36.1 mAs), with gantry angles $-100°$ to $+100°$ sets of 200 2D projections were acquired and 3D volumes were constructed ($1mm^3$ voxel size). A scan time of 1 min averaged out the small breathing motion of the vocal cords in the CBCT [93]. The imaging dose from each CBCT scan was measured to be approximately 1 mGy per scan (dose to the skin at the level of the larynx). This low dose has a negligible contribution to the patient dose compared to the treatment.

Although the image quality of the CBCT scans was inferior to that of the planning CT, they showed sufficient contrast for this study, see figure 3.1 and figure 3.2. A clipbox is defined around the thyroid cartilage containing the volume of interest (VOI) in the planning CT. This is done once by an observer before the start of the treatment fractions. Before each treatment fraction, the CBCT is then automatically registered to the planning CT using the grey value match function of the XVI software within, on average, 1 min. The registration is carried out using only voxels that are inside the 3D volume, defined on the planning CT scan by the alignment clipbox, based on a grey level correlation technique [46]. This method yields translations and rotations about the center of the alignment clipbox prior to each treatment fraction. The results of the automatic registration were always checked by an observer, visually verifying the matching quality of

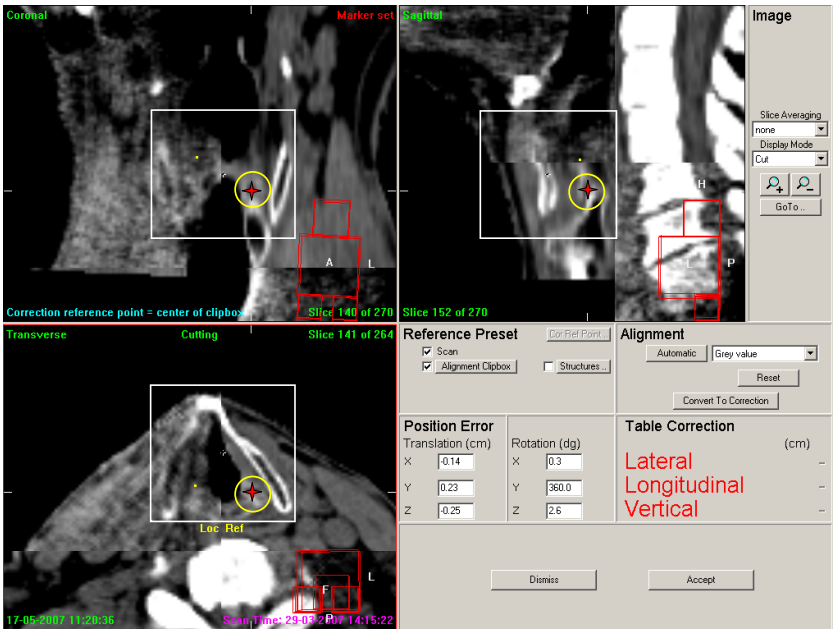

Figure 3.1: *Determination of the residual error in the position of the left arytenoid (indicated by the circle) after XVI automatic grey value matching. Each window shows a cut view of the localization and the reference CT scans.*

the bony structures (cartilages) inside and outside the VOI that is defined by the clipbox using checkerboard overlays. The positioning errors before applying registration-based positional corrections (i.e. initial set-up errors) are reported.

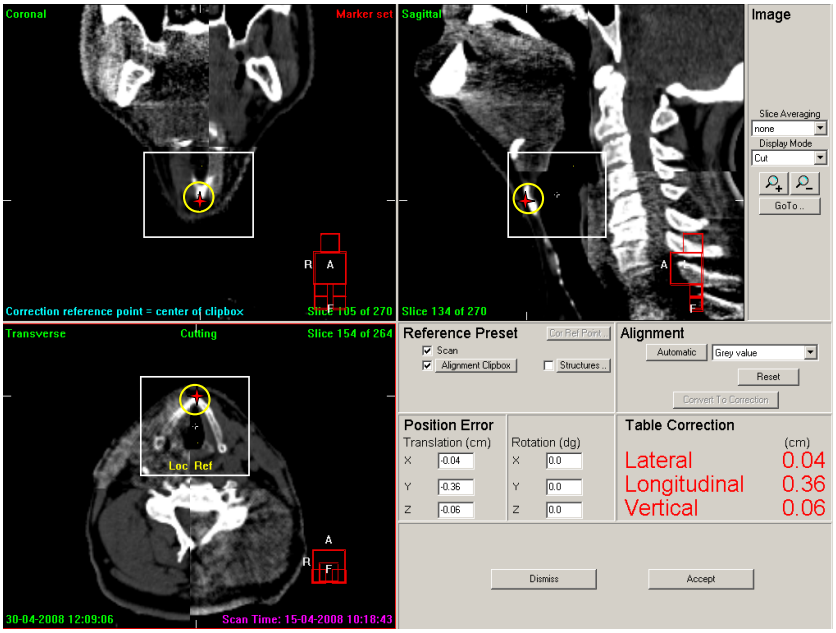

Figure 3.2: *Determination of the residual error on the position of the front node of the thyroid cartilage (indicated by the circle) after XVI automatic grey value matching and applying the translation only automatically derived correction (given by table correction values in the right lower panel).*

3.2.3 Accuracy achievable with CBCT on-line corrections

The translations and rotations obtained from the matches described above were applied to the CBCT scan. It is then possible to check point-by-point the coincidence of anatomic structures on both the planning and the CBCT scans and thus establish the accuracy that can be achieved with optimally executed on-line corrections based on XVI registration. To verify the quality of the registration for the vocal cords, the coordinates of three representative points encompassing the soft tissue region of interest were checked in each CBCT vs planning CT after registration. The anatomical reference points used were; the front node of the thyroid cartilage, and the centers of the left and the right arytenoids (see the red crosses in figure 3.1 and figure 3.2). The residual errors in the position of the center of mass (COM) of these points were calculated.

The residual inter-fractional positional variations were calculated for each

patient and for the entire population and are summarized here in the standard representation of systematic and random errors [123]. Residual average systematic errors (μ) in the in the cranial-caudal (CC), anterior-posterior (AP) and medial-lateral (ML) directions were calculated by determining the mean offset of COM of the vocal cords for each patient from all the fractions and calculating the average over all patients. The standard deviation (SD) of patient systematic errors around this mean is Σ. Population residual random errors (σ) were calculated as the average root-mean-square of individual random variations [123, 130].

In common practice, treatment couch shifts are applied to correct only the translational positioning errors (no rotations). The convert-to-corrections option in XVI calculates such translational table movements, which is ideally corrected at the correction reference point (center of alignment clipbox). We applied this translation-only correction also to the CBCT scans and measured the same residual errors for the anatomical landmarks as described above. Hence, the importance of the rotation corrections in SVCI can be established.

3.2.4 Intra-observer and inter-observer variations

We assessed intra-observer inaccuracies (SD $=\sigma_{Obs}$) introduced by the manual measurement of the anatomical landmarks coordinates by repeating the measurements five times independently in five patients (2 fractions for each patient) (50 measurements). Per fraction, the SD of the landmark 5 matches was obtained, and the average of the thus obtained 10 SDs yielded the estimated intra-observer measurement inaccuracy σ_{Obs}. In addition, the inter-observer variations in placing the clipbox around the VOI and consequently the reproducibility of the XVI-based corrections were tested for 5 patients (2 observers, 179 fractions) (SD = $\sigma_{Clipbox}$).

Table 3.1: *Positioning errors calculated from XVI matching results of the VOI for all the patients for all the fractions before applying the corrections.*

	Translations (mm)			Rotations (°)		
	μ_{Trans}	Σ_{Trans}	σ_{Trans}	μ_{Rot}	Σ_{Rot}	σ_{Rot}
ML	-1.3	1.6	1.3	0.7	1.5	1.4
CC	-2.4	3.3	2.6	0.8	1.2	1.7
AP	0.2	2.2	1.5	-0.4	1.5	1.1

3.2.5 Margins

Finally, to put the errors we found in this study into use, an estimation of the CTV-PTV margin is made using a standard margin recipe:

$$M_{PTV} = 2.5\Sigma + 1.64\sqrt{\sigma^2_{organmotion} + \sigma^2_{set-up} + \sigma^2_p} - 1.64\sigma_p$$

where $\sigma_{organmotion}$ and σ_{set-up} are the SDs of organ motion and set-up random errors, respectively, and σ_p is the SD describing the penumbra width ($\sim 0.3cm$ in water; 6 MV photon beams) [130, 118].

3.3 Results

3.3.1 Analysis of the CBCT-based on-line corrections

A summary of pre-correction positioning errors (translation and rotation) based on clipbox registration is presented in Table 3.1 (μ_{Trans}, Σ_{Trans}, σ_{Trans}, μ_{Rot}, Σ_{Rot}, σ_{Rot}). The largest errors were detected in the CC direction (μ_{Trans} =-2.4mm, Σ_{Trans}=3.3mm, σ_{Trans} =2.6mm, $\mu_{Rot} = 0.8°$, $\Sigma_{Rot} = 1.2°$, $\sigma_{Rot} = 1.7°$). In Table 3.2 we report the residual errors (μ, Σ, σ) calculated at the center of mass of the anatomically representative points if the thus obtained corrections would be executed, including rotations corrections. The largest errors observed were also in the CC direction (μ = -0.2 mm, Σ = 0.5 mm, σ= 0.7 mm). To give a better insight, a scatter plot of XVI detected positioning errors (pre-correction) and the residual errors at the center of mass of the vocal cords (post-correction) is presented in figure 3.3. We have chosen to plot the positioning errors in the AP direction vs CC direction in 2D because the largest errors were continuously measured in the CC direction.

Apart from the accuracy obtained at the COM of the anatomical landmarks, the daily residual set-up errors at the front node of the thyroid cartilage and the centers of the left and right arytenoids are also relevant. In Table 3.2 and Table 3.3 they are given separately for all 10 patients in all the fractions. The data are shown here to give a general impression of how good is this clipbox-based automatic matching procedure for all the relevant structures.

Using the XVI function "convert to table shift", applies only translation positioning correction as explained in the material and methods section of this article. Population residual errors in set-up after applying translation corrections only (no rotation) are presented in Table 3.3. The accuracy is almost identical to the accuracy obtained when including rotation corrections. Once again, the largest residual errors were noticed in the CC direction (μ = 0.1 mm, Σ = 0.3 mm, σ = 0.8 mm).

3.3.2 Intra-observer and Inter-observer effects

The intra-observer inaccuracies (σ_{Obs}) introduced by the manual inspection of the coordinates at the COM were 0.2 mm, 0.6 mm, and 0.4 mm in the ML, CC, and AP directions, respectively, comparable to the observed random residue errors (Table 3.2 and Table 3.3).

The impact of the inter-observer variability in selecting a clipbox around the VOI, on the CBCT registration, yielded a population average SD $\sigma_{Clipbox}$ of 0.3

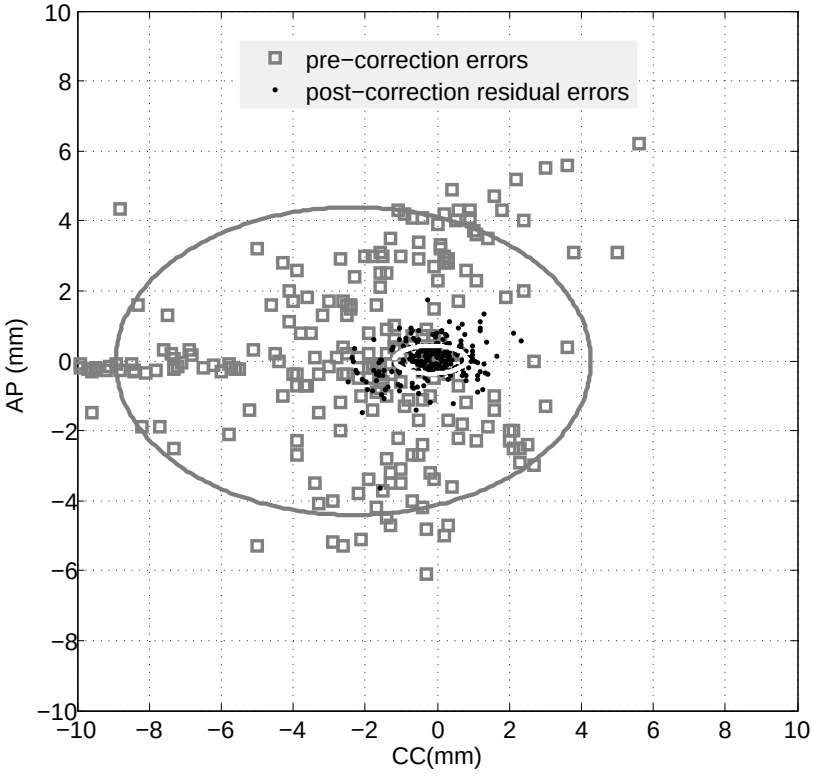

Figure 3.3: *Measured set-up errors of 10 patients in 264 fractions in the CC and AP directions before (grey squares) and after (black dots) applying corrections (translations and rotations). The grey and white ellipses indicate the mean systematic errors within* $\mu \pm 2\Sigma$ *intervals before and after applying the on-line corrections, respectively.*

Table 3.2: *Residual errors at the three representative structures spanning the vocal cords and at the COM of these structures after applying the XVI-based corrections (translations and rotations) calculated for all the patients for all the fractions,* $\sigma_{Corrected} = \sqrt{\sigma^2 - \sigma_{Obs}^2}$

.

mm	μ	Σ	σ	σ_{Obs}	$\sigma_{Corrected}$
ML					
Thyroid	0.0	0.1	0.5	0.1	0.5
R-arytenoid	0.0	0.1	0.6	0.3	0.5
L-arytenoid	0.1	0.1	0.5	0.3	0.4
COM	0.0	0.1	0.3	0.2	0.2
CC					
Thyroid	-0.2	0.5	0.8	0.4	0.7
R-arytenoid	-0.2	0.7	1.1	1.2	0.0
L-arytenoid	-0.1	0.6	1.1	1.0	0.5
COM	-0.2	0.5	0.7	0.6	0.4
AP					
Thyroid	0.1	0.3	0.6	0.3	0.5
R-arytenoid	0.0	0.3	0.7	0.7	0.0
L-arytenoid	0.0	0.5	1.0	0.5	0.9
COM	0.0	0.2	0.5	0.4	0.3

mm, 0.5 mm, and 0.3 mm along the ML, CC, and AP directions, respectively. The corresponding values for rotational errors were 0.7°, 0.8°, and 0.7° about the ML, CC, and AP axes, respectively.

Table 3.3: *Residual errors at the three representative structures spanning the vocal cords and at the COM of these structures after applying the table shift XVI corrections (translational only corrections)* $\sigma_{Corrected} = \sqrt{\sigma^2 - \sigma_{Obs}^2}$.

mm	μ	Σ	σ	σ_{Obs}	$\sigma_{Corrected}$
ML					
Thyroid	0.0	0.2	0.3	0.1	0.3
R-arytenoid	0.0	0.1	0.4	0.3	0.3
L-arytenoid	0.1	0.1	0.4	0.3	0.3
COM	0.0	0.0	0.1	0.2	0.0
CC					
Thyroid	0.2	0.6	1.2	0.4	1.1
R-arytenoid	0.2	0.7	1.0	1.2	0.0
L-arytenoid	0.1	0.4	1.0	1.0	0.0
COM	0.1	0.3	0.8	0.6	0.5
AP					
Thyroid	0.1	0.2	0.6	0.3	0.5
R-arytenoid	0.1	0.3	0.8	0.7	0.4
L-arytenoid	0.2	0.5	0.9	0.5	0.7
COM	0.1	0.2	0.5	0.4	0.3

3.3.3 Margins

For inter-fraction motion, we used the values given in this paper (Table 3.2), uncorrected for observer errors in order to give a conservative estimate of necessary margins. For intra-fraction motion, values were taken from our previously published work [93]. Respiratory-induced random positional deviations of one vocal cord (population based) were calculated assuming symmetrical movements of the two cords towards the midline ($\sigma_{Resp} = \frac{\sigma_{Resp_{tot}}}{\sqrt{2}}$) where σ_{Resp} and $\sigma_{Resp_{tot}}$ are the random error component of one cord movement and from both cords, respectively. This produces random errors of 0.7 mm, 0.8 mm, 0.5 mm in the ML, CC and AP, respectively. Using a single phase from the 4D-CT set that represents the tumor in its time-weighted mean position to plan the treatment, systematic error could be reduced to nearly zero and respiratory motion contribution to the margins will stem from purely random errors. Inserting these values of respiratory

induced and set-up errors into the margin recipe yields margins of 0.4 mm, 1.5 mm, and 0.6 mm in the ML, CC, and AP directions, respectively.

3.4 Discussion

In the present study, we look at inter-fraction motion of the volume of interest using daily CBCT scans. As set-up errors commonly observed in mask-fixed patients [48, 63, 71] are too large for SVCI, we also determined the positioning accuracy that can be obtained with on-line CBCT corrections. The results demonstrate the feasibility of positioning the cords using the described on-line procedure fast and accurately. The residual errors at the COM of the anatomical structures spanning the vocal cords are sub-mm in all three orthogonal directions.

The largest positioning errors both pre-correction and post-correction were observed in the cranial-caudal direction, see Table 3.1, Table 3.2 and Table 3.3. One possible reason is that the reference CT used to register the daily CBCT had 2.5 mm slice thickness. This might cause registration errors in that direction when dealing with small structures of dimensions that are comparable to the CT slice thickness. For clinical SVCI application, the latter slice thickness will be reduced to 1 mm, as allowed by current multi-slice CT scanners [93]. Furthermore, a reason for the relatively large pre-correction cranial-caudal errors (see figure 3.3) may be rooted in the registration of the breathing averaged CBCT scans to a multi-slice spiral CT scan that does not precisely reflect the breathing averaged position. This effect is not particularly relevant for this study as the final systematic errors are reduced to <1 mm by the on-line corrections. Nevertheless, in the clinical SVCI procedure this effect can be avoided by using the 4D-CT scans of patients to construct the breathing averaged positions.

The intra-observer measurement inaccuracies in determining residue errors were comparable to the actual values of the residue errors (see σ_{Obs} and $\sigma_{Corrected} = \sqrt{\sigma^2 - \sigma_{Obs}^2}$ in Table 3.2 and Table 3.3). In Table 3.2 and Table 3.3 more insight is given by reporting the residual errors at the individual anatomical points. These results demonstrate the small residual errors at these points especially after the correction for the intra-observer random variation $\sigma_{Corrected}$. This result indicates that the automatic matching method delivers appropriate corrections for the true volume of interest (vocal cords) and that measured residual errors might originate largely from observer introduced variability (in particular, the exact position of the arytenoids is not trivial to determine). Furthermore, it implies that the already small residue errors reported in this study will in actuality be even smaller (Table 3.1 and Table 3.2). In addition, it was found that with clear guidelines of which structures to include in the clipbox, the effects of inter-observer variation in choosing a clipbox around the VOI were negligible.

The automatic XVI registration of CBCT and planning CT scans was easy, fast and directly successful for nearly all cases. Moreover, the inter-observer variation in the placement of the clipbox around the VOI and its effect on the XVI-based

positional corrections was small ($\leq 0.5mm$). Nevertheless, for one of the patients in this study the grey value match of the last 15 fractions was not satisfactory. This could be explained from unusual large volumetric differences due to patient weight change between the planning CT and the CBCT scan as visually evident from the CBCT scans. In this case, we employed the automatic bone matching of the XVI system. Comparing the residues obtained from these bone-matched fractions with the first 15 fractions (grey-value-based) no significant difference was detected in the SD of residue positioning errors. This example illustrates that it is crucial to monitor the quality of all automatic registration results.

The small translational and rotational set-up corrections detected in this study (Table 3.2) as well as previously reported values for head-and-neck patients immobilized with thermoplastic masks [48, 43] indicate that the initial positioning reproducibility is sufficient to present a good starting point for on-line CBCT registration and corrections. As this study indicates, no special immobilization techniques seem to be required for SVCI as long as on-line 3D corrections can be performed and the fitting of the mask is monitored.

We aim at developing an external beam treatment technique for highly focused irradiation of only the involved vocal cord in early glottic carcinoma for which precision is a prerequisite. Such a single vocal cord irradiation (SVCI) requires advanced techniques to achieve the highest level of conformality possible to fully cover the CTV and simultaneously spare the surrounding structures. The required conformality is always perturbed by variations in organ position (both inter-fraction and intra-fraction) and in beam geometry and fluence delivery. Furthermore, for the very small treatment fields required and the proximity of the CTV to both air and cartilages high accuracy of the dose calculation and robustness of the dose distribution against geometrical variations is not trivial.

In a previous paper, we have assessed the intra-fraction motion of the vocal cords due to breathing using 4D-CT [93]. The intra-fractional breathing movements of the vocal cords were small compared to the gap size between them. Hence, the use of gating seemed not required to counter intra-fraction motion, but 4D-CT scans were useful to determine average organ positions and variations.

Having established the intra-fraction and inter-fraction geometrical delivery inaccuracies, and a method to reduce the latter to sub-mm range, we are now in position to develop an appropriate irradiation technique for SVCI. The full procedure will involve various levels of sophistication.

In a simple procedure we are presently developing for plan design, a 4D-CT scan is obtained from which an appropriate breathing averaged 3D scan is selected. Next, the population statistics we have obtained for the cord motion in regular breathing and CBCT on-line corrections may be applied to calculate CTV-PTV margins. Using the thus obtained PTV, a treatment plan can be created using small fields and (non-co-planar) beam angle optimization. We consider it a minimum requirement that thus calculated dose distributions are verified using Monte Carlo simulations. If necessary, the fluencies must be adapted until appropriate target dose is achieved. Finally, the thus obtained optimized plan

can be delivered using daily CBCT guidance as described in this paper.

For final clinical application, the approximate margin estimation provided by a margin recipe may be too limited. For instance, the recipe derived by van Herk et al. holds for ideal (isotropic) conformal dose distributions with a constant penumbra width along the entire PTV surface while the CTV can only translate and has dimensions » SD of the geometrical variations. For the irradiation of a small, longitudinal structure, partly surrounded by air as well as nearby cartilages, these assumptions obviously break down [6, 18]. Even if these assumptions hold, the margin recipe prescribes a margin that guarantees a minimum dose to the CTV of 95% of the prescribed dose in 90% of the patients. That may not be sufficient coverage to conserve the excellent local control now observed using generous fields. Although the recipe of Stroom et al. is based on clinical treatment plans, it suffers from similar drawbacks as the van Herk recipe.

For future work we therefore extend the method we recently developed for handling organ motion and deformation [21, 129] to design SVCI plans without reliance on a margin recipe. This method allows tracking voxels under all known geometrical uncertainties and performs dose accumulation in simulations of actual treatments. The dose in the voxels is accumulated over all known degrees of freedom to obtain effective delivered dose distributions [21]. Thus, the initial margin design can be evaluated, and margins tuned to the specific patient anatomy and motion patterns.

Another aspect that should be considered is the precision of our system in executing the required positioning corrections. In a previous study, Mutanga et al. reported that the precision of the Theraview Couch Set-up Assistant (TCSA) system used in our institute is 0.3 mm in all three directions [82]. Moreover, other intra-fraction errors, movements inside the mask especially for prolonged treatment [71, 8], are also a subject for investigation. In a new protocol of imaging laryngeal cancer patients in our institute, post-treatment CBCT scans are acquired to investigate and quantify the residual intra-fraction errors. To help reducing the latter errors more attention is paid to make best-fitting masks for positioning the patients and patients' weight changes during the course of treatment will be monitored.

3.5 Conclusions

On-line registration and correction using available CBCT acquisition and registration software can yield sub-mm systematic and random displacements for the vocal cords when combined with standard mask fixation. Thus, the high positioning accuracy required for single vocal cord irradiation may be achieved in a clinically feasible procedure. Estimated safety margins required to account for inter-fraction as well as intra-fractional set-up variations are small enough $(0.4 - 1.5mm)$ to spare the healthy vocal cord.

Chapter 4

IMRT for Image-Guided Single Vocal Cord Irradiation

Sarah O.S. Osman, Eleftheria Astreinidou, Hans C.J. de Boer,
Fatma Keskin-Cambay, Sebastiaan Breedveld, Peter Voet,
Abrahim Al-Mamgani, Ben J.M. Heijmen, and Peter C. Levendag

Published in the International Journal of Radiation Oncology Biology and Physics. ePub ahead of print, 2011

Abstract

Purpose: We have been developing an image-guided single vocal cord irradiation technique to treat patients with stage T1a glottic carcinoma. In the present study, we compared the dose coverage to the affected vocal cord and the dose delivered to the organs at risk using conventional, intensity-modulated radiotherapy (IMRT) coplanar, and IMRT non-coplanar techniques.

Methods and Materials: For 10 patients, conventional treatment plans using two laterally opposed wedged 6-MV photon beams were calculated in XiO (Elekta-CMS treatment planning system). An in-house IMRT/beam angle optimization algorithm was used to obtain coplanar and non-coplanar optimized beam angles. Using these angles, the IMRT plans were generated in Monaco (IMRT treatment planning system, Elekta-CMS) with the implemented Monte Carlo dose calculation algorithm. The organs at risk included the contra-lateral vocal cord, arytenoids, swallowing muscles, carotid arteries, and spinal cord. The prescription dose was 66 Gy in 33 fractions.

Results: For the conventional plans and coplanar and non-coplanar IMRT plans, the population-averaged mean dose $\pm$ standard deviation to the planning target volume was 67 $\pm$1 Gy. The contra-lateral vocal cord dose was reduced from 66 $\pm$ 1 Gy in the conventional plans to 39 $\pm$ 8 Gy and 36 $\pm$ 6 Gy in the coplanar and non-coplanar IMRT plans, respectively. IMRT consistently reduced the doses to the other organs at risk.

Conclusions: Single vocal cord irradiation with IMRT resulted in good target coverage and provided significant sparing of the critical structures. This has the potential to improve the quality-of-life outcomes after RT and maintain the same local control rates.

4.1 Introduction

The ultimate goal of radiotherapy (RT) is the total eradication of tumors while minimizing the toxicity to the surrounding healthy structures. In early glottic carcinoma treated with RT, large box fields, using wedged parallel opposed photon beams, have been used conventionally. The tumor-free contralateral vocal cord, arytenoids, thyroid cartilage, and all muscles responsible for opening and closing the vocal cords receive the full dose of 66 Gy. In this conventional method, the swallowing muscles, carotid arteries, thyroid gland, and thyroid and cricoid cartilages among other structures, are partly in field. Exposure of these structures to high radiation doses (fully or partially) could lead to an increased probability of complications that negatively influence the quality of life of these patients. Typical complications have involved voice/speech impairment, diet problems (swallowing, trismus), arytenoid edema, an increased risk of strokes, and reduced treatment options for previously irradiated patients [26, 100, 104].

Very good local control rates have been obtained with simple parallel opposed beams used conventionally. However, efforts should be made to reduce the dose received by the tumor-free laryngeal structures to reduce the radiation-related complications in this group of patients. Reducing the dose received by the organs at risk (OARs) might also help in increasing the treatment options for patients with second primary tumors in the vicinity of the treated tumor. In patients with successfully treated Stage T1a glottic cancer, the incidence of the development of a second primary tumor (commonly in the upper aerodigestive track) at 5, 10, and 15 years was reported to be 23%, 44%, and 48.7%, respectively [83]. Given the large radiation treatment fields presently used for these patients, those second primary tumors have usually been treated surgically with generous surgical margins that significantly deteriorate the patients' quality of life after treatment [114].

At the Erasmus Medical Center, we have been developing a new focused irradiation technique for early glottic cancer. The introduction of a new technique brings with it the responsibility of investigating, testing, and verifying all aspects of the RT process. The geometric uncertainties must be reduced and the residual uncertainties accounted for by ensuring adequate safety margins for treatment planning. Accurate dose calculation and treatment delivery are also crucial.

In a previous study, we investigated and quantified the intrafraction respiratory motion of the vocal cords using four-dimensional computed tomography (CT) scans. It was found that the movement of the vocal cords with breathing is minimal [93]. In another study, it was shown that it is possible to reduce the interfraction setup errors to submillimeter values using cone beam CT scans in an on-line correction protocol [92].

In the present study, we compared the tumor dose coverage and dose delivered to the OARs using conventional parallel opposed fields with dose delivery using computer-optimized coplanar and non-coplanar beam setups and intensity-modulated beam profiles. The dose calculations were performed using a Monte

Carlo (MC)-based treatment planning system (TPS).

4.2 Methods and Materials

4.2.1 Patients, planning CT scans, and delineations

Ten patients who had been conventionally treated for early-stage glottic carcinoma (Stage T1aN0M0) were included in the present study. All patients had undergone four-dimensional CT scanning (Somatom Sensation Open, Siemens Medical Solutions, New York, NY) before treatment, reconstructed in eight breathing phases. The CT resolution was $1 \times 1 \times 1 mm^3$. For each patient, the reconstruction representing the local anatomy in its average respiratory position was used for planning. The OARs contoured were the contralateral (CL) vocal cord, arytenoids, swallowing muscle at the level of the vocal cords (inferior constrictor muscles [ICM], ipsilateral and CL strap muscles), carotid arteries, thyroid and cricoid cartilages, and spinal cord. The craniocaudal extensions of the contours for these OARs were the $C2$ and $C6$ vertebrae.

In Figure 4.1, an example of a Stage T1 tumor confined to one vocal cord is shown, as well as a schematic drawing of the delineation method used. The clinical target volume (CTV) was defined as the whole affected vocal cord as a conservative measure.

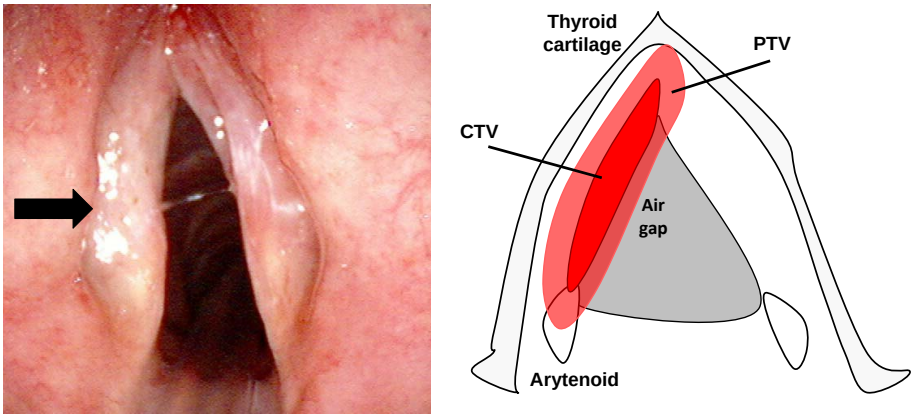

Figure 4.1: *(Left) Endoscopic photograph of tumor on one vocal cord and (Right) schematic drawing showing delineations of clinical target volume (CTV) and corresponding planning target volume (PTV)*

4.2.2 Margins

In line with the International Commission on Radiation Units and Measurements recommendations, a planning target volume (PTV) was constructed around the CTV. A standard margin formula was used:

$$M = 2.5\Sigma_{tot} + 1.64\sigma_{tot} - 1.64\sigma_p,$$

where $\Sigma_{tot} = \sqrt{\Sigma^2_{\text{intrafraction}} + \Sigma^2_{\text{interfraction}}}$, σ_p is the standard deviation describing the penumbra width and $\sigma_{tot} = \sqrt{\sigma^2_{\text{intrafraction}} + \sigma^2_{\text{interfraction}} + \sigma_p}$ [130]. The mean penumbra width was $0.4cm$ (the smallest distance between the 95% and 50% isodose lines in the plans). Using the CT scan with the tumor in its average position for planning, the systematic respiratory error could be reduced to nearly 0, and the respiratory motion contribution to the margins stemmed from purely random errors. We included the uncertainties from the intrafraction respiration [93], and the residual interfraction setup errors (assuming on-line setup corrections to be performed), as measured and explained in our previously published study [92]. For prolonged treatment sessions ($\geq 15min$), the effects of the intrafraction setup errors might not be negligible and should be accounted for [45]. Nevertheless, it has generally been agreed that the magnitude of the intrafraction setup errors will be less than that of the interfractional setup errors [30]. In the present study, the intrafraction setup uncertainties were estimated to be equal to the interfraction uncertainties as a reasonable (upper limit) estimate. Using this procedure, margins of 0.5, 1.7, and $0.8mm$ in the mediolateral, craniocaudal, and anteroposterior directions were calculated. Given the 1 mm^3 resolution of the CT scan, practical margins of $2mm$ in three-dimensions were used for the present study.

4.2.3 Treatment plans

Conventional plans.

Conventional clinical treatment plans using two laterally opposed wedged photon beams were performed using the XiO TPS (version 4.33, Elekta-CMS). The superior border of the treatment fields was the hyoid bone, and the inferior border was the lower edge of the cricoid cartilage. The fields were $1cm$ "falling off" anteriorly, and the posterior border was at the anterior vertebrae [52]. The prescribed dose to the "box" outlined by the treatment fields was 66 Gy at the 100% isodose, given in 33 fractions at six fractions weekly. The dose was calculated using the fast superposition algorithm in XiO.

Design of IMRT plans and optimization procedure.

An in-house-developed IMRT/beam angle optimization algorithm (iCycle) was used to obtain the beam angles for each patient using a set of standardized

Table 4.1: *Wish list used in iCycle showing constraints and objectives used in optimization*

Constraints			
	Volume	Type	Limit (Gy)
	PTV	Minimum	63
	PTV	Maximum	68
	Spinal Cord	Maximum	45
	Unspecified Tissue	Maximum	70
Objectives			
Priority	Volume	Type	Goal (Gy)
1	CL vocal cord	Mean	30
2	CL arytenoid	Mean	50
3	IL arytenoid	Mean	66
4	ICM	Mean	26
5	Unspecified Tissue	Minimize EUD	10

Abbreviations: PTV = planning target volume; CL = contralateral; ICM = inferior constrictor muscles; EUD = equivalent uniform dose

constraints and objectives [110]. iCycle uses a list with constraints and prioritized objectives (a "wish list" for beam angle optimization (Table 4.1). The constraints were hard and must be fulfilled at all times. The objectives were processed in priority. The highest prioritzed objective was to minimize the mean dose to the CL vocal cord to an acceptable level of 30 Gy (i.e., its "goal"). The second priority was to minimize the mean dose to the CL arytenoid to an acceptable level of 50 Gy, and so forth for the ipsilateral arytenoid, ICM, and unspecified tissue. The list was processed in 2 phases. In the first phase, it sought to attain the goals as well as possible. In the second phase, the objectives for which the goal could be attained were minimized to their fullest. From this wish list, iCycle sequentially adds beams to the plan to a maximum of five beams.

The optimized iCycle beam angles were then imported into the Monaco TPS, version 1.00 (Elekta-CMS) to generate plans with a MC dose calculation algorithm. In the Monaco TPS, the plans were configured using biological and physical constraints [42, 126, 111]. For the PTV, a Poisson cell kill model was used combined with a quadratic overdose constraint to avoid hot spots inside the PTV. For the CL vocal cord and the spinal cord, serial complication models were used to limit the maximal dose to both structures. Quadratic overdose constraints were also applied to limit the dose to unspecified tissue. The beams were then segmented, and their weights were optimized in the second optimization phase using a photon MC dose engine (XVMC) based on the voxel MC code [32].

All calculations for the IMRT plans were done for 6-MV photons with a calculation grid spacing of 1.5 mm. The accelerator used was an Elekta Synergy with 40 multileaf collimator leaf pairs, and the leaf width at the isocenter was

4 mm (Elekta Beam Modulator, Elekta Oncology Systems, Crawley, UK). The minimal segment size allowed was 0.5 cm^2. The isocenter was set to the center of the CTV. The dose prescribed to the PTV was 66 Gy, given in 33 fractions (six fractions weekly) using the clinical fractionation scheme. The PTV partially consist of air. No dose was deposited in that part of the PTV. The Monaco TPS feature "auto flash" creates a flash margin of the voxels that extends beyond the surface of the patient (into the air cavity in this case) so that the prescribed dose can be achieved. A "flash margin" of 2 mm around the PTV was used in planning. Thus, dose coverage was also provided for the moving vocal cord (CTV) in and out of the air gap during breathing and in the case of setup errors.

Plan evaluation

The population-averaged dose-volume histograms (DVH), mean doses, and, in some cases, maximal doses were used to evaluate and compare the different plans. For the CTV and selected OARs, the generalized equivalent uniform doses $[EUD(a)]$ [85] were calculated and compared for the different planning techniques. The values of the tissue-specific parameter a used for the CTV were $a = -5$ and $a = -20$, because no clear data are available about the values that should be used for these tumors. For the OAR, $a = 2.2$ was used, as recently recommended by Rancati et al. [100]. Statistical analysis was performed in MatLab using pairwise Wilcoxon signed-rank tests at a significance level of $p \leq .05$. Separate analyses were performed to compare conventional planning with the IMRT coplanar plans and to compare the IMRT coplanar and IMRT non-coplanar plans; no multiple comparison was performed. The fractional volumes of the PTV and CTV that received $\geq 95\%$ of the prescription dose were also reported. For the OARs, the population-averaged mean doses ($\pm$ standard deviation) and the maximal doses to the spinal cord and carotid arteries were reported. It has been recommended to keep the dose in the larynx less than ~ 66 Gy for vocal function preservation [100]. Therefore, the volume of the CL vocal cord that received $\geq 95\%$ of the prescribed dose or more was also reported. It has also been recommended to limit the mean dose to the non-involved larynx to 40 Gy, because the published data have indicated threshold doses of $40-45$ Gy for the onset of other functional complaints [100, 107]. Therefore, we have also reported the fraction of the volume of the CL vocal cord that received a dose of 40 Gy. Furthermore, the volume of the carotid arteries that received ≥ 35 Gy are also reported, because reports have been published of complications with carotid doses 35 Gy [104].

4.3 Results

4.3.1 iCycle optimized coplanar and non-coplanar beam angles

For each patient, a coplanar and non-coplanar set of optimized beam angles was obtained. The distribution of the iCycle beam angles for the 10 coplanar plans is

shown in figure 4.2 for tumors on the left vocal cord. Generally, anterior beams have been favored with a wide range of angles. The class solution beam angles used were indicated with asterisks. Non-coplanar iCycle optimized beam angles are presented in Table 4.2.

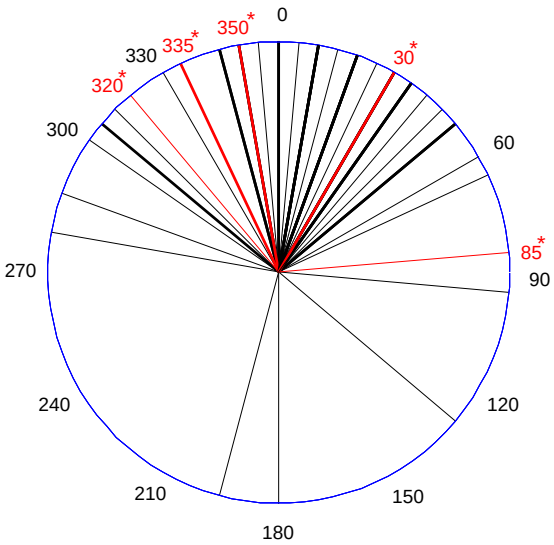

Figure 4.2: *iCycle coplanar beam distributions for left vocal cord tumor. Optimized angles for right side tumors have been mirrored for this representation. Thicker lines indicate directions chosen more than once. Class solution angles shown in red with asterisk.*

4.3.2 Conventional technique vs. coplanar and non-coplanar IMRT

The beam setups obtained with iCycle were used to plan the treatments in the Monaco TPS. Because of the observed similarity in the selected beam angles for the patients (fig 4.2), we selected one set of five beam angles and tested whether this could be used as a class solution for all patients. This could serve for the simplicity and standardization of treatment delivery in practice. For patients with tumor on the left vocal cord, beam angles of 30°, 85°, 320°, 335°, 350° were used. For those with right vocal cord tumors, mirrored angles were used. Figure 4.3 shows the comparisons between doses received by the different structures, using the individualized beam arrangement and the class solution. No significant differences in the delivered doses to the different structures were observed (all

Table 4.2: *iCycle individualized non-coplanar beam arrangements*

Beam	1	2	3	4	5
P1 (Left)	330, 0	15, 270	54, 341	319, 352	337, 333
P2 (Left)	345, 0	344, 289	334, 37	37, 343	329, 10
P3 (Left)	33, 22	342, 56	339, 346	27, 22	330, 0
P4 (Right)	23, 333	18, 56	36, 351	323, 17	54, 341
P5 (Right)	16, 342	344, 289	37, 17	313, 346	34, 333
P6 (Right)	15, 0	344, 71	30, 31	296, 17	49, 340
P7 (Right)	23, 333	0, 0	36, 9	301, 18	27, 22
P8 (Right)	16, 342	15, 90	26, 12	306, 19	22, 315
P9 (Right)	10, 0	44, 338	15, 270	284, 5	18, 34
P10 (Right)	25, 0	344, 71	36, 9	284, 5	26, 323

Abbreviation: P = patient.
Data presented as (gantry, couch) angles; gantry and couch rotate clockwise.

$p > 0.05$). This could have been a result of the degeneracy of the solution space [110, 73]. Although not significant, the class solution seemed to result in somewhat better sparing for some OARs. This could have resulted from the different dose calculation algorithms used; the pencil beam algorithm without adequate MLC segmentation in iCycle in which optimized IMRT beam angles were generated, and in Monaco, with a MC-based dose engine and full MLC segmentation. For the sake of simplicity, all the following results for coplanar IMRT plans were produced with the proposed class solution. For non-coplanar plans, the individualized beam angles, as obtained using iCycle (Table 4.2), were planned in Monaco, because it was more complicated to cluster the beam and couch angles.

Figure 4.4 shows the dosimetric comparisons among the conventional, coplanar IMRT, and non-coplanar IMRT plans. Comparing the conventional plans with the IMRT coplanar plans, similar mean doses to the CTV (p = 0.2) and PTV ($p = 0.1$) were obtained with both techniques. Furthermore, almost all OARs (CL vocal cord, CL arytenoid, carotid arteries, ICM, thyroid, cricoid, and strap muscles) were significantly spared with the IMRT plans compared with the conventional plans (all $p = 0.002$, except for the ipsilateral carotid arteries $p = 0.004$). The PTV extended to partially cover the ipsilateral arytenoids. Accordingly, doses similar to the conventionally delivered doses were achieved using IMRT ($p = 0.4$). Compared with coplanar IMRT, only the CL arytenoid was spared more when using non-coplanar beams ($p = 0.01$).

For coplanar IMRT plans, the smallest field size was $2 \times 2.5cm^2$, and each plan had on average four segments/beam. The average number of monitor units required to deliver the dose was 441 ± 81. Similarly, for non-coplanar plans, an average of four segments/beam was used, and the smallest field size was $2 \times 2cm^2$. The average number of monitor units was 509 ± 145.

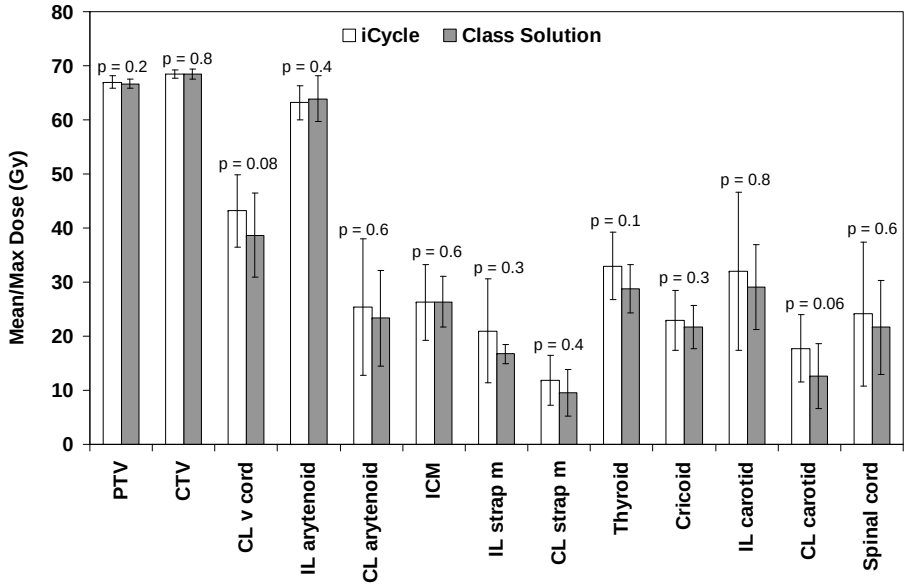

Figure 4.3: *Mean/maximal doses to different structures from coplanar individualized (iCycle) beam angles and for class solution. For carotid arteries and spinal cord, maximal doses shown. Error bars represent ± standard deviation. p Values shown for Wilcoxon signed-ranked tests for individualized beam setups vs. class solution doses. CL = contralateral; v = vocal; IL = ipsilateral; m = muscle.*

In figure 4.5, a typical example of the dose distributions of a conventional plan and IMRT coplanar and non-coplanar setups are shown for 1 patient. The superiority of single vocal cord irradiation (SVCI) is clearly visible. This was also evident in figure 4.6, in which the population mean DVHs for the different planning techniques are presented.

For the CTV, CL vocal cord, and the arytenoids, the EUD mean values (± standard deviation) obtained from the different planning techniques are presented in Table 4.3. The data show substantial and statistically significant sparing of the CL vocal cord and CL arytenoid for SCVI with IMRT. The $EUD(-5)$ and $EUD(-20)$ for the CTV were slightly (but statistically significantly) elevated in the IMRT plans compared with the conventional plans, showing that the large reduction in OAR doses with IMRT could be obtained while also giving a slightly greater dose to the CTV. Several dose-volume parameters for the CTVs and the contralateral vocal cord are listed in Table 4.4. The percentage of the CTV receiving $\geq 95\%$ of the dose was, for all plans, $\geq 99\%$. Only 86% and 88% of the PTV received $\geq 95\%$ of the prescribed dose in the coplanar and non-coplanar plans (see PTV DVH in figure 4.6). This is due to the fact that the PTV extends

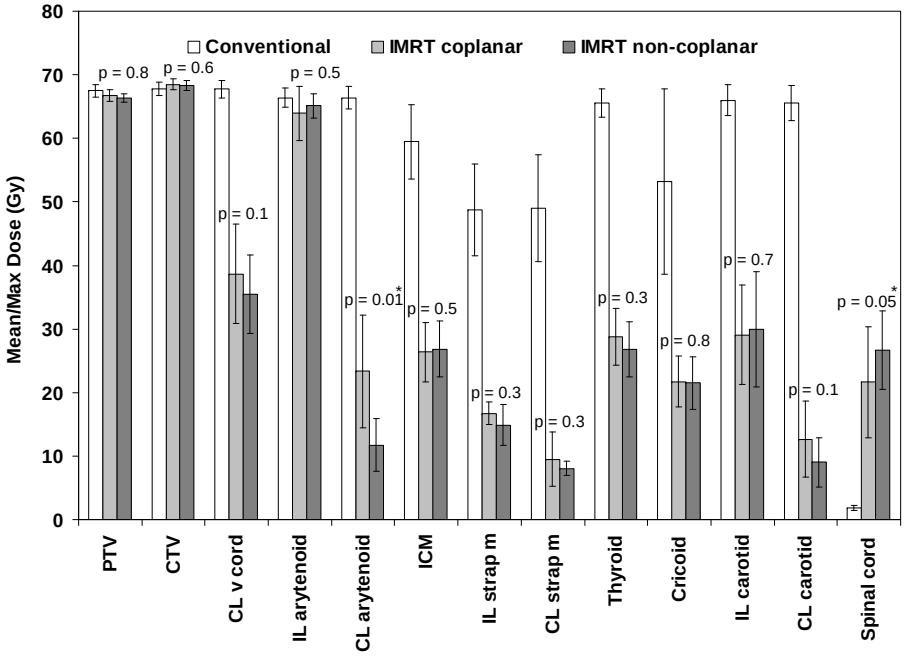

Figure 4.4: *Delivered doses for planning target volume (PTV) and organs at risk (OARs) from conventional and intensity-modulated radiotherapy (IMRT) coplanar and non-coplanar plans. For carotid arteries and spinal cord, population average maximal doses shown. For other structures, mean doses depicted. Error bars represent ± standard deviation. p Values shown for Wilcoxon signed-ranked tests for doses delivered using IMRT coplanar vs. non-coplanar beam setups. CL = contralateral; v = vocal; IL = ipsilateral; m = muscle. *Statistically significant.*

into the air gap of the larynx. Applying a flash margin (see the "Methods and Materials" section), similar fluences were deposited to the PTV (i.e., opening the leaves to conform to a virtual target). The whole CL vocal cord received $\geq 95\%$ of the prescribed dose in the current conventional plans; however, in the IMRT plans, only a small fractional volume received such high doses.

On average, the percentage of the volume of the carotid arteries that received a dose of ≥ 35 Gy in the clinical plans was 86% for the ipsilateral carotid and 92% for the CL carotid artery. However, a major reduction in the dose received to both carotid arteries was achieved using SVC IMRT because no parts of the arteries received any dose > 35 Gy (see also the maximal dose to the carotid arteries in figure 4.4 and the DVHs in figure 4.6.

Figure 4.5: *Transverse views at isocenter level for 1 patient showing dose distributions for (A) conventional, intensity-modulated radiotherapy (B) coplanar (class solution), and (C) non-coplanar plans.*

Table 4.3: *Generalized equivalent uniform dose parameters for different plans*

Variable	Conventional plans	IMRT coplanar	P^1	IMRT non-coplanar	P^2
CTV					
EUD(-5)	67.6 ± 1.0	68.6 ± 0.3	0.03*	68.3 ± 0.8	0.3
EUD(-20)	67.6 ± 1.0	68.4 ± 0.3	0.05*	68.0 ± 0.9	0.3
CL vocal cord					
EUD(2.2)	67.3 ± 1.0	41.2 ± 5.7	0.002*	40.2 ± 5.7	0.3
Ipsilateral arytenoid					
EUD(2.2)	66.2 ± 1.4	63.9 ± 3.9	0.3	65.1 ± 1.7	0.3
CL arytenoid					
EUD(2.2)	66.2 ± 1.7	22.1 ± 8.6	0.002*	12.6 ± 4.1	0.01*

Abbreviations: IMRT=intensity-modulated radiotherapy; CTV=clinical target volume; EUD=equivalent uniform dose; CL=contralateral.
[1] Conventional vs. IMRT coplanar plans.
[2] Coplanar vs. non-coplanar plans.
*Statistically significant.

4.4 Discussion

We have conducted a planning study for one-sided early glottic cancer to compare the conventional RT technique (using wedged parallel opposed fields) with highly focused IMRT. Although IMRT might not be necessary to control early-stage squamous cell carcinoma of the larynx, the added value of normal tissue sparing has made it clinically relevant. We found the dose received by healthy structures in the vicinity of targets can be significantly reduced with the proposed technique without compromising the target coverage ([Table 4.3] and [Table 4.4] and figure 4.4).

In the present report, we have proposed a class solution for coplanar beam angles to be used as a template for SVCI in the treatment of early-stage glottic

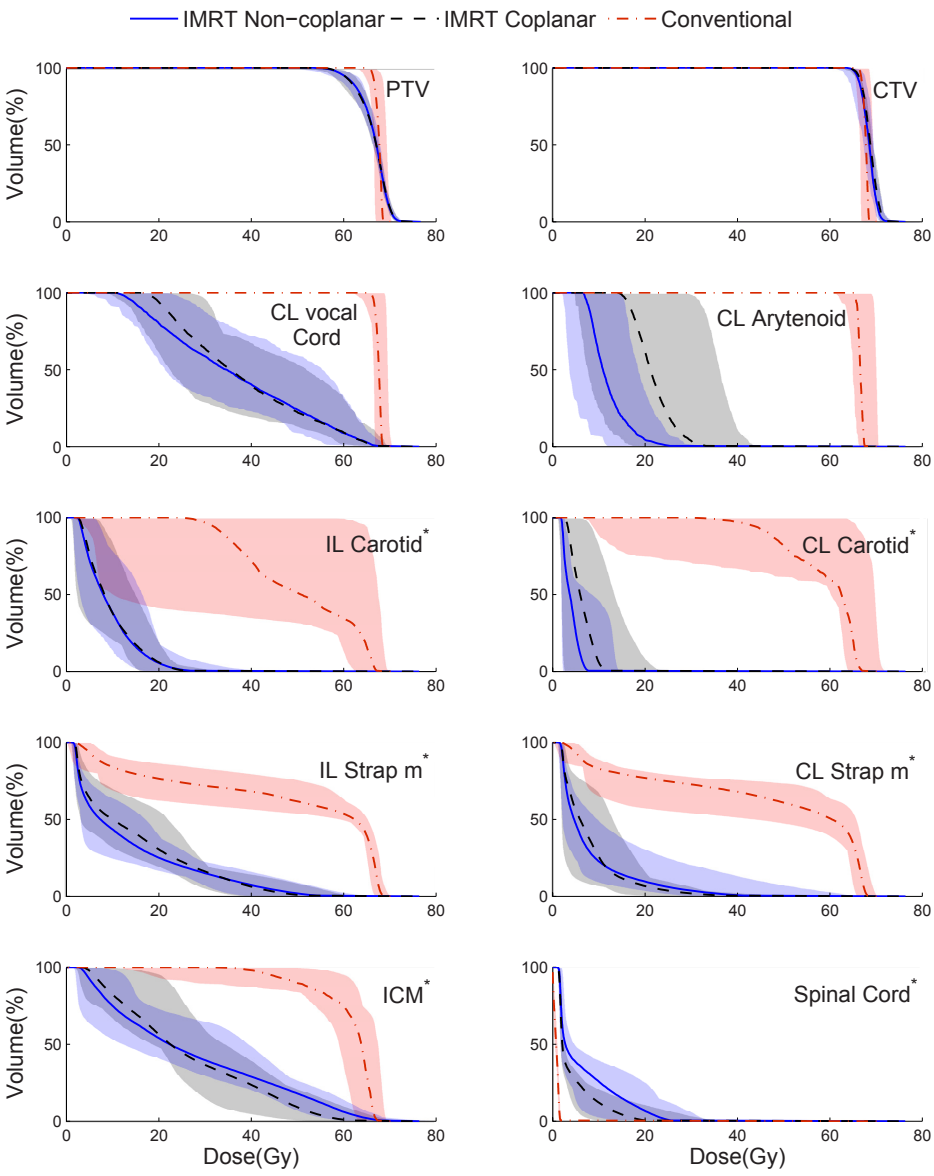

Figure 4.6: *Population mean dose-volume histograms from different planning techniques shown for selected structures. Shaded areas indicate ranges (population minimal and maximal dose-volume histograms). Asterisk indicates partially contoured organs at risk. CL=contralateral; IL = ipsilateral; m = muscle; ICM = inferior constrictor muscle.*

cancer. This class solution was derived from full IMRT/beam angle optimization for the patients in the present study using an in-house-developed optimizer. Comparing the dose parameters for the different OARs using the individualized plans with respect to the proposed class solution, little difference was found, suggesting that the class solution is a valid template (figure 4.3). Using this class solution will reduce the complexity and allow quicker plan generation compared with individualized beam setups. Adding non-coplanar beams resulted in little improvement in plan quality (figure 4.4). Having non-coplanar beams would significantly increase the treatment time compared with coplanar treatment. Moreover, it will introduce positioning difficulties that might not be justified by the small gain in OAR dose reduction.

As demonstrated in figure 4.4 and Table 4.3, SVCI results in major sparing of the CL vocal cord, CL arytenoid, ICM, strap muscles, thyroid and cricoid cartilages, and carotid arteries compared with conventional RT. For the ipsilateral arytenoid and anterior commissure, we allowed high doses (similar to that with the conventional plans) to avoid target underdosage. For the IMRT plans, the dose to the spinal cord increased with respect to the conventional plans but remained far below the specified limit of 45 Gy.

As mentioned in the "Methods and Materials" section, analysis of the target coverage using the PTV concept would be inaccurate for SVCI because of the air present in the volume. The use of the flash margin should guarantee proper target dose delivery in the case of motion. This is a topic for additional investigation.

Although RT was reported superior to laser surgery in terms of voice preservation, a number of studies have reported that the voice does not return to normal after RT [5, 22]. Other studies comparing laser surgery and RT as treatment options reported comparable local control and voice quality outcomes from the two treatment modalities [136]. These studies compared RT techniques using conventional "box" RT fields (with high doses to all structures included) with localized laser surgery. This provided a strong motive to hypothesize that more focused RT techniques could provide better results in terms of quality of life compared with laser surgery. It could also provide better local control among this group of patients by offering the potential for dose escalation. The increased sparing of the OARs might also allow the application of hypofractionation schemes to reduce the overall treatment time and increase patient comfort.

It has generally been agreed that reducing the doses to the laryngeal structures has the potential to reduce the complications related to RT (e.g., swallowing, speech, persistent edema) [26, 100, 4]. More recent studies have also highlighted the increased risk of strokes and direct carotid artery injury that could result from high-dose irradiation of the carotid arteries (usually 66 Gy) [104, 14]. Both groups showed a huge reduction of the dose to the carotid arteries when using IMRT for early glottic carcinoma, which was confirmed by our study. Limiting the dose to the carotid arteries might also allow re-irradiation when necessary.

Several groups have opposed the use of IMRT for early glottic cancer [74, 31]. Their main concern has been that the use of IMRT will compromise local control

Table 4.4: *Dosimetric parameters for CTV and contralateral vocal cord for different planning techniques.*

Variable	Conventional plans	IMRT coplanar	P^1	IMRT non-coplanar	P^2
CTV					
$V_{95\%}$					
Mean ± SD	100.0 ± 0.0	99.9 ± 0.2	1.0	99.6 ± 0.9	0.5
Range	$100 - 100$	$99.4 - 100.0$		$97.4 - 100.0$	
Median	100.0	100.0		100.0	
CL vocal cord					
$V_{95\%}$					
Mean ± SD	100.0 ± 0.0	8.1 ± 6.5	0.004*	8.5 ± 6.7	0.6
Range	$100.0 - 100.0$	$2.0 - 19.4$		$3.0 - 20.2$	
Median	100.0	5.8		6.3	
V_{40Gy}					
Mean ± SD	100.0 ± 0.0	39.9 ± 14.5	0.002*	38.0 ± 15.3	0.5
Range	$100.0 - 100.0$	$19.2 - 65.4$		$22.0 - 72.4$	
Median	100.0	38.5		34.0	

Abbreviations: $V_{95\%}$=fractional volume that received $\geq 95\%$ of prescription dose; SD=standard deviation; V_{40Gy}=volume receiving dose $\geq 40Gy$.
[1] Conventional vs. IMRT coplanar plans.
[2] Coplanar vs. non-coplanar plans.
* Statistically significant.

by failing to deliver adequate doses to a small primary cancer that conventional approaches cannot miss. Another concern has been the limitations of the calculation algorithms that can result in over- or underdosage at the tissue-air interface. Special attention should also be paid to the potential enhanced occurrence of second primaries with the small fields used in SVCI, because evidence has shown that RT might delay the occurrence of these second tumors [101].

All these valid points were carefully taken into consideration in the present study of SVCI. We have proposed that with the introduction of on-line image-guided RT and the availability of more accurate calculation algorithms in commercially available TPSs, the reduction of the treated volumes is a reasonable step to undertake. In contrast to all previous studies, we defined the CTV (the whole affected vocal cord) contoured on the CT scans with $1 - mm^3$ resolution. The intra- and interfractional setup errors have been thoroughly investigated, quantified, and reduced [93, 92]. Residual geometric errors were used to construct the CTV-PTV safety margins. The dose was calculated using MC in the Monaco TPS. The results in the present study indicated a tremendous reduction in the doses received by the OARs using the SVCI technique.

In preparation for the SVCI -IMRT technique we have introduced, studies on the dosimetry and dose modeling, especially in the buildup region, must be carefully conducted. In our clinic, some of the IMRT beams from the presented

plans were verified using a two-dimensional detector array [111]. Gamma analyses showed good agreement between the dose distributions calculated using the Monaco TPS and the measured distributions. Before the clinical introduction of this treatment, more extensive studies on the accuracy of the dose engine near tissue inhomogeneities will be conducted. SVCI should be considered an experimental technique that has yet to be clinically proven. We believe that SVCI should not be applied outside well-controlled clinical studies to prove its efficacy. The extremely high-treatment precision required can only be guaranteed with daily on-line image-guided RT protocols, advanced dose-calculation engines, and a very extensive quality assurance program conducted by experienced personnel.

4.5 Conclusions

Evidence was found that image-guided SVCI using IMRT can provide significant sparing of critical structures without compromising CTV coverage, thus offering the possibility of better voice and swallowing function preservation. A huge reduction in the maximal dose received by the carotid arteries was also observed. This has the potential to reduce the risk of stroke and might also allow re-irradiation (if the need arises because of second primaries in the vicinity), especially in younger patients. A class solution of beam angles was presented to ease and standardize treatment planning for a single vocal cord. The proposed technique also offers the new possibilities of dose escalation and hypofractionation for this group of patients.

Chapter 5

Impact of Geometric Variations on Delivered Dose in Highly Focused Single Vocal Cord IMRT

Sarah O.S. Osman, Eleftheria Astreinidou, Peter C. Levendag, and Ben J.M. Heijmen

Submitted to the International Journal of Radiation Oncology Biology and Physics, August 2011

Abstract

Purpose: To investigate the robustness of single vocal cord IMRT treatment plans for set-up errors, respiration, and deformation.

Methods and Materials: 4D-CT scans of ten early glottic carcinoma patients, previously treated with a conventional technique, were used in this simulation study. For each patient, the pre-treatment 4D-CT was used for IMRT planning, generating the reference dose distribution. Prescribed PTV-dose was 66 Gy. The impact of set-up errors was simulated by applying shifts to the planning CT-scans, followed by dose re-calculation with original beam segments, MUs, etc. Effects of respiration and deformation were determined with inhale and exhale CT-scans, and repeat scans acquired after 22 Gy, 44 Gy, and 66 Gy, respectively. All doses were calculated using Monte Carlo dose simulations.

Results: Considering all investigated geometrical perturbations, reductions in the CTV $V_{95\%}$, $D_{98\%}$, $D_{2\%}$, and generalized equivalent uniform dose($gEUD$) were limited to 1.2 ± 2.2%, 2.4 ± 2.9%, 0.2 ± 1.8%, and 0.6 ± 1.1 Gy, respectively. The near minimum dose, $D_{98\%}$, was always higher than 89%, and $gEUD$ always remained higher than 66 Gy. Planned contra-lateral vocal cord D_{Mean}, $gEUD$, and V_{40Gy} were 38.2 ± 6.0 Gy, 43.4 ± 5.6 Gy, and 42.7 ± 4.9%. With perturbations these values changed by −0.1 ± 4.3 Gy, 0.1 ± 4.0 Gy, and −1.0 ± 9.6%, respectively.

Conclusions: On average, CTV dose reductions due to geometrical perturbations were very low, and sparing of the contra-lateral vocal cord was maintained. In a few observations, the near-minimum CTV-dose was around 90%, requiring attention in deciding on a future clinical protocol.

5.1 Introduction

Intensity modulated radiation therapy (IMRT) is being increasingly investigated for the management of early stage squamous cell carcinoma of the larynx [104, 14, 93, 92, 91, 61]. IMRT produces a conformal dose distribution around the tumor; therefore the surrounding organs at risk (OAR) can be spared more than what could be achieved with conventional RT techniques. Limiting the dose to OAR has the potential of reducing RT related toxicity, such as, vocal dysfunction, dysphagia, trismus, arytenoid edema, carotid arteries injuries, and increased risk of strokes. IMRT appears not widespread as the standard technique for stage T1 laryngeal cancer, and whenever it is applied, both vocal cords are included in the treatment volume [104, 14]. The reason for this forbearance in the implementation of IMRT to this specific tumor site, compared to other head-and-neck tumor sites, may be the good overall survival currently achieved [61]. Nevertheless, reducing the dose to normal tissue potentially reduces long term sequelae and improves the quality of life (QoL), which is important for this category of patients with such a long term survival. Additionally, limiting the dose to the OARs, potentially yields another treatment option for patients with re-current tumors; re-irradiation. The use of IMRT and small target volumes could potentially also allow shorter, more hypo-fractionated schedules. Safety margins (CTV-PTV) are used to ensure that the CTV receives adequate coverage during the multi-fraction course of treatment. IMRT plans usually contain high dose gradients to spare organs at risk adjacent to target volumes, putting an enhanced stress on selection of appropriate margins. This is particularly important as it was shown that a small position variation does not necessarily mean a correspondingly small dose variation and vice versa in the case of head-and-neck RT because of tissue inhomogeneities and body contour variations with respect to the beams [6]. IMRT utilizes 3D anatomic information extracted from CT scans acquired prior to treatment. Nonetheless, several groups have reported anatomic changes occurring throughout fractionated external beam radiotherapy [7, 112]. The CTV-PTV margins have to account for potential anatomical changes during the course of treatment, e.g. caused by tumor regression or weight loss. In single vocal cord IMRT, applied CTV-PTV margins also have to compensate for respiratory tumor motion [93, 91]. Recently, it has been shown that using adaptive radiotherapy (ART) techniques has potential advantages in preventing many of the above mentioned concerns when treating head and neck tumors with IMRT [12, 109].

In Rotterdam we have developed a highly focused IMRT technique to only irradiate the involved vocal cord in early glottic cancer. This was allowed by recent technological advances in image acquisition with 4D-CT, image-guided position verification with cone beam CT, and the clinical availability of a TPS with Monte Carlo dose calculations [93, 92, 91, 61]. With our technique, not only the distant OARs are spared but also the contra-lateral vocal cord that lies in close vicinity to the irradiated vocal cord [91]. Single vocal cord irradiation (SVCI) involves the use of small treatment fields for a tumor surrounded partially by

air, complicating selection of appropriate CTV-PTV margins. For the treatment plans generated in [91] (used as reference in this study, see below), an isotropic CTV-PTV margin of 2mm was used. The current study was conducted to test the robustness of these IMRT plans against different geometrical uncertainties. The uncertainties evaluated were; set-up errors, respiratory movements, and inter-fraction anatomical variations (deformation).

5.2 Methods and Materials

5.2.1 Patients and generation of reference IMRT dose distributions

Ten patients, previously treated for early glottic carcinoma (T1aN0M0) with a conventional technique, were retrospectively included in this study. The involved cases and generation of the reference IMRT dose distributions as used in this study have been described in detail in [91]. Here a brief summary is provided. Each patient had a 4D-CT scan acquired before treatment, used to reconstruct scans for 8 breathing phases [93]. The CT resolution was $1 \times 1 \times 1mm^3$. For each patient, the airgap area at the level of the vocal cords was measured for all breathing phases. The scan from the phase that measured the middle value for the airgap was then used as the planning scan. This CT scan represents the tumor in (or closest to) its average respiratory position. IMRT plans were generated on these planning scans and the corresponding dose distributions were the reference distributions as used in this study. The applied CTV-PTV margin was 2 mm in all directions. A class solution with five beam angles was employed [91]. The prescribed dose to the CTV was always 66 Gy given in 33 fractions (six weekly fractions) using 6-MV photon beams. The IMRT treatment plans were generated with the Monaco TPS, version 1.00 (Elekta-CMS) that uses a MC dose calculation engine.

5.2.2 Simulation of set-up errors

The effects of set-up errors on CTV dose coverage and on the dose received by the CL vocal cord were assessed by re-computing the dose distribution for six shifts of the planning CT-scan (section 5.2.1 above) along the three principal axes (+ and -). Dose re-calculation was performed using the linac parameters (segments, MUs, etc.) as established for generation of the reference dose distribution (section 5.2.1 above). In a previous work [92] we have presented a daily on-line positioning procedure for single vocal cord irradiation. We found that the residual positioning errors after employing this on-line 3D patient setup correction procedure were below a millimeter. Nevertheless, in this present study shifts of $\pm$ 2 mm were simulated as an upper bound estimate of possible systematic set-up errors in clinical settings. As patient 6 had no pre-treatment 4D-CT, the described analyses

were done with the scan acquired after 22 Gy.

5.2.3 Simulation of respiratory motion

For each patient, the extreme inhale and extreme exhale CT scans, reconstructed from the pre-treatment 4D-CT scan, were used for the simulations. The manually delineated planning scan (above) was exported to the Atlas-Based Auto-segmentation (ABAS) software (Elekta/CMS software) to serve as a patient specific atlas [125] for delineation of the two extreme breathing phases CT scans. Where needed, the ABAS delineations were edited by an experienced observer (author 3) [135]. Again, dose calculations for these extreme breathing phases were based on the original linac parameters. As patient 6 had no pre-treatment 4D-CT, the described analyses were done with the scan acquired after $22Gy$.

5.2.4 Simulation of deformations and volumetric changes

The impact of deformations and volumetric changes was simulated utilizing repeat 4D-CT scans that were acquired at 22Gy (8 patients), 44Gy (6 patients) and at the end of the treatment 66 Gy (9 patients). In each repeat 4D-CT scan the middle breathing phase scan was determined and used for this analysis (section 5.2.1). Delineation of these middle CT scans was performed as described in 5.2.3 above. To simulate the treatment positioning, rigid registration of the planning CT scan with each repeat CT scan was performed. The coordinates of three well defined anatomical points; the front node of the thyroid cartilage and the two arytenoids were determined on both CT scans. The registration result of the center of mass (COM) of these three points was then used to determine the shifts applied to the iso-center of the repeat scan, followed by calculation of the corresponding dose distribution. The applied registration method resembles our cone beam CT based, on-line setup verification and correction protocol [92].

5.2.5 Dose calculation and plan evaluation

All dose calculations in this study were done in the Monaco treatment planning system (Elekta/CMS software), using the integrated Monte Carlo based dose calculation algorithm. In total 103 plans were re-calculated to simulate the uncertainties described above. In all cases, re-calculated dose distributions were compared with the corresponding reference distribution as designed for the planning CT-scan (section 5.2.1 above). In all cases, the CTV was used to evaluate tumor dose delivery; the PTV was only a geometrical tool to generate a treatment plan. Apart from the CTV, dose in the contra-lateral vocal cord was evaluated in detail. For the CTVs, the volume that received dose $\geq 95\%$ of the prescribed dose, $V_{95\%}$, the dose received by 98% of the structure, $D_{98\%}$,(near-minimum dose), the dose received by the hottest 2% of the volume, $D_{2\%}$, and the generalized equivalent uniform dose, $gEUD$, were calculated. The latter was computed using;

$gEUD(a) = (\sum_{i=1}(v_i D_i^a)^{1/a})$, were a is a unit-less model parameter that has a structure specific value, v_i represents the $i'th$ partial volume receiving dose D_i in Gy [85]. The value of the volume specific parameter for the CTV was chosen to be $(a = -13)$ [36]. For the contra-lateral vocal cord, the mean dose D_{Mean}, the generalized equivalent uniform dose $gEUD(a = 2.2)$ [100], and the percentage of the volume that received $40Gy$ or more, (V_{40Gy}), were assessed.

5.3 Results

5.3.1 CTV-delineation

Population mean CTV volume was 0.5 ± 0.1 cc, ranging from $0.2 - 0.8$ cc. A small repeat study pointed at an intra-observer uncertainty of $\pm$ 0.08 cc in vocal cord delineation. Delineated CT volumes in the various CT-scans (pre-treatment and repeat scans) used in this study were analyzed. It was found that, CTV delineations for the different time points were consistent.

5.3.2 Impact of geometric perturbations on CTV dose distributions

Changes in the CTV dose parameters due to geometric perturbations are presented in figures 5.1, 5.2, and 5.3. Averaged over all patients and shifts, changes in the CTV $V_{95\%}$, $D_{98\%}$, $D_{2\%}$, and generalized equivalent uniform dose ($gEUD$) compared to the reference dose distributions were $1.1 \pm 2.4\%$, $2.7 \pm 2.9\%$, $0.4 \pm 1.4\%$, and 0.8 ± 1.0 Gy, respectively (figure 5.1). Largest changes were generally observed for 'into-tissue' lateral shifts. Even for patient 10, with lowest $V_{95\%}$ and $D_{98\%}$, the $gEUD$ value remained above 66Gy with$D_{98\%} = 89\%$.

Figure 5.2 shows a relatively small impact of respiration phase on CTV dose parameters. Averaged over the 10 patients and considering both inhale and exhale scans, $V_{95\%}$, $D_{98\%}$, $D_{2\%}$, and the generalized equivalent uniform dose ($gEUD$) changed by $1.0 \pm 2.0\%$, $1.9 \pm 2.8\%$, $0.7 \pm 1.0\%$, and 0.6 ± 0.7 Gy, respectively (figure 5.2).

Figure 5.3 shows the impact of deformations and other volumetric changes during the course of fractionated treatment. Apart from the 22 Gy scans of patients 4 and 9, all deviations from the 0 Gy planning scan are minor. No clear explanation for the larger deviations is available as there is no indication of a change in delineated CTV (see section 5.3.1). Anyway, in all cases, the gEUD values were larger than 67 Gy, and $D_{98\%}$ values were never lower than 93%. For all 22 Gy, 44 Gy and 66 Gy scans together, $V_{95\%}$, $D_{98\%}$, $D_{2\%}$, and the generalized equivalent uniform dose ($gEUD$) changed by $1.0 \pm 1.9\%$, $1.9 \pm 3.0\%$, $-0.5 \pm 2.8\%$, and 0.1 ± 1.5 Gy on average.

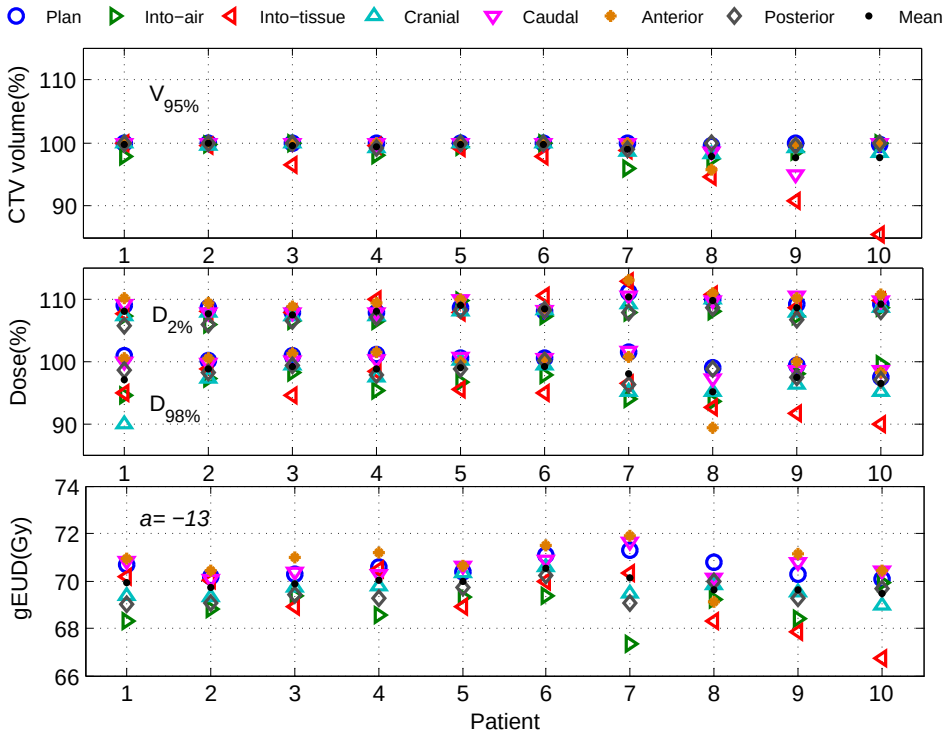

Figure 5.1: *Variations in CTV dose parameters with shifting the isocenter by 2 mm in different directions. In the upper panel the percentage of the CTV volume receiving dose of* $\geq 95\%$ *of the prescribed dose is shown. The dose received by* 98% *of the CTV volume , and the dose percentage received by the hottest* 2% *of the CTV volumes are presented in the middle panel. In the lower panel the CTV generalized equivalent uniform dose for each simulated situation is shown.*

5.3.3 Impact of geometric perturbations on CL vocal cord sparing

The population averages of the planned D_{Mean}, $gEUD$, and V_{40Gy} as presented with circles in figures 5.4, 5.5, and 5.6 are 38.2 ± 6.0 Gy, 43.4 ± 5.6 Gy, and 42.7 ± 14.9%, respectively. As expected, the shift analyses in figure 5.4 show largest increase of the CL vocal cord dose with iso-centric shifts towards airgap and the contrary with shifts away from the airgap. Considering all shifts in all patients, D_{Mean}, $gEUD$, and V_{40Gy}, changed compared to planning by -0.4 ± 4.9 Gy, −0.2 ± 4.7 Gy, and −1.2 ± 10.7%, respectively. Clearly, the large gain relative to a conventional RT technique (D_{Mean}= 66 Gy, V_{40Gy}= 100%) is maintained. Even for the shifts giving highest parameters, there is still a considerable gain in terms of sparing.

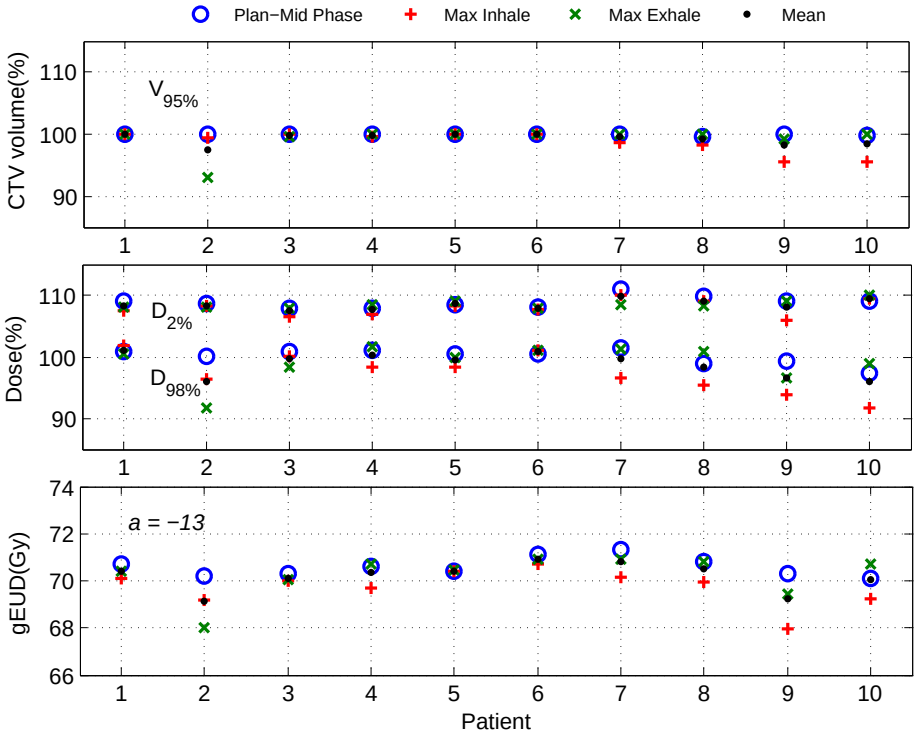

Figure 5.2: *Variations in the dose to the CTV in extreme inhale and exhale respiration phases compared to average phase that was used for planning. In the upper panel the percentage of the CTV volume receiving dose of* $\geq 95\%$ *of the prescribed dose, middle panel the dose received by* 98% *of the CTV volume, and the dose percentage received by the hottest* 2% *of the CTV volumes are shown. In the lower panel the CTV generalized equivalent uniform dose for each simulated situation is shown*

As for the CTV, change in respiration phase resulted in the smallest changes in dose parameters (compare figure 5.5 with figures 5.4 and 5.6). Changes in respiration phase resulted in 1.2 ± 2.3 Gy, 1.2 ± 2.1 Gy, and $1.4 \pm 5.1\%$ changes in D_{Mean}, $gEUD$, and V_{40Gy}, respectively. For the 22 Gy, 44 Gy and 66 Gy scans (figure 5.6), these parameters changed by -0.8 ± 3.6 Gy, -0.1 ± 3.2 Gy, and $-2.5 \pm 9.3\%$, respectively.

In eight of nine patients with a 0 Gy CT-scan available, V_{40Gy} after $66Gy$ is higher than at planning (figure 5.6). For this reason, we studied the airgap between the vocal cords as a function of delivered dose. For the 10 patients, when plotting the mean airgap area as a function of the dose, the average of the slopes of the regression lines was negative ($p = 0.004$), indicating that there is an overall decrease in the airgap areas with progressing treatment time. This

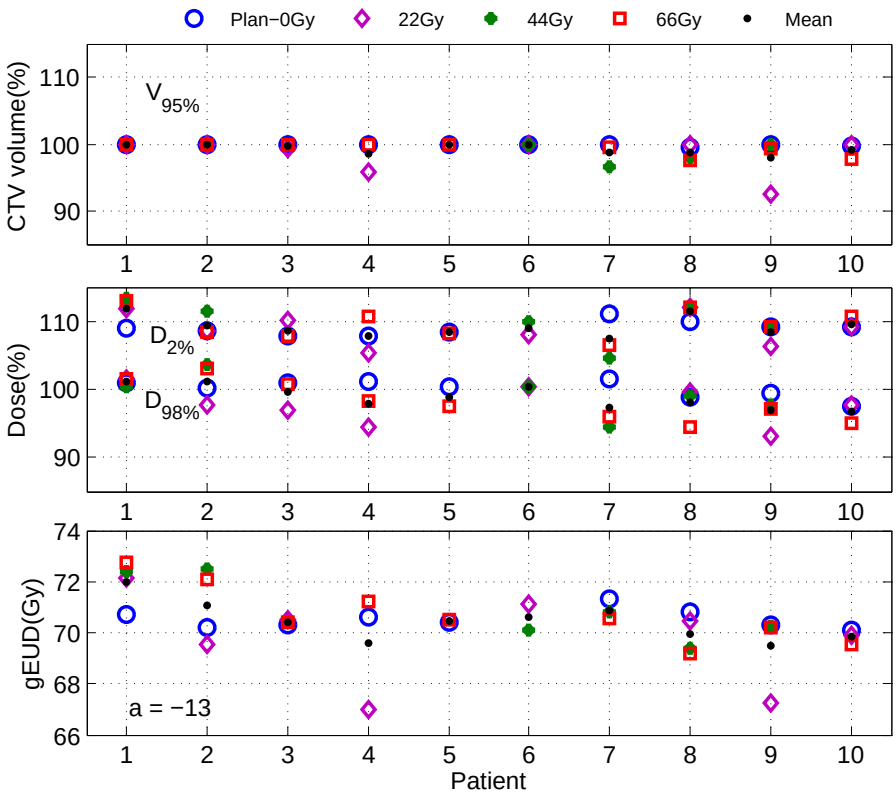

Figure 5.3: *Variations in some CTV dose parameters with preceding treatment time shown at time points 0Gy, 22Gy, 44Gy, and 66Gy for all patients.*

could possibly be explained by the incidence of arytenoid edema or synechia in the anterior commissure that are known acute RT side effects.

5.4 Discussion

We have been the first group to propose a complete systematic image-guided procedure for the delivery of highly focused IMRT plans for single vocal cord irradiation [93, 92, 91, 61]. The design of CTV-PTV margins for small tumors, partially surrounded by air, is non-trivial. Based on assessed geometrical uncertainties, in a previous study [91], we decided on the use of a 2 mm margin for SVCI. The present analysis was performed to dosimetrically test the robustness of the IMRT plans generated with this 2 mm margin [91]. We used the PTV for planning and the CTV to evaluate target dose for investigated geometrical

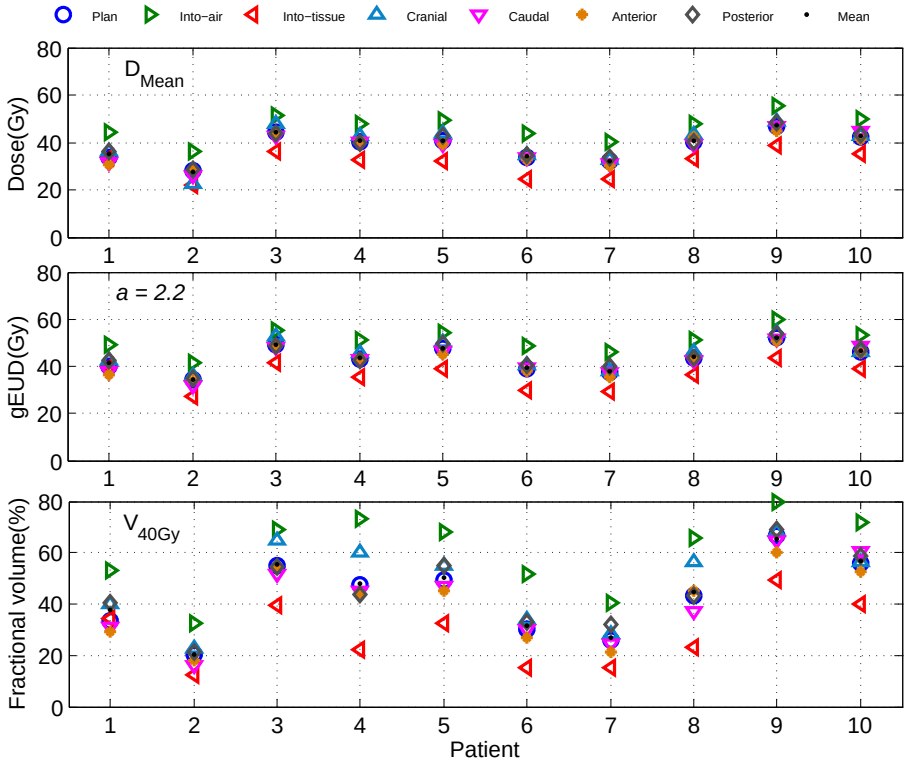

Figure 5.4: *Variations in the mean dose* (D_{Mean})*,* $(gEUD)$ *and* (D_{40Gy}) *received by the CL vocal cord with iso-centers shifts of* $2mm$ *in the specified directions.*

variations. Dose was always recalculated using beam angles, segments, MUs, etc. as established during treatment plan generation. Dose distributions were (re-)calculated with Monte Carlo simulation, taking into account all real internal inhomogeneities and surface curvatures.

Three possible sources of geometrical variation, i.e. set-up errors, respiratory movements, and inter-fraction volumetric changes and deformation were investigated. Planned IMRT dose distributions were compared with re-calculated dose distributions for the perturbed geometries. It was found that the good CTV dose coverage and the CL vocal cord sparing achieved in the static reference plans were largely maintained under the influence of treatment simulated geometrical variations. For the CTV, coverage ($V_{95\%}$), near-minimum dose ($D_{98\%}$), and $gEUD$ were on average reduced by 1.2%, 2.4% and 0.6 Gy, respectively. In a few instances, the near-minimum doses, $D_{98\%}$, in perturbed geometries (see figure 5.1) were around 90% of the prescribed dose, instead of 95%. These were exceptions, and it should also be taken in mind that in the shift analyses, for each

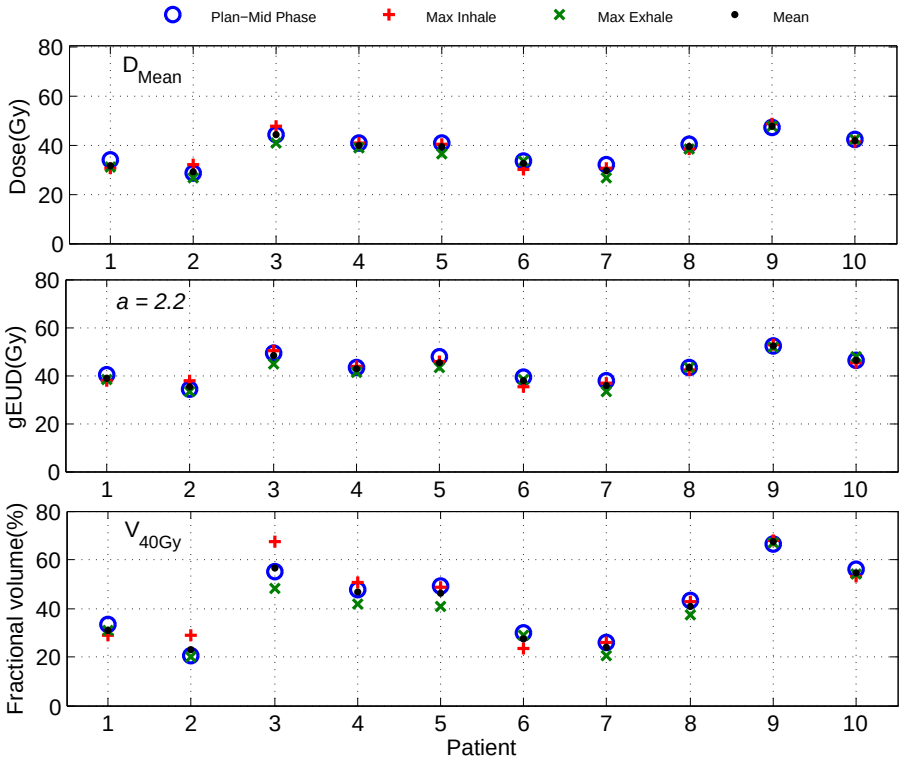

Figure 5.5: *Variations in the mean dose (D_{Mean}), ($gEUD$) and (D_{40Gy}) received by the CL vocal cord in extreme inhale and exhale respiration phases compared to middle breathing phase that was used for planning.*

individual patient, this only occurred at maximum in 1/6 of the simulated shifts. Moreover, with the proposed on-line protocol in place, 2 mm shifts are unlikely to occur [92], and it is even less likely that they are systematic, i.e. repeating each fraction. In the repeat CT analyses, a lower $D_{98\%}$ in a patient repeat scan was always accompanied by higher values at different time points (figure 5.3).

With the current, conventional treatment technique, local failure because of tumor miss is virtually impossible. Based on our results obtained sofar ([93, 92, 91, 61], this paper), we believe that with daily on-line CBCT-based re-positioning, probability of local failure with our planned IMRT dose distributions will also be very low. However, given the discussion above, there may be some risk that it not as low as for the conventional RT technique. Gowda et al [39] reported an excellent 5-years local control of 93% following treatment with $50-52.5$ Gy in 16 fractions in an overall treatment time (OTT) of 21-26 days. In our current ideas for SVCI, a total dose of 58.1 Gy may be delivered in 16 fractions, 5 fractions per

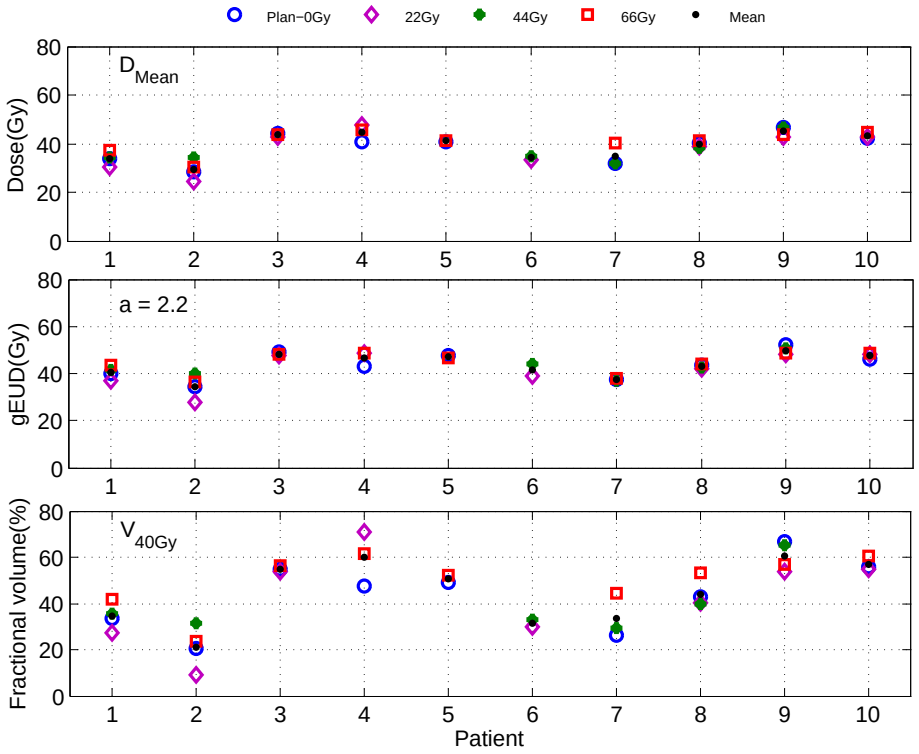

Figure 5.6: *Variations in the mean dose* (D_{Mean})*,* $(gEUD)$ *and* (D_{40Gy}) *received by the CL vocal cord with preceding treatment time shown at time points* $0Gy$ *(planning),* $22Gy$*,* $44Gy$*, and* $66Gy$ *for all patients.*

week, yielding a higher total dose than Gowda et al, and an EQD_{2Gy} of 66 Gy as in our current treatment approach, but in a shorter overall treatment time. A default 3 mm CTV-PTV margin is considered for single vocal cord IMRT (increase by 1 mm). A check on robustness of generated plan against potential anatomy shifts during treatment as described in section 5.2.2 can be performed for each individual patient prior to the start of treatment. Such a procedure may be used to verify the initially selected default CTV-PTV margin on a per patient basis and adapt the margins and the plan if needed, also in the context of potential inter-patient variations in plan conformity. Van Asselen et al. [127] showed that the amplitude of larynx movements due to swallowing may be $> 1cm$, but they also demonstrated that the incidence and duration of swallowing are low for most of the patients. Nonetheless, in a clinical protocol, swallowing during imaging and treatment has to be minimized, e.g. by patient instruction and monitoring.

5.5 Conclusions

This simulation study shows that with isotropic margins as small as 2 mm and daily cone beam CT-guided repositioning, CTV dose remained generally high, and large sparing of the contra-lateral vocal cord was maintained, when considering realistic intra- and inter-fraction geometric variations. Occasionally observed modest reductions in CTV dose have to be considered when deciding on a clinical protocol.

Chapter 6

Single Vocal Cord Irradiation: A Competitive Treatment Strategy in Early Glottic Cancer

Peter C. Levendag, David N. Teguh, Fatma Keskin-Cambay, Abrahim Al-Mamgani, Peter van Rooij, Eleftheria Astreinidou, Stefan L.S. Kwa, Ben Heijmen, Dominique A. Monsereza, and Sarah O.S. Osman

Published in Radiotherapy and Oncology. ePub ahead of printing 2011

Abstract

Introduction: The treatment of choice for early glottic cancer is still being debated; ultimately it relies on the functional outcome. This paper reports on a novel sparing 4D conformal technique for single vocal cord irradiation (SVCI).

Methods and Materials: The records of 164 T1a patients with SCC of the vocal cord, irradiated in the Erasmus MC between 2000 and 2008, were analyzed for local control and overall survival. The quality of life was determined by *EORTC H&N*35 questionnaires. Also the VHI (voice handicap index), and the TSH (thyroid stimulating hormone) blood levels, were established. On-line image guided SVCI, using cone beam CT and stereotactic radiation therapy (SRT) techniques, were developed.

Results: A LC rate at five-years of 93% and a VHI of 12.7(0−63) was determined. It appeared feasible to irradiate one vocal cord within $1-2$ mm accuracy. This way sparing of the contralateral (CL) vocal cord and CL normal tissues, could be achieved.

Conclusions: Given the accuracy ($1-2$ mm) and small volume disease (CTV limited to one vocal cord), for the use of stereotactic RT techniques SVCI with large fraction sizes is currently being investigated in clinic. It is argued that hypofractionated SVCI can be a competitive alternative to laser surgery.

6.1 Introduction

Of all head and neck cancers (HNCs), approximately 30 percent originates from the larynx. In Europe, annually 52.000 patients are diagnosed with cancer of the larynx. Local control (LC) varies, depending on the subsite and/or extent of the disease (T-and N-stage). This paper analyzes patients with early glottic cancer (EGC), that is, as defined by the UICC/AJCC classification system, disease confined to one (T1a) true vocal cord [88]. Radiation therapy (RT) and carbon dioxide endoscopic laser surgery (LS) have both proven to be effective treatment modalities for T1a glottic cancers. A high cure rate is often cited using either one modality. A summary of the literature by Sjogren et al. [115, 116] reported for T1 lesions treated with RT alone a LC rate at five-years of 84% (range $78-89\%$) and an average larynx preservation rate of 93%. Same author published in 2008 on 143 T1a lesions treated by RT (70) and LS (73); a local recurrence of 21% vs. 10% for RT and LS, respectively, was observed [115]. However, 16% of the LS group needed additional treatment consisting of LS (4%) and/or RT (11%). No significant difference in VHI was found for both treatment modalities [116]. Mendenhall and colleagues, reported in their review paper on T1 lesions treated by primary RT, local control rates of $85-94\%$. Recently, Mendenhall [13] updated their own results on T1, T2 glottic cancer. A five-year LC rate of 94% was reported for T1a lesions. Also, of the 585 patients analyzed, ten (1.7%) experienced severe or fatal complications [13]. In a summary paper by Grant et al. [41], local control rates for transoral laser microsurgery (TLM) varied between 71% and 97% [137, 121, 119, 108, 103, 96, 79, 78, 72, 66, 57, 47, 40, 35, 28]. Cohen et al., in a meta-analysis of non-randomized studies comparing the VHI of patients receiving RT or LS, found the voice to be similar in both modalities ($p = 0.1$) [16]. Similarly, in the most detailed retrospective study published by Loughran et al. when using the full armamentarium of validated scoring systems for studying vocal performance no difference was observed [67]. With regard to the quality of voice in EGC; LS is in principle performed as a highly focussed treatment for a clinical target volume (CTV) located on one vocal cord, while in conventional RT, the radiation fields do not conform to the tumor volume per se but in fact both vocal cords are irradiated. Moreover, in a number of cases LS is still to be followed by EBRT of the larynx.

A comparative dosimetric analysis of vocal cord irradiation using different techniques, that is conventional (box technique) vs. IMRT of the larynx vs. single vocal cord irradiation, has recently been published by our group. This paper focuses on the comparison of the dose distribution in many of the normal tissues at risk, using either one of the aforementioned techniques. The reduction of potential side effects, such as pain, poor quality of voice, speech, xerostomia, dysphagia, incidence of stroke or transient ischemic attack following radiation of the neck, and hypothyroidism, will be discussed. Given the fact that one is dealing with small volume disease (CTV [part of] one vocal cord), when using SRT techniques, the role of (hypo) fractionation can be analyzed. It is argued that single vocal cord

irradiation by hypofractionation, considering the low probability of normal tissue side-effects, can be a future way to treat early (T1a) glottic cancers. Good local control rates, improvement of VHI, short overall treatment times and potential room for retreatment with preservation of the larynx, can be anticipated.

6.2 Methods and Materials

The purpose of this paper is to report on treatment optimization when radiating T1a vocal cord lesions. As a base line observation, first the results from our own institution on LC, OS, quality of life (QoL) and voice handicap index (VHI) of EGC treated with conventional radiation therapy were analyzed. For a clinical review on LS, the reader is referred to the many papers on this issue reported in the literature. These data have been briefly summarized in the introduction section of this paper.

6.2.1 LC and survival using conventional radiotherapy of early glottic tumor

To analyze the LC rate and QoL results, all records of patients with SCC of the glottis were reviewed (figure 6.1); newly diagnosed carcinoma in situ (35 Tis), T1b lesions (38; both vocal cords) were excluded from the present analysis. The remaining patients with SCC of the true vocal cords (164 T1a) treated between 2000 and 2008 at our institute, were studied. All patients were simulated in supine position; for immobilization purposes a custom made head shell was manufactured. Lateral parallel-opposed wedged 6 MV photon beams, mean field size $\leq 36cm^2$ $[6 \times 6cm^2]$, with the iso-center placed at the center of the vocal cord lesion, were used. One fraction per day, fraction size of $2 - 2.3$ Gy, was given five days per week, up to a total dose of $60 - 66$ Gy. The dose was prescribed according to ICRU guidelines (with dose in the target varying between 95% and 107%) [89]. The absence of a lymphatic network and consequently the low incidence of nodal spread do not warrant elective nodal irradiation. Patients of the current series were analyzed for local control with or without salvage, and overall survival. Also, QoL using the $EORTC\ H\&N35$ questionnaires, the quality of voice using the VHI (voice handicap index), and the thyroid function status (TSH [thyroid stimulating hormone] blood levels), were determined.

6.2.2 Intensity modulated radiotherapy for T1a early glottic cancers, single vocal cord irradiation technique

Ten patients with T1aN0M0 glottic carcinomas were previously treated at our institute by lateral P-O fields (box technique), and were retrospectively used for the current investigation. The conventional treatment plans were originally made using the CadPlan treatment planning system (Varian Medical Systems, Palo

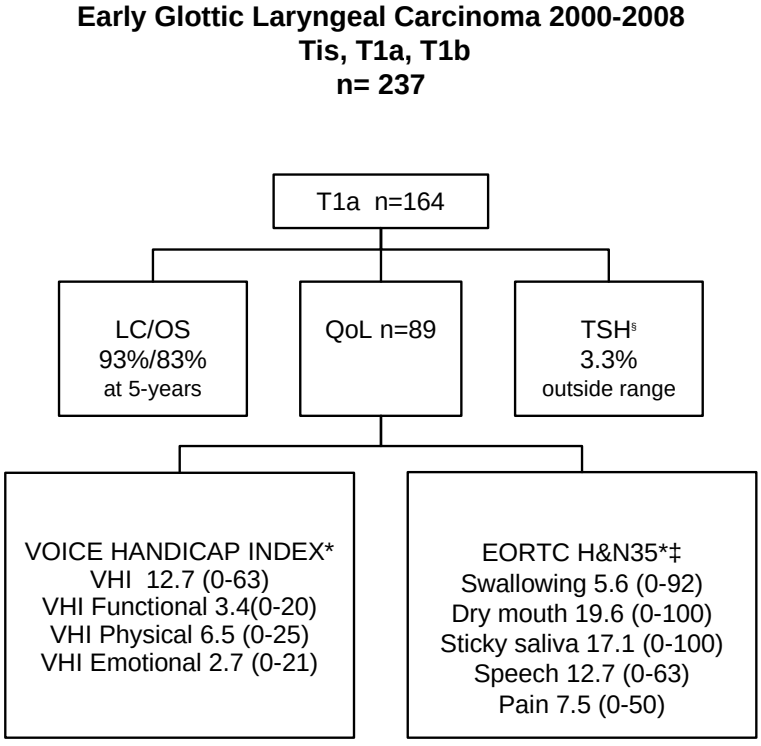

Figure 6.1: *For patients treated in the Erasmus Medical Center-Daniel den Hoed Cancer Center, figure 6.1 depicts the LC (local control) and OS (overall survival), the QoL (quality of life) scales and VHI (voice handicap index). Also presented are the blood levels TSH (thyroid stimulating hormone) reflecting the thyroid function post radiotherapy.*

Alto, USA), and were regenerated in the XiO treatment planning system (V 4.33 Elekta-CMS Software), using heterogeneity corrections and a fast convolution superposition algorithm. In all planning CT scans (resolution $1mm^3$) the clinical target volume (CTV, margin 3 mm) and the organs at risk (OARs) were delineated. The delineated structures were the vocal cords, arytenoids, swallowing muscle at the level of the vocal cords (inferior constrictor muscle, ICM), ipsi- and contra-lateral strap muscles, carotid arteries, thyroid gland, thyroid and ricoids cartilages, and the spinal cord. The cranial-caudal extensions of the contours of these OARs were at the level of the vertebra C2 and C7. IMRT and SVCI treatment planning was performed for an Elekta Synergy linear accelerator with 40 MLC leaf pairs and a leaf width at the isocenter of 4 mm (Elekta Beam ModulatorTM, Elekta Oncology Systems, Crawley, UK) at 6-MV. The minimum segment size allowed was $0.5cm^2$. The isocenter of the treatment was set to the center of one of the vocal cords. The radiation schedule proposed to be used in combination with the SVCI technique, is discussed in the next section.

6.3 Results and Discussion

6.3.1 Laser surgery or radiotherapy

Carbon dioxide endoscopic LS is an established treatment technique for early glottic cancer. According to Sjogren et al. [116] LS was introduced in the Leiden University Medical Center, for T1a midcord lesions, in 1996. The results were summarized as follows; "T1a glottic carcinoma allocated to radiotherapy have a poorer outcome in terms of local control and laryngectomy free survival than do T1a patients selected for laser surgery". Motta et al. [80] assessed the vocal function of patients who had undergone CO_2 laser cordectomy. No functional compensation enabled the patients to achieve a voice quality comparable with that of controls. Vilaseca et al. [134] studied the voice quality after CO_2 laser cordectomy. They concluded that the voice improved in almost 60% of the patients, returning to normal in 45%. Nunez et al. [86] analyzed functional outcome and self-evaluation of the voice of patients with T1 glottic carcinoma treated with endoscopic LS and RT. When comparing the VHI scores, this was in apparent favor for RT, in functional and emotional ratings as well as for the global scores. VHI scores of the T1a larynx cancer group after radiotherapy in our hospital has been listed in Table 6.1.

Despite the (sometimes contradictory) reports on post-treatment voice quality, it is mostly agreed upon that radiotherapy results in equal or even better voice quality post treatment as opposed to LS [116]. Moreover, even better outcomes are to be expected with the emerging more focused RT techniques (see below). Apart from this, the comparison of LS with conventional RT techniques is not really valid due to patient selection. For example, since patients treated for small, early lesions are exposed more commonly to LS and, therefore, a favorable outcome for

Table 6.1: *Mean and range of the VHI-scores T1a larynx group after radiotherapy. VHI: voice handicap index, VHI-F: VHI-functional, VHI-E: VHI-emotional, VHI-P: VHI-physical.*

VHI-total, mean (range)	12.7 (0-63)
VHI-F, mean (range)	3.4 (02-0)
VH-E, mean (range)	2.7 (0-21)
VHI-P, mean (range)	6.5 (0-25)

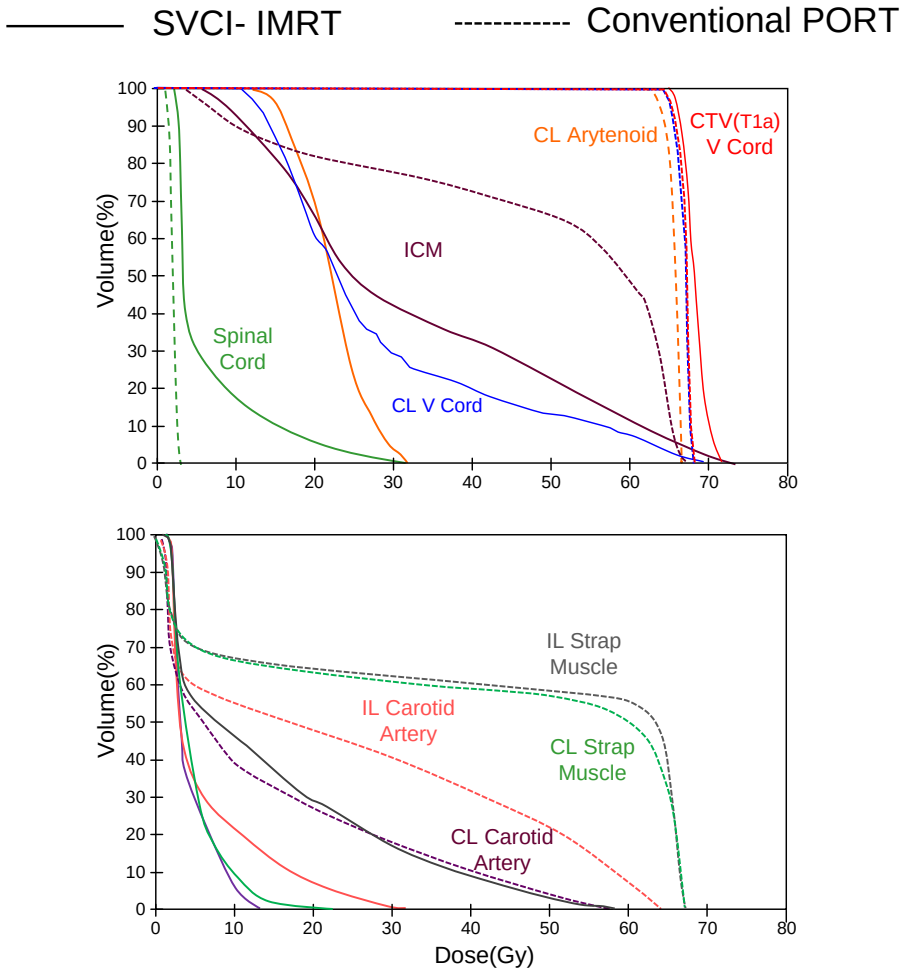

Figure 6.2: *An example of typical dose volume histograms (DVH) comparing the dose received by the CTV (panel 1). Also depicted are the organs at risk when using conventional parallel opposed beam (dotted lines) and IMRT for single cord irradiation (solid lines).*

this patient group is anticipated. This bias can only be overcome by the design of prospective randomized trials.

In addition to a localized tumor growth confined to one or both vocal cords, geometrically complex tumors could also be treated with RT using IMRT techniques and still achieve excellent normal tissue sparing. These include tumors involving the anterior commissure (AC) which are most often not amenable for LS. Moreover, for T2 tumors extending into to the sub- or supra-glottic regions, so far insufficient data with regard to LS are available.

6.3.2 Single vocal cord irradiation (SVCI) with IMRT

In the Erasmus Medical Center a study was undertaken by Osman et al. on the feasibility of unilateral vocal cord irradiation (SVCI) for T1a lesions. The concept was to see whether unilateral vocal cord irradiation could reliably be re-produced on a daily basis (i.e. in case of fractionated RT). In 2008, our first study was published showing that the intra-fraction movement of the vocal cords was small and not prohibitive for executing such a delicate treatment technique [93]. A second publication dealt with the adequacy of daily on-line re-positioning [92]. A subsequent paper showed the superiority of IMRT as opposed to lateral P-O irradiation techniques with regard to normal tissue involvement [91].

6.3.3 Risk of ischemic vascular side effects after neck irradiation

In recent years attention has increasingly been devoted to vascular effects when radiation is the treatment of choice for a primary cancer in the head & neck region [11, 104]. RT of the head and neck is found to be a significant risk factor for carotid artery stenosis. In a paper by Brown et al. [11], an incidence of 18% carotid artery stenosis in the ipsilateral irradiated neck vs. 7% in the contralateral non-irradiated neck was reported. Lateral P-O portals include in part the carotid arteries; consequentially, since one of the causes of stroke is carotid artery stenosis. Stroke could be considered as a typical side effect associated with irradiation of the head and neck. According to Dorrestein et al. [27], the overall risk of strokes after RT was significantly increased compared to the general population. Rosenthal et al. [104] concluded from a literature survey that 50 Gy could be considered the approximate threshold dose for vascular (i.e. carotid arteries) damage in the neck after post-irradiation. Consequently, treatment options for previously irradiated patients (with conventional RT methods) are potentially limited due because of increased risk for carotid injury. In our planning study using SVCI techniques with IMRT, no part of the carotid arteries received doses as high as 50 Gy (see mean and maximum dose received by the carotid arteries Table 6.2). Therefore, this might allow for re-irradiation of these tumors. In conclusion, additional treatment options for recurrent tumors or second primary tumors in the upper aerodigestive track are another benefit for using IMRT. These tumors are usually salvaged with

surgery with very generous surgical margins (e.g. by laryngectomy), obviously negating the effect on the QoL of these patients.

Table 6.2: *Mean dose to PTV, CTV and critical structures. IL = ipsi-lateral, CL, contra-lateral.*

	Dose (Gy)	SVCI with IMRT	BVCI with IMRT	PO clinical plans
PTV	$Mean \pm SD$	67 ± 1	67 ± 1	67 ± 1
CTV	$Mean \pm SD$	67 ± 1	67 ± 1	67 ± 1
CL vocal cord	$Mean \pm SD$	39 ± 8	(n.a.)	67 ± 1
IL arytenoid	$Mean \pm SD$	64 ± 3	65 ± 1	66 ± 1
CL arytenoid	$Mean \pm SD$	20 ± 8	66 ± 2	66 ± 1
ICM	$Mean \pm SD$	28 ± 4	39 ± 5	61 ± 3
IL strap muscle	$Mean \pm SD$	17 ± 2	18 ± 3	49 ± 8
CL strap muscle	$Mean \pm SD$	9 ± 4	18 ± 3	49 ± 10
Thyroid gland	$Mean \pm SD$	3 ± 1	3 ± 1	17 ± 11
Thyroid gland	$Max \pm SD$	10 ± 8	10 ± 9	15 ± 11
Thyroid cartilage	$Mean \pm SD$	28 ± 5	38 ± 7	66 ± 1
Cricoid	$Mean \pm SD$	22 ± 4	28 ± 4	61 ± 4
IL carotid artery	$Max \pm SD$	24 ± 5	31 ± 4	66 ± 3
CL carotid artery	$Max \pm SD$	12 ± 2	30 ± 5	66 ± 2
Spinal cord	$Max \pm SD$	22 ± 10	27 ± 6	2 ± 0

6.3.4 Hypothyroidism

Hypothyroidism remains an underreported and often under-appreciated late sequel of RT or thyroid surgery [34]. Early recognition and suppletion with thyroid hormones may prevent the development of clinical symptoms of hypothyroidism. In the laboratory of the Erasmus MC, TSH normal values range from 0-4.3 mUnits. In the patients under investigation, a maximum of 6% had abnormal values of TSH (that is outside the normal range), see also figure 6.1. This low number is probably due to the anatomical position of the thyroid gland. Thus, a small dose is apparently to be received by the thyroid glands with normal anatomical positioning (see Table 6.2 in general). However, a simple TSH routine check in follow-up is still worthwhile for picking up these isolated cases (6%). A detailed analysis of hypothyroidism is beyond the scope of the present paper.

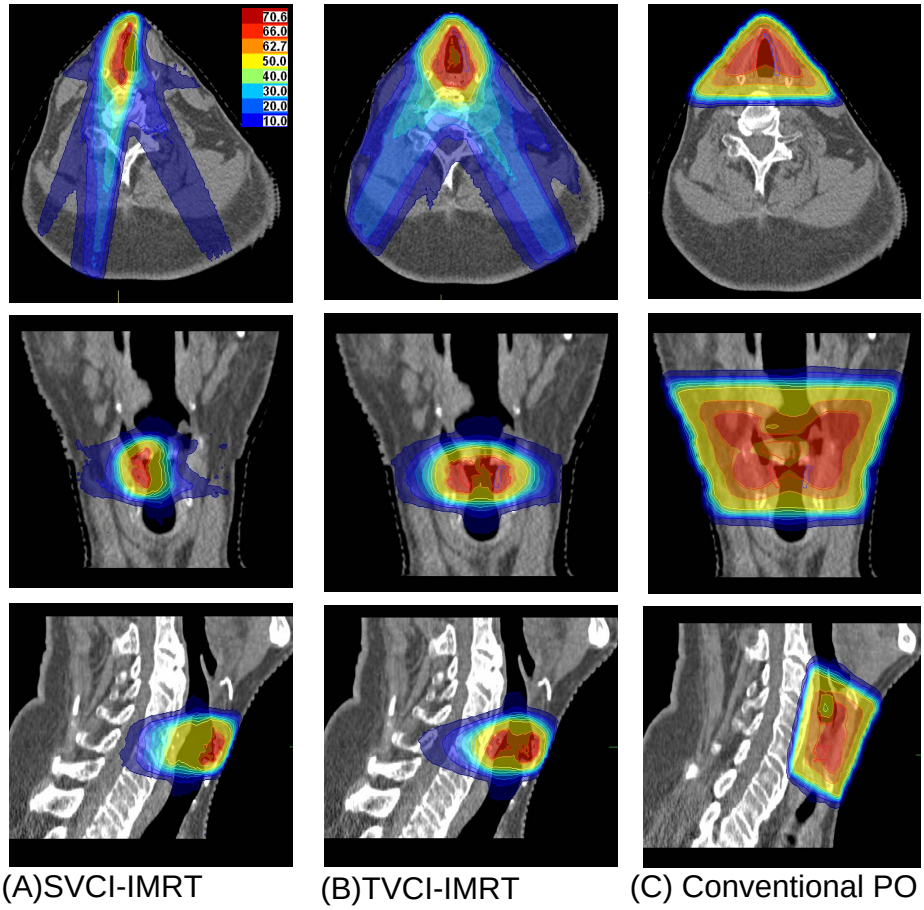

Figure 6.3: *Transverse (top), coronal (middle), sagittal (bottom) slices showing typical dose distributions (iso-dose fill) obtained using IMRT for the right vocal cord (first column), IMRT for both vocal cords (second column), and P-O plans (third column).*

6.3.5 Radiotherapy for the management of early glottic tumors

A comparison of the dose received by the various structures from the different radiotherapy techniques is shown in [figure 6.2] and [figure 6.3]. In figure 6.2 examples of typical dose-volume-histogram (DVH) comparisons are shown, illustrating the dose received by the vocal cords, arytenoids, inferior constrictor muscle (ICM), spinal cord, strap muscles, and the arytenoids when using lateral P-O wedged photon beams (dotted lines), IMRT for two vocal cords (dashed lines) vs. IMRT for a single vocal cord (solid lines). In the lateral P-O beam plans most of the structures receive the full dose as opposed to IMRT plans, where notable sparing of normal tissue is obtained (also see Table 6.2). figure 6.3 shows examples of three dose distributions; column (A) for SVCI with IMRT for a T1a tumor on the right vocal cord. In addition, in column B, an example of a T1b-IMRT plan is shown for both vocal cords. Finally, column C, a typical dose distribution for lateral P-O beams is presented. At present accurate treatment techniques are available to apply highly focused radiation, e.g. with the use of cone beam CT and stereotactic radiation. Given the small target and the large amount of sparing of different normal tissues, apparently the CTV and PTV margin can be small and the benefit of hypofractionation becomes an issue. We have, therefore, proposed to start a clinical pilot study using five fractions of 8.5 Gy per fraction, with the dose prescribed to the 80% isodose line. Finally, we have not discussed the issue of costs per treatment modality since they differ substantially given the variations in health care providers (national guidelines) per country.

6.4 Conclusions

Treatment modalities of T1 vocal cord lesions differ substantially per institution. Many of the selection factors involved were evaluated in this study in order to arrive at the best treatment option. The analyzed selection factors were LC, OS, QoL, preservation of voice, potential for vascular side effects, and hypothyroidism. The weight given to each of the QoL factors and the potential side effects of LS will guide the preference for either LS or RT. The outcome in QoL and the preservation of voice have, in general, favorably been reported for RT; this is despite the fact the RT involves a larger surface area than is the case with LS (i.e. two vocal cords in stead of one). Vascular side effects and hypothyroidism are not present when using LS. The risk for the occurrence of these side effects is, however, extremely small in the case of RT and can be further reduced by using advanced RT techniques, such as IMRT and SVCI. For good reasons (see paragraph before), it has been argued to start the clinical testing of the role of hypofractionation in these very small target volumes. Finally, of obvious advantage is the fact that RT is a non-invasive technique. However, in terms of evidence based medicine, randomized trials for the outcome of SVCI by IMRT techniques and LS are absent but are definitely needed in order to make a more balanced comparison for these

competitive techniques.

Chapter 7

General Discussion

7.1 Radiotherapy for early stage glottic tumors

The treatment of early stage glottic cancers is still widely debated because there are many effective treatment modalities that are equally successful in terms of local control. The most common choices are radiotherapy and endoscopic laser surgery that have very comparable outcomes. Therefore, besides cure the choice between treatment modalities should rely on laryngeal preservation, voice preservation, minimal morbidity, expense and convenience (i.e. patient's preference).

Despite the increased popularity of endoscopic laser surgery in recent years, many still consider radiotherapy to be the treatment of choice. This is because patients treated with radiotherapy are reported to have superior voice quality as opposed to those treated with laser surgery [86, 59]. This conclusion is supported by quantitative acoustic measurements, auditive perception (perceived voice quality) and more importantly patient self evaluation voice handicap index (VHI) questionnaires. This VHI questionnaire reviews situations grouped into three areas (functional, physiological and emotional) and gives an idea of the subjective impact that a vocal problem produces in a specific individual [23].

Additionally, in contrast with laser surgery, practically all types of early glottic tumors can be treated with RT. In conventional radiotherapy, parallel opposed wedged photon beams are generally used to cover the tumor and the surrounding healthy structures conservatively. With this conventional treatment technique the tumor as well as all laryngeal structures receive the total prescribed dose (e.g. 66 Gy in 33 fractions of Gy at our institute). This is a well established treatment technique with excellent results. Nevertheless, this treatment technique could be optimized further by sparing healthy structures that are unnecessarily irradiated. This has the potential of reducing radiotherapy related side effects for this group of patients.

Moreover, despite the very good outcome of this treatment, recurrent tumors are encountered. One reason could be that many patients do not quit smoking after the treatment for the initial tumor [128]. Another reason might stem from technical pitfalls of the conventional radiotherapy settings. Among these, the most commonly discussed limitation is the underdosage due to inadequate build-up of electrons [53, 94, 120]. This problem is unrealized by most of commercially available treatment planning systems (TPS) due to accuracy limitations of their dose calculation engines [53, 132]. The problem is more pronounced for tumors that lie close to the anterior skin and also on the surface of the air cavity in the interior of the larynx. This could possibly also explain why anterior commissure involvement is associated with inferior local control as reported by a number of authors [70, 87]. Inadequate build-up of electrons may be found beneath the skin of the neck as the anterior commissure is only $1cm$ from the skin, resulting in underdosing of these regions. Patients with recurrent tumors are usually referred to surgery and not infrequently a laryngectomy is performed which has a negative impact on the quality of life of these patients. Another technical difficulty that

conventional RT techniques are faced with is treating patients with short necks, which makes the use of lateral opposed fields troublesome. In such cases oblique fields are used leading to more spread of the high dose regions to other OAR.

In addition to the technical challenges there also exist some clinical problems. These problems are directly linked to delivering high doses to healthy tissues. Among these problems, voice/speech impairment, persistent edema of the arytenoids, the increased risk of xerostomia, trismus, strokes and hypothyroidism. This topic is discussed in greater detail in chapter 6.

There have been some attempts in the past to reduce the dose received by the arytenoids to prevent persistent edema of the arytenoids [4]. Recently, some institutes have incorporated intensity modulated radiotherapy (IMRT) in the treatment of early glottic cancers [104, 14]. Their main goal was to spare the carotid arteries in an attempt to reduce the risk of stroke in this group of patients. However, given the excellent results of a conventional technique, some people have been reluctant and stood against the use of small treatment fields and IMRT for these patients, as the use of small fields could increase the risk of a geographic miss [31]. Moreover, as a result of limitations of dose calculation algorithms, problems of underedosage at the air-tissue interface and at the anterior commissure might remain undetected without the use of advanced dose calculation engines. These technical concerns were taken into account in the studies described in this thesis.

In this thesis we have presented a novel radiotherapy procedure to treat patients with early glottic tumors with highly conformal dose distributions. In chapters $2-5$, single vocal cord irradiation with IMRT is presented as a potential solution for limitations of conventional RT techniques mentioned above. Because of the availability of an advanced treatment planning system with a Monte Carlo (MC) dose calculation engine, also for smaller treatment fields with air around the tumor, good estimates of the of the delivered tumor dose can be obtained. From the dosimetric point of view, this allowed the introduction of small field treatments. All treatment steps are conducted with caution to ensure the high precision that is crucial for this treatment technique. We have employed 4D-CT to monitor and quantify patient respiration correlated movement of the tumor [93]. Cone beam CT scans were investigated for daily positioning of the patients with high accuracy [92]. The studies pointed at possibilities for tremendous sparing of OAR. This has the potential of reducing RT related side effects while still maintaining the good local controls achieved by conventional RT techniques.

Moreover, limiting the dose to normal structures might increase treatment options for patients with recurrent tumors or second primary tumors, especially in younger patients. In chapter 6, we have presented SVCI as a competitive treatment technique to conventional RT as well as to laser surgery. We have also presented some of our own institutional results on quality of life of early glottic cancer patients and we related our results to those published for laser surgery.

It is important to realize that the studies in this thesis pointing at good possibilities for focused radiotherapy were done in a retrospective setting, no patients were treated with IMRT. All involved CT datasets were acquired for

patients treated with the conventional technique. Also, the number of studied patients was low. Therefore, caution is needed in clinical introduction.

7.2 A clinical protocol

So far, five early glottic patients have been entered into a clinical protocol for highly focused IMRT. Here, some details are briefly discussed.

7.2.1 CTV delineation and CTV-PTV margin

CTVs are delineated on a pre-treatment contrast-enhanced planning CT scan with the aid of an endoscopic photograph of the patient's vocal cords. In this process, the central axial CT slice of the vocal cords is fused with the endoscopic photograph of the patient's vocal cords. Goal is to delineate at least the volume that would have been surgically resected if the patient was referred to endoscopic laser surgery rather than radiotherapy. If only the CT scan is used for tumor delineation, it is of great difficulty to define the borders of the CTV. For extra safety, three millimeter isotropic margins are used for CTV-PTV extension instead of the 2 mm mentioned in chapters 4 and 5. A study evaluating inclusion of MR images to further enhance tumor delineation accuracy is being discussed.

7.2.2 Dose fractionation and overall treatment time (OTT)

Reducing the overall treatment time could reduce the re-population of tumor cells between sessions and result in better tumor control. On the other hand, the main concern against less fractions and so increased dose per fraction is the risk of increased toxicity. The subject of clinical outcomes of altered fractionation schemes in early glottic cancer has been investigated by a number of groups [39, 90, 9]. Nevertheless, it is difficult to distinguish the effect of dose per fraction and overall treatment time (OTT) from these studies as most of them alter both parameters. Gowda et. al. [39] reported an excellent 5-year LC of 93% following treatment with $50 - 52.5$ Gy in 16 fractions and an OTT of 21-26 days.

As our dose distributions for single vocal cord IMRT are really focused compared to conventional treatment (Chapter 4), the enhanced toxicity risk following a moderate OTT reduction is expected to be compensated. In our current protocol, a total dose of 58.08 Gy is delivered in 16 fractions (fraction dose $d = 3.63$ Gy), 5 fractions are delivered per week. Using the linear-quadratic model, the biological equivalent dose given in fractions of 2 Gy (EQD_{2Gy}) is given by $EQD_{2Gy} = D * [\alpha/\beta + d]/[\alpha/\beta + 2]$, where α/β is the alpha-beta ratio in Gy and d is the dose per fraction. In the selected scheme $EQD_{2Gy} = 66$ Gy for the tumor (using $\alpha/\beta = 10$ Gy), which is identical to the total dose we are used to give in non-IMRT larynx treatments.

7.2.3 Daily image-guidance

To minimize tumor miss probability and monitor adequate dose delivery, three daily cone beam CT scans are made. The first is used to re-position the patient, aiming at the set-up as established during planning. The second is acquired immediately after re-positioning to check proper execution of the required set-up correction. The third scan is acquired after delivery of all treatment beams (around 10 minutes after switching on the first beam).

Adaptive radiotherapy (ART) is an approach to correct for non-rigid anatomical changes during fractionated treatment through on-line or off-line modification of the original IMRT treatment plan, based on acquired images. Many groups have demonstrated the potential benefit of using ART in the treatment of head and neck cancers with IMRT [12, 49, 2]. In chapter 5 we have shown that the impact of anatomy deformations on delivered dose in single vocal cord IMRT may be limited. However, there was also evidence for time trends in the air gap between the vocal cords. Possibly, the daily acquired CBCT could be used to further study the potential role of ART in single vocal cord IMRT. The CBCT might even be useful in adapting the treatment plans if needed [25, 58, 44, 64, 131].

7.3 Swallowing during imaging and treatment

It is known that the displacement of the larynx due to swallowing is large. Van Asselen et al. [127] showed that the amplitude of the larynx movements is $> 1cm$, but they also demonstrated that the incidence and duration of swallowing are low for most of the patients. In our protocol, patients are instructed not to swallow during image acquisition as well as during treatment delivery. We also instruct them to give a signal if they can not avoid swallowing at any moment.

7.4 Non-coplanar treatment set-ups

Chapter 4 includes a preliminary study on the of use of non-coplanar vs coplanar optimized beam angles. Because of the involved couch rotations, non-coplanar treatments at a linear accelerator are time-consuming. Moreover, the couch rotations might also comprise treatment accuracy. The Cyberknife (Accuray) has the interesting option to irradiate patients with non-coplanar beams without the need for couch rotations. It would be of interest to investigate plan quality with this system, compared to coplanar treatment on a conventional linac. Part of the investigations should focus on the accuracy of tumor set-up using planar kV-images as obtained with the Cyberknife system. Possibly, the Cyberknife could also be upgraded with 3D/4D imaging facilities.

Bibliography

[1] J. P. Agarwal, G. K. Baccher, C. M. Waghmare, I. Mallick, S. Ghosh-Laskar, A. Budrukkar, P. Pai, P. Chaturvedi, A. D'Cruz, S. K. Shrivastava, and K. A. Dinshaw. Factors affecting the quality of voice in the early glottic cancer treated with radiotherapy. *Radiotherapy and Oncology*, 90(2):177 – 182, 2009.

[2] P. H. Ahn, C.-C. Chen, A. I. Ahn, L. Hong, P. G. Scripes, J. Shen, C.-C. Lee, E. Miller, S. Kalnicki, and M. Garg. Adaptive planning in intensity-modulated radiation therapy for head and neck cancers: Single-institution experience and clinical implications. *International Journal of Radiation Oncology*Biology*Physics*, In Press, Corrected Proof:–, 2010.

[3] Y. Akine, N. Tokita, T. Ogino, I. Tsukiyama, S. Egawa, M. Saikawa, W. Ohyama, T. Yoshizumi, and S. Ebihara. Radiotherapy of T1 glottic cancer with 6 MeV X rays. *International Journal of Radiation Oncology*Biology*Physics*, 20(6):1215 – 1218, 1991.

[4] A. S. Allal, R. Miralbell, W. Lehmann, and J. M. Kurtz. Effect of arytenoid sparing during radiation therapy of early stage glottic carcinoma. *Radiotherapy and Oncology*, 43(1):63 – 65, 1997.

[5] A. Aref, J. Dworkin, S. Devi, L. Denton, and J. Fontanesi. Objective evaluation of the quality of voice following radiation therapy for T1 glottic cancer. *Radiotherapy and Oncology*, 45(2):149 – 153, 1997.

[6] E. Astreinidou, A. Bel, C. P. Raaijmakers, C. H. Terhaard, and J. J. Lagendijk. Adequate margins for random setup uncertainties in head-and-neck IMRT. *International Journal of Radiation Oncology*Biology*Physics*, 61(3):938 – 944, 2005.

[7] J. L. Barker, A. S. Garden, K. Ang, J. C. O'Daniel, H. Wang, L. E. Court, W. H. Morrison, D. I. Rosenthal, K. Chao, S. L. Tucker, R. Mohan, and L. Dong. Quantification of volumetric and geometric changes occurring during fractionated radiotherapy for head-and-neck cancer using an integrated CT/linear accelerator system. *International Journal of Radiation Oncology * Biology * Physics*, 59(4):960 – 970, 2004.

[8] J. Boda-Heggemann, C. Walter, A. Rahn, H. Wertz, I. Loeb, F. Lohr, and F. Wenz. Repositioning accuracy of two different mask systems-3D revisited: Comparison using true 3D/3D matching with cone-beam CT. *International Journal of Radiation Oncology*Biology*Physics*, 66(5):1568 – 1575, 2006.

[9] J. Bourhis, J. Overgaard, H. Audry, K. K. Ang, M. Saunders, J. Bernier, J.-C. Horiot, A. L. Maître, T. F. Pajak, M. G. Poulsen, B. O'Sullivan, W. Dobrowsky, A. Hliniak, K. Skladowski, J. H. Hay, L. H. Pinto, C. Fallai, K. K. Fu, R. Sylvester, and J.-P. Pignon. Hyperfractionated or accelerated radiotherapy in head and neck cancer: a meta-analysis. *The Lancet*, 368(9538):843 – 854, 2006.

[10] J. Brandenburg. Laser cordotomy versus radiotherapy: An objective cost analysis. *Annals of Otology, Rhinology and Laryngology*, 110(4):312–318, 2001.

[11] P. D. Brown, R. L. Foote, M. P. McLaughlin, M. Y. Halyard, K. V. Ballman, A. C. Collie, R. C. Miller, K. D. Flemming, and J. W. Hallett. A historical prospective cohort study of carotid artery stenosis after radiotherapy for head and neck malignancies. *International Journal of Radiation Oncology*Biology*Physics*, 63(5):1361 – 1367, 2005.

[12] P. Castadot, J. A. Lee, X. Geets, and V. Gregoire. Adaptive radiotherapy of head and neck cancer. *Seminars in Radiation Oncology*, 20(2):84 – 93, 2010.

[13] B. S. Chera, R. J. Amdur, C. G. Morris, J. M. Kirwan, and W. M. Mendenhall. T1N0 to T2N0 squamous cell carcinoma of the glottic larynx treated with definitive radiotherapy. *International Journal of Radiation Oncology*Biology*Physics*, 78(2):461 – 466, 2010.

[14] B. S. Chera, R. J. Amdur, C. G. Morris, and W. M. Mendenhall. Carotid-sparing intensity-modulated radiotherapy for early-stage squamous cell carcinoma of the true vocal cord. *International Journal of Radiation Oncology*Biology*Physics*, 77(5):1380 – 1385, 2010.

[15] I. K. C.K. Bomford, S.B. Sherriff and H. Miller. *Walter and Miller's textbook of radiotherapy-radiation physics, therapy and oncology*, pages 350 – −353. Churchill Livingstone, Edinburgh, fifth edition, 1993.

[16] S. Cohen, C. Garrett, W. Dupont, R. Ossoff, and M. Courey. Voice-related quality of life in T1 glottic cancer: Irradiation versus endoscopic excision. *Annals of Otology, Rhinology and Laryngology*, 115(8):581–586, 2006.

[17] S. Cragle and J. Brandenburg. Laser cordectomy or radiotherapy: Cure rates, communication, and cost. *Otolaryngology - Head and Neck Surgery*, 108(6):648–654, 1993.

[18] T. Craig, J. Battista, and J. V. Dyk. Limitations of a convolution method for modeling geometric uncertainties in radiation therapy. i. the effect of shift invariance. *Medical Physics*, 30(8):2001–2011, 2003.

[19] D.A.Fein, W. Lee, A.L.Hanlon, J.A.Ridge, W. C. Jr., and L. Coia. Do overall treatment time, field size, and treatment energy influence local control of T1-T2 squamous cell carcinomas of the glottic larynx? *International Journal of Radiation Oncology Biology Physics*, 34(4):823–831, 1996.

[20] A. S. Dagli, H. F. Mahieu, and J. M. Festen. Quantitative analysis of voice quality in early glottic laryngeal carcinomas treated with radiotherapy. *European Archives of Oto-Rhino-Laryngology*, 254:78–80, 1997.

[21] J. de Boer, T. Mutanga, G. van der Wielen, L. Incrocci, and B. Heijmen. Efficacy of on-line translation and rotation corrections for seminal vesicle coverage in prostate radiotherapy. *International Journal of Radiation Oncology*Biology*Physics*, 72(1, Supplement 1):S574 – S574, 2008.

[22] I. M. V. de Leeuw, R. B. Keus, F. J. M. Hilgers, F. J. K. van Beinum, A. J. Greven, J. M. A. de Jong, G. Vreeburg, and H. Bartelink. Consequences of voice impairment in daily life for patients following radiotherapy for early glottic cancer: voice quality, vocal function, and vocal performance. *International Journal of Radiation Oncology*Biology*Physics*, 44(5):1071 – 1078, 1999.

[23] I. V. de Leeuw, D. Kuik, M. D. Bodt, I. Guimaraes, E. Holmberg, T. Nawka, C. Rosen, A. Schindler, R. Whurr, and V. Woisard. Validation of the voice handicap index by assessing equivalence of european translations. *Folia Phoniatr Logop*, 60(4):173–8, 2008.

[24] J. de Pooter, A. M. Romero, W. Jansen, P. Storchi, E. Woudstra, P. Levendag, and B. Heijmen. Computer optimization of noncoplanar beam setups improves stereotactic treatment of liver tumors. *International Journal of Radiation Oncology Biology Physics*, 66(3):913–922, 2006.

[25] G. X. Ding, D. M. Duggan, C. W. Coffey, M. Deeley, D. E. Hallahan, A. Cmelak, and A. Malcolm. A study on adaptive IMRT treatment planning using kv cone-beam CT. *Radiotherapy and Oncology*, 85(1):116 – 125, 2007.

[26] K. Dornfeld, J. R. Simmons, L. Karnell, M. Karnell, G. Funk, M. Yao, J. Wacha, B. Zimmerman, and J. M. Buatti. Radiation doses to structures within and adjacent to the larynx are correlated with long-term diet- and speech-related quality of life. *International Journal of Radiation Oncology*Biology*Physics*, 68(3):750 – 757, 2007.

[27] L. D. Dorresteijn, A. C. Kappelle, N. M. Scholz, M. Munneke, J. T. Scholma, A. J. Balm, H. Bartelink, and W. Boogerd. Increased carotid wall thickening after radiotherapy on the neck. *European Journal of Cancer*, 41(7):1026 – 1030, 2005.

[28] H. Eckel, W.F.Thumfart, M. Jungehulsing, C. Sittel, and E. Stennert. Transoral laser surgery for early glottic carcinoma. *European Archives of Oto-Rhino-Laryngology*, 257(4):221–226, 2000.

[29] F. S. Elner, A. Carbon dioxide laser as primary treatment of glottic T1s and T1a tumours. *Acta Oto-Laryngologica, Supplement*, 106(449):135–139, 1988.

[30] M. Engelsman, S. Rosenthal, S. Michaud, J.A.Adams, R. Schneider, S. Bradley, J. Flanz, and H. Kooy. Intra- and interfractional patient motion for a variety of immobilization devices. *Medical Physics*, 32(11):3468–3474, 2005.

[31] S. J. Feigenberg, M. Lango, N. Nicolaou, and J. A. Ridge. Intensity-modulated radiotherapy for early larynx cancer: Is there a role? *International Journal of Radiation Oncology*Biology*Physics*, 68(1):2 – 3, 2007.

[32] M. Fippel. Fast monte carlo dose calculation for photon beams based on the vmc electron algorithm. *Medical Physics*, 26(8):1466–1475, 1999.

[33] K. Fung, J. Yoo, H. Leeper, B. Bogue, S.Hawkins, J. Hammond, J.A.Gilchrist, and V. Venkatesan. Effects of head and neck radiation therapy on vocal function. *Journal of Otolaryngology*, 30(3):133–139, 2001.

[34] A. L. Galbo, R. D. Bree, P. Lips, and C. R. Leemans. Detecting hypothyroidism after treatment for laryngeal or hypopharyngeal carcinomas: A nationwide survey in the netherlands. *European Archives of Oto-Rhino-Laryngology*, 266(5):713–718, 2009.

[35] A. Gallo, M. D. Vincentiis, V. Manciocco, M. Simonelli, M. Fiorella, and J. Shah. CO_2 laser cordectomy for early-stage glottic carcinoma: A long-term follow-up of 156 cases. *Laryngoscope*, 112(2):370–374, 2002.

[36] H. A. Gay and A. Niemierko. A free program for calculating eud-based ntcp and tcp in external beam radiotherapy. *Physica Medica*, 23(3-4):115 – 125, 2007.

[37] C. V. Gogh, I. V.-D. Leeuw, B. Boon-Kamma, R. R. ., M. D. Bruin, J. Langendijk, D. Kuik, and H. Mahieu. The efficacy of voice therapy in patients after treatment for early glottic carcinoma. *Cancer*, 106(1):95–105, 2006.

[38] J. Gordon and J. V. Siebers. Convolution method and CTV-to-PTV margins for finite fractions and small systematic errors. *Physics in Medicine and Biology*, 52, 1997.

[39] R. V. Gowda, J. M. Henk, K. L. Mais, A. J. Sykes, R. Swindell, and N. J. Slevin. Three weeks radiotherapy for T1 glottic cancer: the christie and royal marsden hospital experience. *Radiotherapy and Oncology*, 68(2):105 – 111, 2003.

[40] D. G. Grant, J. R. Salassa, M. L. Hinni, B. W. Pearson, R. E. Hayden, and W. C. Perry. Transoral laser microsurgery for untreated glottic carcinoma. *Otolaryngology - Head and Neck Surgery*, 137(3):482 – 486, 2007.

[41] D. G. Grant, J. R. Salassa, M. L. Hinni, B. W. Pearson, R. E. Hayden, and W. C. Perry. Transoral laser microsurgery for recurrent laryngeal and pharyngeal cancer. *Otolaryngology - Head and Neck Surgery*, 138(5):606 – 613, 2008.

[42] D. Grofsmid, M. Dirkx, H. Marijnissen, E. Woudstra, and B. Heijmen. Dosimetric validation of a commercial monte carlo based IMRT planning system. *Medical Physics*, 37(2):540–549, 2010.

[43] M. Guckenberger, J. Meyer, D. Vordermark, K. Baier, J. Wilbert, and M. Flentje. Magnitude and clinical relevance of translational and rotational patient setup errors: A cone-beam CT study. *International Journal of Radiation Oncology*Biology*Physics*, 65(3):934 – 942, 2006.

[44] J. A. Hatton, P. B. Greer, C. Tang, P. Wright, A. Capp, S. Gupta, J. Parker, C. Wratten, and J. W. Denham. Does the planning dose-volume histogram represent treatment doses in image-guided prostate radiation therapy? assessment with cone-beam computerised tomography scans. *Radiotherapy and Oncology*, 98(2):162 – 168, 2011.

[45] M. S. Hoogeman, J. J. Nuyttens, P. C. Levendag, and B. J. Heijmen. Time dependence of intrafraction patient motion assessed by repeat stereoscopic imaging. *International Journal of Radiation Oncology*Biology*Physics*, 70(2):609 – 618, 2008.

[46] F. B. Hristov, D.H. A grey-level image alignment algorithm for registration of portal images and digitally reconstructed radiographs. *Medical Physics*, 23(1):75–84, 1996.

[47] Z. Huang, D. Han, Z. Yu, X. Ni, and X. Ge. Evaluate the curative effect of CO_2 laser in treatment of glottic carcinoma. *Zhonghua Er Bi Yan Hou Ke Za Zhi*, 37(3):219 – 222, 2002.

[48] C. W. Hurkmans, P. Remeijer, J. V. Lebesque, and B. J. Mijnheer. Set-up verification using portal imaging; review of current clinical practice. *Radiotherapy and Oncology*, 58(2):105 – 120, 2001.

[49] A. D. Jensen, S. Nill, P. E. Huber, R. Bendl, J. Debus, and M. W. Münter. A clinical concept for interfractional adaptive radiation therapy in the treatment of head and neck cancer. *International Journal of Radiation Oncology*Biology*Physics*, In Press, Corrected Proof:–, 2011.

[50] A. S. Jones, B. Fish, J. E. Fenton, and D. J. Husband. The treatment of early laryngeal cancers (T1a-T2 N0): surgery or irradiation? *Head & Neck*, 26(2):127–135, 2004.

[51] P. Keall, S. Vedam, R. George, C. Bartee, J. Siebers, F. Lerma, and E. W. .and T.Chung. The clinical implementation of respiratory-gated intensity-modulated radiotherapy. *Medical Dosimetry*, 31(2):152–162, 2006.

[52] G. Kian Ang .K. *Radiotherapy for head and neck cancers: indications and techniques*, pages 118 – −133. PA Philadelphia, Lippincott Williams & Wilkins, third edition, 2006.

[53] E. E. Klein, L. M. Chin, R. K. Rice, and B. J. Mijnheer. The influence of air cavities on interface doses for photon beams. *International Journal of Radiation Oncology*Biology*Physics*, 27(2):419 – 427, 1993.

[54] D. Kooper, P. V. den Broek, J. Manni, R. Tiwari, and G. Snow. Partial vertical laryngectomy for recurrent glottic carcinoma. *Clinical Otolaryngology and Allied Sciences*, 20(2):167–170, 1995.

[55] M. Krengli, M. Policarpo, I. Manfredda, P. Aluffi, G. Gambaro, M. Panella, and F. Pia. Voice quality after treatment for T1a glottic carcinoma: Radiotherapy versus laser cordectomy. *Acta Oncologica*, 43(3):284–289, 2004.

[56] Q. X. Le, K. K. Fu, S. Kroll, J. K. Ryu, J. M. Quivey, T. S. Meyler, R. M. Krieg, and T. L. Phillips. Influence of fraction size, total dose, and overall time on local control of T1-T2 glottic carcinoma. *International Journal of Radiation Oncology*Biology*Physics*, 39(1):115 – 126, 1997.

[57] G. P. Ledda and R. Puxeddu. Carbon dioxide laser microsurgery for early glottic carcinoma. *Otolaryngology - Head and Neck Surgery*, 134(6):911 – 915, 2006.

[58] L. Lee, Q.-T. Le, and L. Xing. Retrospective IMRT dose reconstruction based on cone-beam CT and MLC log-file. *International Journal of Radiation Oncology*Biology*Physics*, 70(2):634 – 644, 2008.

[59] I. V.-D. Leeuw, F. Hilgers, R. Keus, F. K.-V. Beinum, A. Greven, J. D. Jong, G. Vreeburg, and H. Bartelink. Multidimensional assessment of voice characteristics after radiotherapy for early glottic cancer. *Laryngoscope*, 109(2 I):241–248, 1999.

[60] H. Lesnicar, L. Smid, and B. Zakotnik. Early glottic cancer: The influence of primary treatment on voice preservation. *International Journal of Radiation Oncology*Biology*Physics*, 36(5):1025 – 1032, 1996.

[61] P. C. Levendag, D. N. Teguh, F. Keskin-Cambay, A. Al-Mamgani, P. van Rooij, E. Astreinidou, S. L. Kwa, B. Heijmen, D. A. Monserez, and S. Osman. Single vocal cord irradiation: A competitive treatment strategy in early glottic cancer. *Radiotherapy and Oncology*, In Press, Corrected Proof:–, 2011.

[62] P. C. Levendag, D. N. Teguh, P. Voet, H. van der Est, I. Noever, W. J. de Kruijf, I.-K. Kolkman-Deurloo, J.-B. Prevost, J. Poll, P. I. Schmitz, and B. J. Heijmen. Dysphagia disorders in patients with cancer of the oropharynx are significantly affected by the radiation therapy dose to the superior and middle constrictor muscle: A dose-effect relationship. *Radiotherapy and Oncology*, 85(1):64 – 73, 2007.

[63] H. Li, X. R. Zhu, L. Zhang, L. Dong, S. Tung, A. Ahamad, K. S. C. Chao, W. H. Morrison, D. I. Rosenthal, D. L. Schwartz, R. Mohan, and A. S. Garden. Comparison of 2d radiographic images and 3d cone beam computed tomography for positioning head-and-neck radiotherapy patients. *International Journal of Radiation Oncology*Biology*Physics*, 71(3):916 – 925, 2008.

[64] T. Li and L. Xing. Optimizing 4D cone-beam CT acquisition protocol for external beam radiotherapy. *International Journal of Radiation Oncology*Biology*Physics*, 67(4):1211 – 1219, 2007.

[65] L. Licitra, J. Bernier, C. Grandi, L. Locati, M. Merlano, G. Gatta, and J.-L. Lefebvre. Cancer of the larynx. *Critical Reviews in Oncology/Hematology*, 47(1):65 – 80, 2003.

[66] L. Lopez, B. Nunez, J. L. Pendas, V. Puente, B. Aldama, and N. Suarez. Laser cordectomy: oncologic outcome and functional results. *Acta Otorrinolaringol Esp*, 55:30–40, 2004.

[67] S. Loughran, N. Calder, F. MacGregor, P. Carding, and K. MacKenzie. Quality of life and voice following endoscopic resection or radiotherapy for early glottic cancer. *Clinical Otolaryngology*, 30(1):42–47, 2005.

[68] M. Luscher, U. Pedersen, and L. Johansen. Treatment outcome after laser excision of early glottic squamous cell carcinoma - a literature survey. *Acta Oncologica*, 40(7):796–800, 2001.

[69] A. Lusinchi, P. Dube, P. Wibault, I. Kunkler, B. Luboinski, and F. Eschwege. Radiation therapy in the treatment of early glottic carcinoma: the experience of villejuif. *Radiotherapy and Oncology*, 15(4):313–319, 1989.

[70] R. Mantravadi, E. Liebner, R. Haas, E. Skolnik, and E. Applebaum. Cancer of the glottis: prognostic factors in radiation therapy. *Radiology*, 149(1):311 – 4, 1983.

[71] L. Masi, F. Casamassima, C. Polli, C. Menichelli, I. Bonucci, and C. Cavedon. Cone beam CT image guidance for intracranial stereotactic treatments: Comparison with a frame guided set-up. *International Journal of Radiation Oncology*Biology*Physics*, 71(3):926 – 933, 2008.

[72] M. Maurizi, G. Almadori, G. Plaudetti, D. C. Eugenio, and J. Galli. Laser carbon dioxide cordectomy versus open surgery in the treatment of glottic carcinoma: Our results. *Otolaryngology - Head and Neck Surgery*, 132(6):857 – 861, 2005.

[73] G. Meedt, M. Alber, and F. Nasslin. Non-coplanar beam direction optimization for intensity-modulated radiotherapy. *Physics in Medicine and Biology*, 48(18):2999–3019, 2003.

[74] W. M. Mendenhall, R. J. Amdur, and J. R. Palta. Intensity-modulated radiotherapy in the standard management of head and neck cancer: Promises and pitfalls. *Journal of Clinical Oncology*, 24(17):2618–2623, 2006.

[75] B. Mittal, D. Rao, J. Marks, and C. Perez. Role of radiation in the management of early vocal cord carcinoma. *International Journal of Radiation Oncology*Biology*Physics*, 9(7):997 – 1002, 1983.

[76] H. M.M., Wieringa, M.H., Gerritsma, E.J., and L. Feenstra. Reproducibility of the dutch version of the voice handicap index. *Folia Phoniatrica et Logopaedica*, 58(2):132–138, 2006.

[77] G. K. Moose, B.D. Definitive radiation management for carcinoma of the glottic larynx. *Otolaryngologic Clinics of North America*, 30(1):131–143, 1997.

[78] F. J. W. E. C. D. Mortuaire, G. Local recurrence after CO_2 laser cordectomy for early glottic carcinoma. *Laryngoscope*, 116(1):101–105, 2006.

[79] G. Motta, E. Esposito, S. Motta, G. Tartaro, and D.Testa. CO_2 laser surgery in the treatment of glottic cancer. *Head and Neck*, 27(7):566–573, 2005.

[80] S. Motta, U. Cesari, M. Mesolella, and G. Motta. Functional vocal results after CO_2 laser endoscopic surgery for glottic tumours. *Journal of Laryngology and Otology*, 122(9):948–951, 2008.

[81] T. F. Mutanga, H. C. de Boer, G. J. van der Wielen, , and B. Heijmen. Fast on-line prostate positioning with stereographic targeting on KV/MV image pairs. *Medical Physics*, 34:2624, 2007.

[82] T. F. Mutanga, H. C. de Boer, G. J. van der Wielen, D. Wentzler, J. Barnhoorn, L. Incrocci, and B. J. Heijmen. Stereographic targeting in prostate radiotherapy: Speed and precision by daily automatic positioning corrections using kilovoltage/megavoltage image pairs. *International Journal of Radiation Oncology*Biology*Physics*, 71(4):1074 – 1083, 2008.

[83] A. Narayana, A. Vaughan, S. Fisher, and S. Reddy. Second primary tumors in laryngeal cancer: results of long-term follow-up. *International Journal of Radiation Oncology*Biology*Physics*, 42(3):557 – 562, 1998.

[84] K.-I. Nibu, S.-E. Kamata, K. Kawabata, M. Nakamizo, T. Nigauri, and K. Hoki. Partial laryngectomy in the treatment of radiation-failure of early glottic carcinoma. *Head and Neck*, 19(2):116–120, 1997.

[85] A. Niemierko. Reporting and analyzing dose distributions: A concept of equivalent uniform dose. *Medical Physics*, 24(1):103–110, 1997.

[86] B. Nunez, M. C. Cueva, and G. Senaris. Voice quality after endoscopic laser surgery and radiotherapy for early glottic cancer: objective measurements emphasizing the voice handicap index. *Eur Arch Otorhinolaryngol*, 265(5):543–548, 2008.

[87] S. J. Olszewski, J. M. Vaeth, J. P. Green, A. F. Schroeder, and B. Chauser. The influence of field size, treatment modality, commissure involvement and histology in the treatment of early vocal cord cancer with irradiation. *International Journal of Radiation Oncology*Biology*Physics*, 11(7):1333 – 1337, 1985.

[88] A. J. C. on Cancer. *Manual for Staging of Cancer*, page abstract. New York: Springer-Verlag, 6th edition, 2002.

[89] A. J. C. on Cancer. ICRU50, prescribing, recording and reporting photon beam therapy ICRU report 50: prescribing, recording and reporting photon beam therapy. Technical report, 2006.

[90] R. Onimaru, M. Hasegawa, K. Yasuda, A. Homma, N. Oridate, S. Fukuda, and H. Shirato. Radiotherapy for glottic T1N0 carcinoma with slight hypofractionation and standard overall treatment time: importance of overall treatment time. *Japanese Journal of Clinical Oncology*, 41(1):103 – 9, 2011.

[91] S. O. Osman, E. Astreinidou, H. C. de Boer, F. Keskin-Cambay, S. Breedveld, P. Voet, A. Al-Mamgani, B. J. Heijmen, and P. C. Levendag. IMRT for image-guided single vocal cord irradiation. *International Journal of Radiation Oncology*Biology*Physics*, In Press, Corrected Proof:–, 2011.

[92] S. O. Osman, H. C. de Boer, E. Astreinidou, A. Gangsaas, B. J. Heijmen, and P. C. Levendag. On-line cone beam CT image guidance for vocal cord tumor targeting. *Radiotherapy and Oncology*, 93(1):8 – 13, 2009.

[93] S. O. Osman, H. C. de Boer, B. J. Heijmen, and P. C. Levendag. Four-dimensional CT analysis of vocal cords mobility for highly focused single vocal cord irradiation. *Radiotherapy and Oncology*, 89(1):19 – 27, 2008.

[94] P. Ostwald, T. Kron, and C. Hamilton. Assessment of mucosal underdosing in larynx irradiation. *International Journal of Radiation Oncology Biology Physics*, 36(1):181–187, 1996.

[95] A. Peeters, van C.D. Gogh, K. Goor, I. V. de Leeuw, J. Langendijk, and H. Mahieu. Health status and voice outcome after treatment for T1a glottic carcinoma. *European archives of oto-rhino-laryngology : official journal of the European Federation of Oto-Rhino-Laryngological Societies (EUFOS) : affiliated with the German Society for Oto-Rhino-Laryngology - Head and Neck Surgery*, 261(10):534–540, 2004.

[96] G. Peretti, C. Piazza, D. Cocco, L. D. Benedetto, F. D. Bon, L. R. D. Zinis, and P. Nicolai. Transoral CO_2 laser treatment for tis-t3 glottic cancer: The university of brescia experience on 595 patients. *Head and Neck*, 32(8):977–983, 2010.

[97] S. Pradhan and K. R. *Surgery for laryngeal cancer: anatomy and patterns of spread, in Voice conservation surgery for laryngeal and hypopharyngeal cancer*, pages 10–105. Lloyds Publishing House: Mumbai, third edition, 2006.

[98] J.-B. Prevost, H. de Boer, J. Poll, P. Voet, and P. Levendag. Analysis of the motion of oropharyngeal tumors and consequences in planning target volume determination. *Radiotherapy and Oncology*, 87(2):268 – 273, 2008.

[99] R. Puxeddu, C. Piazza, M. Mensi, G. Ledda, F. Argiolas, and G. Peretti. Carbon dioxide laser salvage surgery after radiotherapy failure in T1 and T2 glottic carcinoma. *Otolaryngology - Head and Neck Surgery*, 130(1):84–88, 2004.

[100] T. Rancati, M. Schwarz, A. M. Allen, F. Feng, A. Popovtzer, B. Mittal, and A. Eisbruch. Radiation dose-volume effects in the larynx and pharynx. *International Journal of Radiation Oncology*Biology*Physics*, 76(3, Supplement 1):S64 – S69, 2010.

[101] E. Rennemo, U. Zätterström, J. Evensen, and M. Boysen. Reduced risk of head and neck second primary tumors after radiotherapy. *Radiotherapy and Oncology*, 93(3):559 – 562, 2009.

[102] L. F. Robert, J. B. Steven, L. G. Gordon, and A. B. James. Has radiotherapy become too expensive to be considered a treatment option for early glottic cancer? *Head and Neck*, 19(8):692–700, 1997.

[103] R. Rodel, W. Steiner, R. Muller, M. Kron, and C. Matthias. Endoscopic laser surgery of early glottic cancer: Involvement of the anterior commissure. *Head and Neck*, 31(5):583–592, 2009.

[104] D. I. Rosenthal, C. D. Fuller, J. L. B. Jr., B. Mason, J. A. Garcia, J. S. Lewin, F. C. Holsinger, C. R. Stasney, S. J. Frank, D. L. Schwartz, W. H. Morrison, A. S. Garden, and K. K. Ang. Simple carotid-sparing intensity-modulated radiotherapy technique and preliminary experience for T1-2 glottic cancer. *International Journal of Radiation Oncology*Biology*Physics*, 77(2):455 – 461, 2010.

[105] J.-F. Rosier, V. Grégoire, H. Counoy, M. Octave-Prignot, P. Rombaut, P. Scalliet, F. Vanderlinden, and M. Hamoir. Comparison of external radiotherapy, laser microsurgery and partial laryngectomy for the treatment of T1N0M0 glottic carcinomas: a retrospective evaluation. *Radiotherapy and Oncology*, 48(2):175 – 183, 1998.

[106] R. Rydell, L. Schalen, and S. F. A. Elner. Voice evaluation before and after laser excision vs. radiotherapy of T1a glottic carcinoma. *Acta Oto-Laryngologica*, 115(4):560–565, 1995.

[107] G. Sanguineti, P. Adapala, E. J. Endres, C. Brack, C. Fiorino, M. P. Sormani, and B. Parker. Dosimetric predictors of laryngeal edema. *International Journal of Radiation Oncology*Biology*Physics*, 68(3):741 – 749, 2007.

[108] M. Schrijvers, E. V. Riel, Langendijk, F. Dikkers, E. Schuuring, J. V. D. Wal, and B. V. D. Laan. Higher laryngeal preservation rate after CO_2 laser surgery compared with radiotherapy in T1a glottic laryngeal carcinoma. *Head and Neck*, 31(6):759–764, 2009.

[109] D. L. Schwartz and L. Dong. Adaptive radiation therapy for head and neck cancer can an old goal evolve into a new standard? *Journal of Oncology*, 2011:1–14, 2011.

[110] B. H. Sebastiaan Breedveld, Pascal Storchi. Multi-criteria beam angle IMRT optimization with icycle. *Radiotherapy and Oncology*, 92(1):S204, 2009.

[111] V. A. Semenenko, B. Reitz, E. Day, X. S. Qi, M. Miften, and X. A. Li. Evaluation of a commercial biologically based IMRT treatment planning system. *Medical Physics*, 35(12):5851–5860, 2008.

[112] E. Senkus-Konefka, E. Naczk, I. Borowska, A. Badzio, and J. Jassem. Changes in lateral dimensions of irradiated volume and their impact on the accuracy of dose delivery during radiotherapy for head and neck cancer. *Radiotherapy and Oncology*, 79(3):304 – 309, 2006.

[113] Y. Seppenwoolde, R. Berbeco, S. Nishioka, H. Shirato, and B. Heijmen. Accuracy of tumor motion compensation algorithm from a robotic respiratory tracking system: A simulation study. *Medical Physics*, 34(7):2774–2784, 2007.

[114] A. Sewnaik, C. Meeuwis, T. V. D. Kwast, and J. Kerrebijn. Partial laryngectomy for recurrent glottic carcinoma after radiotherapy. *Head and Neck*, 27(2):101–107, 2005.

[115] E. Sjogren, T. Langeveld, and R. D. Jong. Clinical outcome of T1 glottic carcinoma since the introduction of endoscopic CO_2 laser surgery as treatment option. *Head and Neck*, 30(9):1167–1174, 2008.

[116] E. Sjogren, M. V. Rossum, T. Langeveld, M. Voerman, V. V. D. Kamp, M. Friebel, R. Wolterbeek, and R. D. Jong. Voice outcome in Tla midcord glottic carcinoma. *Archives of Otolaryngology - Head and Neck Surgery*, 134(9):965–972, 2008.

[117] J. C. Smith, J. T. Johnson, and E. N. Myers. Management and outcome of early glottic carcinoma. *Otolaryngology - Head and Neck Surgery*, 126(4):356 – 364, 2002.

[118] J.-J. Sonke, J. Lebesque, and M. van Herk. Variability of four-dimensional computed tomography patient models. *International Journal of Radiation Oncology*Biology*Physics*, 70(2):590 – 598, 2008.

[119] J. Spector, Sessions, K. Chao, B. Haughey, J. Hanson, J. Simpson, and C. Perez. Stage i (T1 N0 M0) squamous cell carcinoma of the laryngeal glottis: Therapeutic results and voice preservation. *Head and Neck*, 21(8):707–717, 1999.

[120] S. Spirydovich, L. Papiez, V. Moskvin, and P. Desrosiers. Evaluation of underdosage in the external photon beam radiotherapy of glottic carcinoma: Monte carlo study. *Radiotherapy and Oncology*, 78(2):159 – 164, 2006.

[121] W. Steiner. Results of curative laser microsurgery of laryngeal carcinomas. *American Journal of Otolaryngology*, 14(2):116 – 121, 1993.

[122] M. Stewart, A. Chen, and C. Stach. Outcomes analysis of voice and quality of life in patients with laryngeal cancer. *Archives of Otolaryngology - Head and Neck Surgery*, 124(2):143–148, 1998.

[123] J. Stroom, H. D. Boer, H. Huizenga, and A. Visser. Inclusion of geometrical uncertainties in radiotherapy treatment planning by means of coverage probability. *International Journal of Radiation Oncology Biology Physics*, 43(4):905–919, 1999.

[124] D. N. Teguh, P. C. Levendag, A. Sewnaik, M. M. Hakkesteegt, I. Noever, P. Voet, H. van der Est, D. Sipkema, P. van Rooij, R. J. B. de Jong, and P. I. Schmitz. Results of fiberoptic endoscopic evaluation of swallowing vs. radiation dose in the swallowing muscles after radiotherapy of cancer in the oropharynx. *Radiotherapy and Oncology*, 89(1):57 – 63, 2008.

[125] D. N. Teguh, P. C. Levendag, P. W. Voet, A. Al-Mamgani, X. Han, T. K. Wolf, L. S. Hibbard, P. Nowak, H. Akhiat, M. L. Dirkx, B. J. Heijmen, and M. S. Hoogeman. Clinical validation of atlas-based auto-segmentation of multiple target volumes and normal tissue (swallowing/mastication) structures in the head and neck. *International Journal of Radiation Oncology*Biology*Physics*, In Press, Corrected Proof:–, 2010.

[126] J. U. and A. M. A finite size pencil beam algorithm for IMRT dose optimization: Density corrections. *Physics in Medicine and Biology*, 52(3):617–633, 2007.

[127] B. van Asselen, C. P. J. Raaijmakers, J. J. W. Lagendijk, and C. H. J. Terhaard. Intrafraction motions of the larynx during radiotherapy. *International Journal of Radiation Oncology*Biology*Physics*, 56(2):384 – 390, 2003.

[128] J. C. M. van der Voet, R. B. Keus, A. A. M. Hart, F. J. M. Hilgers, and H. Bartelink. The impact of treatment time and smoking on local control and complications in T1 glottic cancer. *International Journal of Radiation Oncology*Biology*Physics*, 42(2):247 – 255, 1998.

[129] G. J. van der Wielen, M. S. Hoogeman, G. R. Dohle, W. L. van Putten, and L. Incrocci. Dose-volume parameters of the corpora cavernosa do not correlate with erectile dysfunction after external beam radiotherapy for prostate cancer: Results from a dose-escalation trial. *International Journal of Radiation Oncology*Biology*Physics*, 71(3):795 – 800, 2008.

[130] M. van Herk, P. Remeijer, C. Rasch, and J. V. Lebesque. The probability of correct target dosage: dose-population histograms for deriving treatment margins in radiotherapy. *International Journal of Radiation Oncology*Biology*Physics*, 47(4):1121 – 1135, 2000.

[131] M. van Zijtveld, M. Dirkx, and B. Heijmen. Correction of cone beam CT values using a planning CT for derivation of the (dose of the day). *Radiotherapy and Oncology*, 85(2):195 – 200, 2007.

[132] B. Vanderstraeten, N. Reynaert, L. Paelinck, I. Madani, C. D. Wagter, W. D. Gersem, W. D. Neve, and H. Thierens. Accuracy of patient dose calculation for lung IMRT: A comparison of monte carlo, convolution/superposition, and pencil beam computations. *Medical Physics*, 33(9):3149 – 58, 2006.

[133] S. Vedam, P. Keall, V. Kini, H. Mostafavi, H. Shukla, and R. Mohan. Acquiring a four-dimensional computed tomography dataset using an external respiratory signal. *Physics in Medicine and Biology*, 48(1):45–62, 2003.

[134] I. Vilaseca, P. Huerta, J. Blanch, A. Fernández-Planas, C. Jiménez, and M. Bernal-Sprekelsen. Voice quality after CO_2 laser cordectomy - what can we really expect? *Head and Neck*, 30(1):43–49, 2008.

[135] P. W. Voet, M. L. Dirkx, D. N. Teguh, M. S. Hoogeman, P. C. Levendag, and B. J. Heijmen. Does atlas-based autosegmentation of neck levels require subsequent manual contour editing to avoid risk of severe target underdosage? a dosimetric analysis. *Radiotherapy and Oncology*, 98(3):373 –377, 2011.

[136] J. Wedman, J. Heimdal, I. Elstad, and J. Olofsson. Voice results in patients with T1a glottic cancer treated by radiotherapy or endoscopic measures. *European Archives of Oto-Rhino-Laryngology*, 259(10):547–550, 2002.

[137] G. Weinstein, B. O. Jr., W. Snyder, and N. G.Hockstein. Transoral robotic surgery: Supraglottic partial laryngectomy. *Annals of Otology, Rhinology and Laryngology*, 116(1):19–23, 2007.

[138] J. Werner, M. Schunke, H. Rudert, and B.Tillmann. Description and clinical importance of the lymphatics of the vocal fold. *Otolaryngology - Head and Neck Surgery*, 102(1):13–19, 1990.

[139] J. Wong, M. Sharpe, D. Jaffray, V. Kini, J. Robertson, J. Stromberg, and A. Martinez. The use of active breathing control (abc) to reduce margin for breathing motion. *International Journal of Radiation Oncology Biology Physics*, 44(4):911–919, 1999.

List of publications

[1] J. B. Malherbe, N. G. van der Berg, F. Claudel, S. O. S. Osman, R. Q. Odendaal, F. Krok, and M. Szymonski. Fluence dependence of the surface roughness of InP after bombardment. *Nuclear Instruments and Methods in Physics Research Section B: Beam Interactions with Materials and Atoms*, 230(1-4):533 – 538, 2005. Atomic Collisions in Solids - Proceedings of the 21st International Conference on Atomic Collisions in Solids.

[2] S. O. S. Osman, H. C. J. de Boer, B. J. M. Heijmen, and P. C. Levendag. Four-dimensional CT analysis of vocal cords mobility for highly focused single vocal cord irradiation. *Radiotherapy and Oncology*, 89(1):19 – 27, 2008.

[3] S. O. S. Osman, H. C. J. de Boer, E. Astreinidou, A. Gangsaas, B. J. M. Heijmen, and P. C. Levendag. On-line cone beam CT image guidance for vocal cord tumor targeting. *Radiotherapy and Oncology*, 93(1):8 – 13, 2009.

[4] P. C. Levendag, D. N. Teguh, F. Keskin-Cambay, A. Al-Mamgani, P. van Rooij, E. Astreinidou, S. L.S. Kwa, B. J. M. Heijmen, D. A. Monserez, and S. O. S. Osman. Single vocal cord irradiation: A competitive treatment strategy in early glottic cancer. *Radiotherapy and Oncology*, In Press, Corrected Proof:–, 2011.

[5] S. O. S. Osman, E. Astreinidou, H. C. J. de Boer, F. Keskin-Cambay, S. Breedveld, P. Voet, A. Al-Mamgani, B. J. M. Heijmen, and P. C. Levendag. Imrt for image-guided single vocal cord irradiation. *International Journal of Radiation Oncology*Biology*Physics*, In Press, Corrected Proof:–, 2011.

[6] S. O. S. Osman, E. Astreinidou, P. C. Levendag, and B. J. M. Heijmen. Impact of geometric variations on delivered dose in highly focused single vocal

cord IMRT. *International Journal of Radiation Oncology*Biology*Physics*, submitted:–, 2011.

[7] P. C. Levendag, A. Al-Mamgani, and D.Teguh. *Contouring in Head and Neck Cancer*, pages 166–174. Elsevier GmbH, Munich, first edition, 2009.

Summary

An early stage glotic cancer can effectively be treated using RT alone, showing excellent results ($80 - 90\%$ probability of cure). Conventionally, for the RT treatment, tumors are irradiated using two parallel opposed wedged photon beams (typical field size $25 - 50cm^2$). A conservative approach is used where the fields generously cover the tumor and surrounding healthy structures are greatly involved. Among the structures that are unnecessarily irradiated ; the contra-lateral vocal cord, arytenoids, swallowing muscles and carotid arteries at the level of the vocal cords. This might give rise to complaints such as; impaired voice, persistent arytenoid edema, dysphagia, and increased risk of strokes. Evidence was found of an inverse relationship between the dose to the laryngeal structures and quality of life (QoL) indicators concerning e.g., speech, diet. This highlights the need for a more optimized focused RT technique. Moreover, as early stage glottic tumors are known to be very localized and limited to the mucosa with no lymphatic vessels involvement this promotes the use a more localized technique for treatment. Therefore, we have been developing a technique for highly focused vocal cord irradiation in early glottic carcinoma, namely single vocal cord irradiation (SVCI) with intensity-modulated RT (IMRT). This technique aims at optimally treating a target volume confined to a single cord while sparing the surrounding healthy structures as much as possible. An overview of the steps involved in the development of this image-guided radiotherapy (IGRT) technique, are presented in this thesis.

In chapter 1 of this thesis a general introduction to the anatomy of the larynx and the conventional RT techniques used in the management of early stage glottic cancers is given.

As a first step in realizing SVCI, 4D-CT were used to assess respiratory vocal cord motion as described in chapter 2 . Nine discrete phase-resolved CT scans were reconstructed for each patient . Movement of the vocal cords with breathing were quantified using the 4D-CT data. Maximum displacements of the vocal cords were observed in the lateral direction towards the back of the larynx. The patient-averaged standard deviation (SD) with breathing here was 1.3mm while

the corresponding average lateral air gap width was 11mm. It was concluded that vocal cords movements due to breathing are generally small. Therefore, breathing motion does not seem to be a limiting factor for SVCI. In the preparatory phase for the treatment a 4D-CT should be acquired for each patient, using the methods described in chapter 2. Based on this 4D-CT scan, the average anatomy and deformation due to breathing motion could be monitored on an individual basis to identify any outliers. If a mid-phase CT scan is used for planning this can rule out intra-fraction systematic errors. In this case, the clinical target volumes (CTV) will be expanded with margins to take into account only the small residue random errors.

In daily treatment execution, highly focused SVCI requires sub-mm daily targeting accuracy to be effective. In chapter 3, a protocol for daily positioning corrections with on-line kV-cone beam CT (CBCT) is presented. From the statistics of the population under study, the residue systematic and random set-up errors (after using this on-line correction procedure) were measured and used to derive the safety margins required to expand the CTV volumes. While before correction the systematic displacements of the vocal cords were as large as 2.4 ± 3.3mm (cranial-caudal population mean $\pm$ SD Σ), daily CBCT registration and correction reduced these values to less than 0.2 ± 0.5mm in all directions. Random positioning errors (SDσ) were reduced to less than 1mm. The added imaging dose (approximately 1mGy per scan) from each CBCT scan was negligible compared to the treatment dose. In conclusion, on-line registration and correction using available CBCT acquisition and registration software can yield sub-mm systematic and random displacements for the vocal cords when combined with standard mask fixation. Thus, the high positioning accuracy required for single vocal cord irradiation may be achieved in a clinically feasible procedure. Estimated safety margins required to account for inter-fraction as well as intra-fractional set-up variations are small enough to spare the healthy vocal cord ($<$2mm in all directions).

Image-guided SVCI using IMRT is presented in chapter 4. An in-house IMRT/beam angle optimization algorithm was used to obtain coplanar and non-coplanar optimized beam angles. Using these angles, IMRT plans targeting a single vocal cord were generated. For the sake of comparison, conventional treatment plans using two laterally opposed wedged 6-MV photon beams are also presented. The tumor dose coverage and dose delivered to the OARs using conventional parallel opposed fields, IMRT using computer-optimized coplanar and non-coplanar beam setups are compared. The dose calculations were performed using a Monte Carlo (MC)-based treatment planning system (TPS). In conventional plans as well as in IMRT plans, the population-averaged mean tumor dose $\pm$ standard deviation to the planning target volume was 67 ± 1Gy. The contra-lateral vocal cord dose was reduced from 66 ± 1Gy in the conventional plans to 39 ± 8Gy and 36 ± 6Gy in the coplanar and non-coplanar IMRT plans, respectively. IMRT consistently reduced the doses to the other organs at risk. In conclusion, evidence was found that image-guided SVCI using IMRT can provide

significant sparing of critical structures without compromising CTV coverage. This might also allow re-irradiation (if the need arises because of second primaries in the vicinity), especially in younger patients. In this study (chapter 4) we also presented a class solution of beam angles to ease and standardize the IMRT treatment planning for a single vocal cord.

It is known that the increasingly conformal dose distributions provided by intensity modulated radiotherapy (IMRT) can be sensitive to geometrical treatment uncertainties. In chapter 5 we have conducted a study to test the sensitivity of single vocal cord IMRT treatment plans to set-up errors, respiration, and deformation. Pre-treatment 4D-CT scans were used for IMRT planning, generating the reference dose distribution. The impact of set-up errors was simulated by applying shifts to the planning CT-scans, followed by dose re-calculation with original beam segments, MUs, etc. Effects of respiration and deformation were determined with inhale and exhale CT-scans, and repeat scans acquired after 22Gy, 44Gy, and 66Gy, respectively. This simulation study shows that with isotropic margins as small as 2mm and daily cone beam CT-guided repositioning, CTV dose remained high, and large sparing of the contra-lateral vocal cord was maintained, when considering realistic intra- and inter-fraction geometric variations.

In chapter 6, SVCI as a competitive treatment strategy for early glottic cancer is presented. Given the very comparable outcome of conventional RT and laser surgery (LS) in the management of early glottic tumors in terms of cure, the treatment of choice ultimately relies on the functional outcome. The outcome in QoL and the preservation of voice have, in general, favorably been reported for RT despite the fact the RT involves a larger surface area than is the case with LS (i.e. two vocal cords instead of one). SVCI using IMRT in combination with hypo-fractionation is also discussed in chapter 6. Good local control rates, improved voice, short overall treatment times and potential room for re-treatment with preservation of the larynx, can be anticipated. It is therefore argued that hypo-fractionated SVCI can be a competitive alternative to laser surgery. However, It is concluded that in terms of evidence based medicine, randomized trials for the outcome of SVCI with IMRT techniques and LS are absent but are definitely needed in order to make a more balanced comparison for these competing techniques.

In chapter 7, a general discussion of the topics presented in this thesis is given. The potential benefits of using SVCI with IMRT in the management of early stage glottic cancers is stressed. In chapter 7 we also present our early clinical experience of treating patient using the SVCI with IMRT technique as described in this thesis.

Samenvatting

Een vroeg stadium glottische kanker (vroeg ontdekte stembandkanker) kan effectief met radiotherapie worden behandeld en geeft een uitstekende kans op genezing van 80-90%. Voor de conventionele Radiotherapie (RT) techniek die gebruikt wordt om deze tumoren te bestralen, maakt men gebruik van parallelle tegengestelde, wigvormige, fotonbundels (typische veldgrootte 25-50 cm^2). De behandeling is conservatief van opzet waarbij de velden de tumor ruim afdekken maar waarbij ook veel gezond weefsel wordt meebestraald. De kritieke structuren die onnodig worden bestraald zijn onder andere: de contra–laterale stembanden, de arytnoid (bekerkraakbeentjes), slikspieren en de carotid arteriën (de halsslagader). Ten gevolgen hiervan kunnen klachten zoals: stem beschadiging, aanhoudend arytenoid oedeem, trismus en verhoogde risico op een hartaanval onstaan. Er is een omgekeerd verband aangetoond tussen de dosering van de laryngeal structuren en de kwaliteit van leven betreffende stem- en eetfuncties. Dit stelt duidelijk de behoefte aan een nauwkeurige geoptimaliseerde RT techniek. Voorts is bekend dat vroeg stadium glottische tumoren zeer gelokaliseerd zijn, waarbij wél het slijmvlies maar niet de lymfevaten zijn aangetast. Het gebruik van een meer gelokaliseerde behandeltechniek zou daarom grote voordelen kunnen hebben. Voor het veilig en nauwkeurig bestralen van vroeg stadium glottische kanker streeft men naar zo klein mogelijk positioneringfouten, waarbij intra- en inter-fractiefouten zoveel mogelijk beperkt worden. Voor dit onderzoek is een techniek ontwikkeld voor gerichte bestraling van vroeg stadium glottische tumoren, waarbij slechts één stemband wordt bestraald (single vocal cord irradiation, SVCI) met intensiteit -gemoduleerde radiotherapie (IMRT). Deze techniek heeft als doel om de stemband optimaal te bestralen, zodanig dat omliggend gezond weefsel zo min mogelijk wordt beschadigd. De ontwikkeling van deze beeldgestuurde gerichte radiotherapie techniek (Image Guided Radiotherapy, IGRT) vormt het onderwerp van dit proefschrift en is samengevat in onderstaande paragrafen.

Hoofdstuk 1 is een introductie in de anatomie van het layrnx (strottenhoofd), waarbij de conventionele radiotherapie (RT) techniek voor de behandeling van

vroeg stadium glottische kanker word beschreven.

In hoofdstuk 2 wordt een eerste stap voor het realiseren van de SVCI techniek beschreven, die van 4DCT gebruikt maakt om ademhalingsbewegingen te beoordelen. Voor elke patiënt werden CT- beelden in negen fasen geconstrueerd. De respiratoire beweging werd aan de hand van deze 4DCT data vastgesteld. De maximale verschuiving van de stembanden werd vastgesteld in de laterale richting, aan de achterkant van het layrnx. Hierbij bedroeg de gemiddelde standaard deviatie van de populatie aan patiënten 1.3 mm, met een overeenkomstige gemiddelde breedte van de luchtspleet van 11 mm. Er werd gesteld dat stembandbewegingen door ademhaling in het algemeen klein waren en geen beperkende factor voor SVCI vormden.

In de voorbereidende fase van de behandeling wordt een 4D-CT van elke patiënt gemaakt, volgens de methoden die in hoofdstuk 2 zijn beschreven. Per patiënt kon zo een gemiddelde anatomie en vervorming door ademhaling gemeten worden en uitzonderlijke afwijkingen worden vastgesteld. Met het gebruik van een middenfase CT-scan voor dosisplanning kunnen intra-fractie-systematische fouten voorkomen worden. Het klinisch doelvolume (Clinical Target Volume, CTV) wordt dan uitgebreid met geometrische marges die slechts deze residu fouten zullen afdekken.

Voor een effectief dagelijks klinisch gebruik vereist de zeer gerichte SVCI techniek een submillimeter precisie. In hoofdstuk 3 wordt een protocol omschreven, waarbij met behulp van CT op het bestralingstoestel (cone-beam CT, CBCT), dagelijks de patiëntpositie wordt gecorrigeerd (on-line protocol). Van de populatiestatistieken werden systematische en random residufouten afgeleid (na toepassing van de dagelijkse correctie) en de noodzakelijke CTV marges bepaald. Waar vóór correctie de systematische verschuivingen van de stembanden nog 2.4 $\pm$ 3.3 mm (cranial-caudal population mean $\pm$SD, Σ) bedroegen, met een dagelijkse CBCT correctie werden deze verminderd tot 0.2 $\pm$ 0.5 mm in alle richtingen. Random positioneringsfouten (SD, σ) werden verminderd tot 1 mm. De extra dosis ten gevolge van het maken van afbeeldingen (ongeveer 1 mGy per scan) was verwaarloosbaar ten opzichte van de behandeldosis. Gesteld kan worden dat het on-line registreren en corrigeren met behulp van CBCT en bijbehorende registratiesoftware resulteert in submillimeter random en systematische verschuivingen van de stembanden in combinatie met een standaard masker voor fixatie. Deze hoge nauwkeurigheid, die vereist is voor het bestralen van één stemband, kan onder klinische omstandigheden worden gehaald. De geschatte geometrische veiligheidsmarges, noodzakelijk voor het ondervangen van inter- en intra-fractie-positioneringsvariatie, zijn klein genoeg ($<$ 2 mm in alle richtingen) om de gezonde stemband nog te kunnen sparen.

In hoofdstuk 4 wordt beeldgestuurde SVCI met IMRT behandeld. Een in eigen beheer ontwikkeld IMRT bundelhoekoptimalisatie algorithme werd gebruikt om optimale coplanaire en niet-coplanaire bundelhoeken te verkrijgen. De hoeken werden gebruikt om IMRT plannen te construeren voor één stemband. Ter vergelijking werden ook conventionele behandelplannen met wigvormige 6 MV

fotonbundels beschouwd. We vergeleken de tumordosering en de dosering van kritieke organen van de conventioneel parallel tegengestelde bundels met die van computergeoptimaliseerde coplanaire en niet coplanaire bundelplaatsingen met intensiteitsgemoduleerde bundelprofielen. De dosisberekeningen werden uitgevoerd in een Monte-Carlo-gebaseerd (MC) dosisplanningssysteem (Treatment Planning System, TPS). Voor zowel de conventionele als voor de IMRT plannen, was de gemiddelde tumordosis, gemiddeld over de populatie ($\pm$SD) 67 $\pm$ 1 Gy. De dosis in de contralaterale stemband werd teruggebracht van 66$\pm$1Gy in de conventionele plannen tot 39 $\pm$ 8 Gy en 36 $\pm$ 6 Gy bij de coplanaire en niet-coplanaire IMRT plannen. IMRT gaf consequent een vermindering in dosis in kritieke organen. We concludeerden dat beeldgestuurde SVCI met IMRT een significante bijdrage kan leveren aan het sparen van gezonde weefsels zonder daarbij CTV dekking op te offeren. Ook opent dit de mogelijkheid tot herbestraling voor de jongere patiënt (mocht dit noodzakelijk zijn in verband met secundaire primaire tumoren in de omgeving). In dit onderzoek (Hoofdstuk 4) presenteren we tevens een klasseoplossing van bundelhoeken met als doel de IMRT behandeling voor één stemband te standaardiseren.

Het is bekend dat de hoge conformiteit, die kenmerkend is voor IMRT behandelingen, erg gevoelig is voor geometrische onzekerheid tijdens een behandeling. In hoofdstuk 5 hebben we de gevoeligheid van IMRT plannen voor positioneringsfouten, ademhaling en vervorming onderzocht. Een 4DCT beelden die voorafgaand aan de behandeling werd gemaakt, werd gebruikt voor constructie van het IMRT dosisplan dat als referentie diende. De invloed van positioneringsfouten werd gesimuleerd door het toepassen van verschuivingen in de CT scans voor planning, gevolgd door een herberekening met originele bundelsegmenten, monitoreenheden, etc. De effecten van ademhaling en vervorming werden afgeleid uit de CT-scans bij in- en uitgeademde toestand, en vervolgscans na 22 Gy, 44 Gy en 66 Gy. Deze simulatie toont, dat bij beschouwing van realistische intra- en interfractie geometrische variaties, het gebruik van 2 mm isotrope marges in combinatie met CBCT-gestuurde repositionering, handhaving van de CTV dosis en sparing van de contralaterale stemband toelaat.

Hoofdstuk 6 introduceert SVCI als een concurrerende kandidaat voor de behandeling van vroeg glottische kanker. Gegeven de zeer vergelijkbare uitkomsten van conventionele RT en laser chirurgie (LS), wanneer het aankomt op genezing van vroeg glottische kanker, zal de uiteindelijke keuze afhangen van de functionele uitkomst. Uitkomsten in termen van QoL en het behoud van de stemfunctie pleiten in het algemeen voor RT, ondanks het feit dat RT een groter oppervlak bestrijkt dan LS (twee stembanden in plaats van één). Met het gebruik van hypogefractioneerde SVCI met IMRT wordt een verbetering in het stemgebruik, een korte behandeltijd en de mogelijkheid tot herbehandeling met sparing van de larynx voorzien. We pleiten dan ook voor hypogefractioneerde SVCI als concurrerende kandidaat voor LS. Desalniettemin ontbreekt het aan gerandomiseerde onderzoeken voor het vergelijk tussen SVCI met IMRT en LS technieken, hetgeen noodzakelijk is voor een juiste afweging tussen deze twee

kandidaten.

Hoofdstuk 7 geeft een overzicht van de onderwerpen in dit proefschrift met een nadruk op de mogelijke voordelen van SVCI met IMRT in het beheersen van vroeg glottische kanker. Ook presenteren we de eerste klinische resultaten van de behandeling van een patiënt met de SVCI-IMRT techniek die beschreven is in dit proefschrift.

Acknowledgments

Thank you to:

The patients that participated in my studies. Beside the fact that the data obtained was of great and indispensable value to this research, I have personally learnt some priceless lessons from your constant kindness and patience. Thank you for your willingness to participate in this study, knowing that it is only for research purposes and that its findings may not benefit you directly but benefit future patients. Your acceptance and endurance throughout the process gave me an extreme sense of responsibility towards this mission; it has motivated me during many difficult times.

Prof. Ben Heijmen, your support, stimulating suggestions and encouragement have helped me throughout the research and during the writing of this thesis. I am also sincerely grateful for your (and your family's) kindness not only to me but also to fellow international students.

Prof. Peter Levendag; without your dedication, motivation and more importantly your trust, this research would have never reached this far.

Dr. Willy de Kruijf, Dr. Hans de Boer, and Dr. Eleftheria Astreinidou, my supervisors, for their help, insight and inspiration. It has been a privilege to have been able to work with you.

Hafid Akhiat, Eliana Vásquez Osorio, Hans Joosten, Wilco Schillemans, Davy Wentzler, Andras Zolnay for their technical support and contributions to make this work possible.

Prof. Levendag for hosting the Thursday meetings in English so that I can be part of it. My thanks also go to Dr. Maarten Dirkx, Peter Voet, David Teguh and Peter van Rooij. I have enjoyed and benefited greatly from our discussions in these meetings over the last years.

Anne Gangsaas, for your enthusiasm for new projects. Your clinical experience introduced me to a more holistic approach; giving the entire project further perspective.

Stefan Kwa, although I only had the chance to know you for a short time, I

am truly grateful for your assistance and coaching.

Mischa Hoogman, Sebastiaan Breedveld, Wouter Wunderink, Yvette Seppenwoolde, Theodore Mutanga, Inger-Karine Kolkman-Deurloo, Dennis Grofsmid, Luiza Bondar, Rozie Ahmed and Steven Petit for all their support, interest and invaluable input.

Gerard Schaap who was of great help at critical times. The same goes to Jacqueline and Jolanda, the secretaries at the department, whose support during my first months in the Netherlands, I truly appreciate.

Special thanks to:

My Sudanese friends in the Netherlands, France, Saudi Arabia, Germany and of course Sudan, for their care, interest, and moral support.

Eliana and Wouter, for so many things but most importantly for being my family in the Netherlands.

My parents: mama Asia and baba Omer; their motivation and endless support and much more kept me going.

Ilham, Amira and Ali for always providing me with advice, support and family warmth.

Special thanks to my husband Aymen, whose patience and love enabled me to complete this work. Thank you for always being there.

Erasmus MC
University Medical Center Rotterdam

PhD Portfolio

Summary of PhD training and teaching

Name PhD student: S.O.S. Osman	PhD period: 2005 - 2011
Erasmus MC Department: Radiotherapy	Promotors: Prof.dr. B.J.M. Heijmen
Research School: Molecular medicine	Prof.dr. P.C. Levendag

1. PhD training	Year
Courses	
Biomedical English Writing and Communication. Erasmus MC, Rotterdam	2007
MathWorks training on Matlab Fundamentals and Statistical Methods. Erasmus MC, Rotterdam	2009
Seminars and workshops	
Monte Carlo Treatment Planning of the European Work group. Gent, Belgium	2006
BEAMnrc Monte Carlo workshop, National research council of Canada (NRC) and Carleton University. Ottawa, Canada	2007
Specific training	
Determination of k_Q Factors for Medium Energy X-ray using Monte Carlo Techniques. VSL, Delft	2011
Presentations and posters at international conferences	
9th Biennial ESTRO Meeting on Physics and Radiation Technology for Clinical Radiotherapy. Barcelona, Spain	2007
27th meeting of the European Society for Therapeutic Radiology and Oncology ESTRO. Gothenburg, Sweden	2008
10th Biennial ESTRO meeting on Physics and Radiation Technology for Clinical Radiotherapy. Maastricht, the Netherlands	2009

2. Teaching	Year
Lecturing	
Journal club: State of the Art Treatment of Early Stage Vocal Cord Cancers	2006
Journal club: Radiation Induced Xerostomia	2007
Journal club: Monte Carlo Treatment Planning, An Introduction.NCS Report 16	2008